



Technical Note

No. 135

Boulder Laboratories

IONOSONDE OBSERVATIONS OF
ARTIFICIALLY PRODUCED
ELECTRON CLOUDS
FIREFLY 1960

BY J. W. WRIGHT



U. S. DEPARTMENT OF COMMERCE
NATIONAL BUREAU OF STANDARDS

THE NATIONAL BUREAU OF STANDARDS

Functions and Activities

The functions of the National Bureau of Standards are set forth in the Act of Congress, March 3, 1901, as amended by Congress in Public Law 619, 1950. These include the development and maintenance of the national standards of measurement and the provision of means and methods for making measurements consistent with these standards; the determination of physical constants and properties of materials; the development of methods and instruments for testing materials, devices, and structures; advisory services to government agencies on scientific and technical problems; invention and development of devices to serve special needs of the Government; and the development of standard practices, codes, and specifications. The work includes basic and applied research, development, engineering, instrumentation, testing, evaluation, calibration services, and various consultation and information services. Research projects are also performed for other government agencies when the work relates to and supplements the basic program of the Bureau or when the Bureau's unique competence is required. The scope of activities is suggested by the listing of divisions and sections on the inside of the back cover.

Publications

The results of the Bureau's research are published either in the Bureau's own series of publications or in the journals of professional and scientific societies. The Bureau itself publishes three periodicals available from the Government Printing Office: The Journal of Research, published in four separate sections, presents complete scientific and technical papers; the Technical News Bulletin presents summary and preliminary reports on work in progress; and Basic Radio Propagation Predictions provides data for determining the best frequencies to use for radio communications throughout the world. There are also five series of non-periodical publications: Monographs, Applied Mathematics Series, Handbooks, Miscellaneous Publications, and Technical Notes.

A complete listing of the Bureau's publications can be found in National Bureau of Standards Circular 460, Publications of the National Bureau of Standards, 1901 to June 1947 (\$1.25), and the Supplement to National Bureau of Standards Circular 460, July 1947 to June 1957 (\$1.50), and Miscellaneous Publication 240, July 1957 to June 1960 (Includes Titles of Papers Published in Outside Journals 1950 to 1959) (\$2.25); available from the Superintendent of Documents, Government Printing Office, Washington 25, D. C.

NATIONAL BUREAU OF STANDARDS

Technical Note

April 1, 1962

IONOSONDE OBSERVATIONS OF ARTIFICIALLY PRODUCED ELECTRON CLOUDS: FIREFLY 1960

By J. W. Wright

The work described here was conducted with support from the United States Air Force Cambridge Research Laboratories under Contract No. PRO 60 - 599.

NBS Technical Notes are designed to supplement the Bureau's regular publications program. They provide a means for making available scientific data that are of transient or limited interest. Technical Notes may be listed or referred to in the open literature. They are for sale by the Office of Technical Services, U. S. Department of Commerce, Washington 25, D. C.

DISTRIBUTED BY
UNITED STATES DEPARTMENT OF COMMERCE
OFFICE OF TECHNICAL SERVICES
WASHINGTON 25, D. C.

Price \$2.50

CONTENTS

	<u>PAGE</u>
ABSTRACT.....	ii
FOREWORD.....	iii
I. INTRODUCTION.....	1
Summary Table of 1960 Experiments and Results.....	3
II. CONDITION OF THE IONOSPHERE.....	4
A. Solar Activity.....	8
1. General Variations 1959/1960.....	8
2. Solar Flare Effects.....	10
B. Geomagnetic Activity.....	12
C. Ionization Below the Nighttime F Region.....	12
D. Sporadic E.....	15
1. Occurrence by Type.....	15
2. Electron Densities in Sporadic E.....	19
E. Meteoric Influx.....	20
F. f-plots for Selected Shot Days.....	22
III. DETAILS OF INDIVIDUAL EXPERIMENTS, FIREFLY 1960.....	32
A. Dawn Electron Clouds.....	32
Margie (August 13; 74 km).....	33
Marie (August 9; 82 km).....	36
Lola (August 15; 83 km).....	36
Zelda (August 25; 102 km).....	39
Peggy (August 16; 103 km).....	42
Olive (August 19; 106 km).....	47
Jeannie (August 10; 109 km).....	50
Susan (August 17; 114 km).....	53
Dolly (July 27; 115 km).....	56

CONTENTS
(Continued)

	<u>PAGE</u>	
B. Night Electron Clouds	60	
Cathy (July 29; 94 km)	60	
Betsy (August 8; 108 km)	61	
Amy (July 28; 111 km)	64	
Ruthy (August 1; 113 km)	67	
Gerta (August 6; 138 km)	67	
C. Trail Electron Clouds (Janet, Hilda)	70	
D. High Explosive Detonations (Carry, Arlene)	72	
E. ONR Project TP Arc Experiments (Annie, Norma) ..	74	
F. Electron Removal (Rena; August 19; 105 km)	76	
G. Other Experiments (Linda, Mavis, Francis, Lily, Hedy, Ida)	80	
IV. SUMMARY: POSITION, DRIFT AND GROWTH OF ELECTRON CLOUDS	83	
V. RECOMMENDATIONS FOR FUTURE PROGRAMS	89	
REFERENCES	91	
APPENDIX I -- NOTES ON INSTRUMENTATION		
A. Characteristics of the Ionosondes, 1959/1960	92	
B. Antennas	95	
C. Range Accuracies	95	
D. Amplitude/Range vs. Time Recordings	98	
APPENDIX 2 -- METHODS FOR DETERMINATION OF CLOUD POSITION, DRIFT, AND GROWTH FROM IONOSONDE RANGE DATA		100
APPENDIX 3 -- A SUGGESTION FOR THE STUDY OF ELECTRON RECOMBINATION IN THE F2 REGION BY THE RELEASE OF GASES FROM ROCKETS		104

IONOSONDE OBSERVATIONS OF ARTIFICIALLY PRODUCED
ELECTRON CLOUDS: FIREFLY 1960

by

J. W. Wright

ABSTRACT

Ionospheric soundings obtained at four sites near Eglin AFB during Firefly 1960 are analyzed for Point Electron Cloud position and movement. The condition of the ionosphere during these experiments is discussed and compared with conditions during the Firefly 1959 series.

FOREWORD

The July-August 1960 series of chemical releases from rockets in the upper atmosphere was conducted at Eglin Air Force Base, Florida by the Air Force Cambridge Research Laboratories (GRD) with the support of ARPA. This series and its previous counterpart in September-October 1959, have a variety of objectives of military significance in missile and communications work which will not directly concern us here. However, the experiments have a very considerable scientific value in studies of the photochemistry and aerodynamics of the upper atmosphere; progress in these fields is perhaps as important to the practical objectives noted above as the direct engineering results themselves.

The National Bureau of Standards has played an increasingly active role in this program, initially (Smokepuff and Firefly 1959), by providing technical guidance to the U. S. Army Signal Corps in ionosonde instrumentation. In the current series NBS has been responsible for the development of echo-amplitude recording techniques, for the refinement of range measuring accuracy, for the operation of the "central" ionosonde installation (A-4), and for the analysis of the resulting data for position and drift information, control data, and some comparisons of results from the 1959 and 1960 series. This report does not -- and could not, with the time and information available -- attempt to exhaust even these data-analysis opportunities; much still remains to be done, particularly in the relation of our results to those of other observers and workers participating in the program.

NBS participation in the 1960 Firefly program has depended heavily on the combined efforts of members of the Equipment Development Group and The Electron Density Profile Group of the Ionosphere Research and Propagation Division. Especially to be mentioned are Mr. E.J. Violette, Mr. J. J. Pitts, and Mr. R. Schumaker, of the former group, and Mr. G. H. Stonehocker, Mrs. L. Wescott, Mr. S. Opitz,

Mr. D. J. Brown, and Mrs. I. Ford, of the latter group. The assistance of Mr. D. McKinnis in the analysis of the data and in programming the CDC 1604 computer is also gratefully acknowledged.

IONOSONDE OBSERVATIONS OF ARTIFICIALLY PRODUCED
ELECTRON CLOUDS: FIREFLY 1960

by
J. W. Wright

I. INTRODUCTION

It is the purpose of this report to describe and discuss some of the results obtained by the use of conventional ionosphere sounders (ionosondes) in the observation of effects of the release of chemicals in the upper atmosphere from research rockets. This report is directed especially to the data collected during "Project Firefly 1960", but comparisons with the results of "Firefly 1959" have been made wherever practical.

By permitting a measurement of the radio distance to ionized clouds over a wide range of radio frequencies, the ionosonde is a valuable tool for the study of cloud position, drift, and growth. Additional information on the electron content of such clouds, and on their radar cross section, results from the variable frequency nature of these observations. (The latter form the subject of a parallel report from the U. S. Army Signal Corps Radio Propagation Agency, based upon data from the same installations as used here). Finally, as the basic tool for ionospheric exploration, the ionosonde gives information on the condition of the ionosphere -- on the electron distribution, occurrence of disturbances and "sporadic E", and on the interaction -- if any -- of the chemical cloud with the ionized medium.

The 1960 Firefly series was observed by four model C-4 ionosondes, located at A-4, Eglin Auxiliary Field-1, Barin NAS Alabama, and Tyndall AFB. Florida. The disposition of the stations may be seen on any of the maps of Section III, showing cloud loci.

This report is organized in 5 sections. We start with a general, and then specific, discussion of the condition of the ionosphere during the 1959 and 1960 Firefly series in Section II, attempting to relate our conclusions to the observed frequency and height variations of the electron clouds. In Section III there follows a more detailed discussion of the various experiments comprising Firefly 1960, based upon the ionosonde range and frequency data. A discussion and survey of position and drift results is given in Section IV. Finally, in Section V some suggestions for future programs are offered.

Appendices at the back of the report describe the instrumentation, our efforts to eliminate range errors, and the methods of computing position and drift results.

II. CONDITION OF THE IONOSPHERE

INTRODUCTION

In many ways, the E region is probably the most difficult -- and the most interesting -- region of the ionosphere in which to do experiments of the kind under discussion here. It is perhaps the least understood of the three main regions of the ionosphere, and is almost as difficult to observe accurately as the D region. These difficulties stem from the relatively low electron densities of the E region (particularly at night) requiring observations on the medium and low radio frequencies where radio interference is especially troublesome; from the high absorption levels for these radio frequencies in this region; and finally, from the great complexity of the E region itself: it is the seat of the ionospheric "dynamo" system, of strong winds at highly variable velocity, and of such poorly understood phenomena as those known collectively as "sporadic E."

Clearly, any discussion of man-made phenomena in the E region should proceed from an understanding of the natural E region, or, failing that, from a knowledge of how E region conditions during the experiments compare with each other and with what might be called "average" conditions. Unfortunately, adequate control data do not exist for the Eglin AFB area, partly because no long series of observations have been made at that location, partly because of the previously mentioned difficulties of making nighttime E region electron density measurements under any circumstances.

In the following sections, we present some data on the observable (and inferrable) condition of the ionosphere and the solar and geomagnetic conditions affecting it. Clear conclusions regarding the relation of ionospheric conditions to the chemical release experiments are still not possible, but some indication may be found of the natural phenomena which should be taken into account in future experiments.

FIREFLY 1959 DAWN ELECTRON CLOUDS

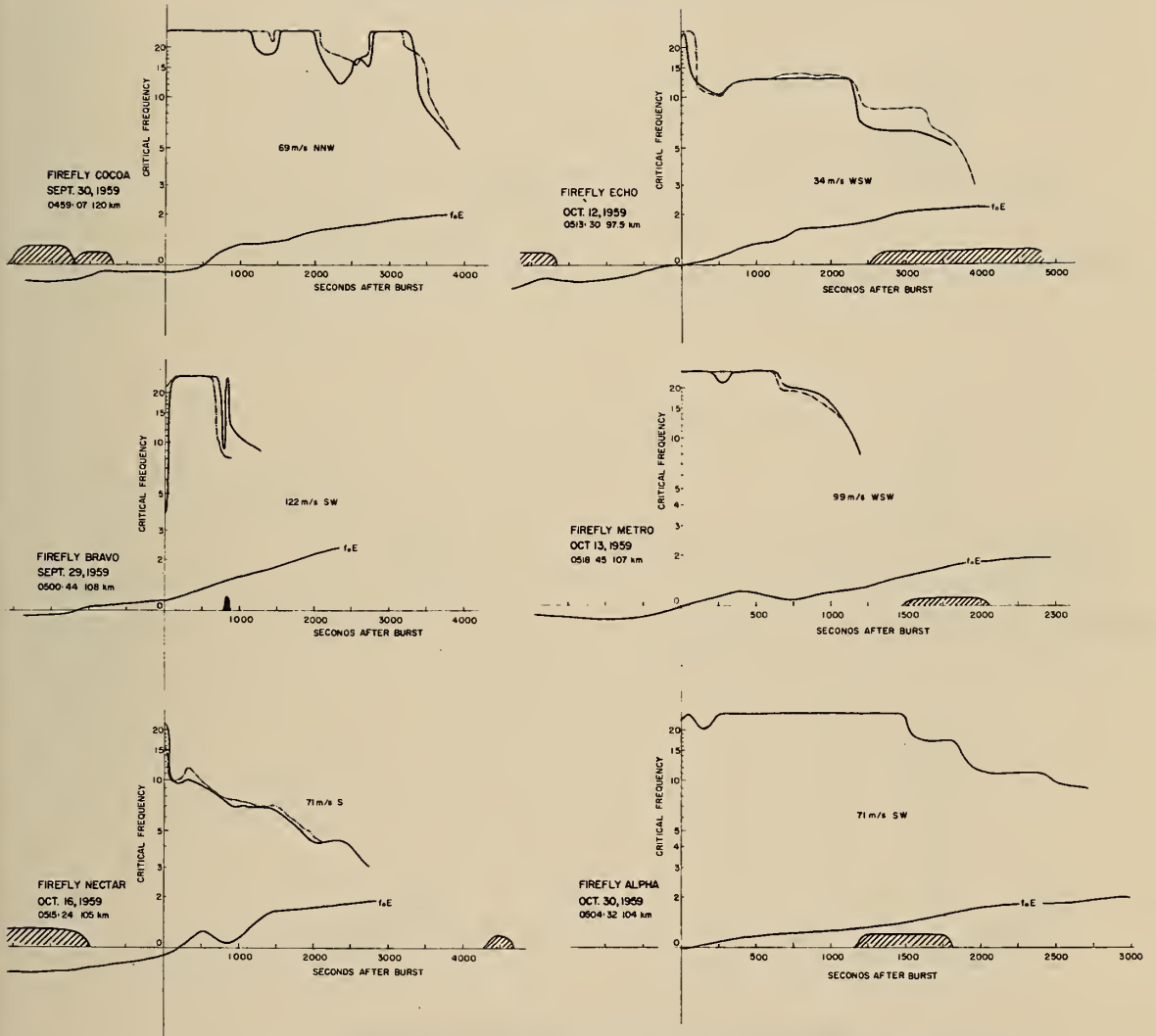


Figure 2: ELECTRON CLOUD CRITICAL FREQUENCIES VS TIME, FIREFLY 1959, DAWN SERIES. STATION A-4 ———; WEAVER SITE - - - - - . HATCHED AREAS SHOW THE DURATION AND MAGNITUDE OF SOLAR FLARES OCCURRING DURING THE EXPERIMENT. VALUES OF AVERAGE f_oE (---) AND INSTANTANEOUS f_oE (——) AS INFERRED IN SECTION II C ARE ALSO SHOWN.

FIREFLY 1959/1960 NIGHT ELECTRON CLOUDS

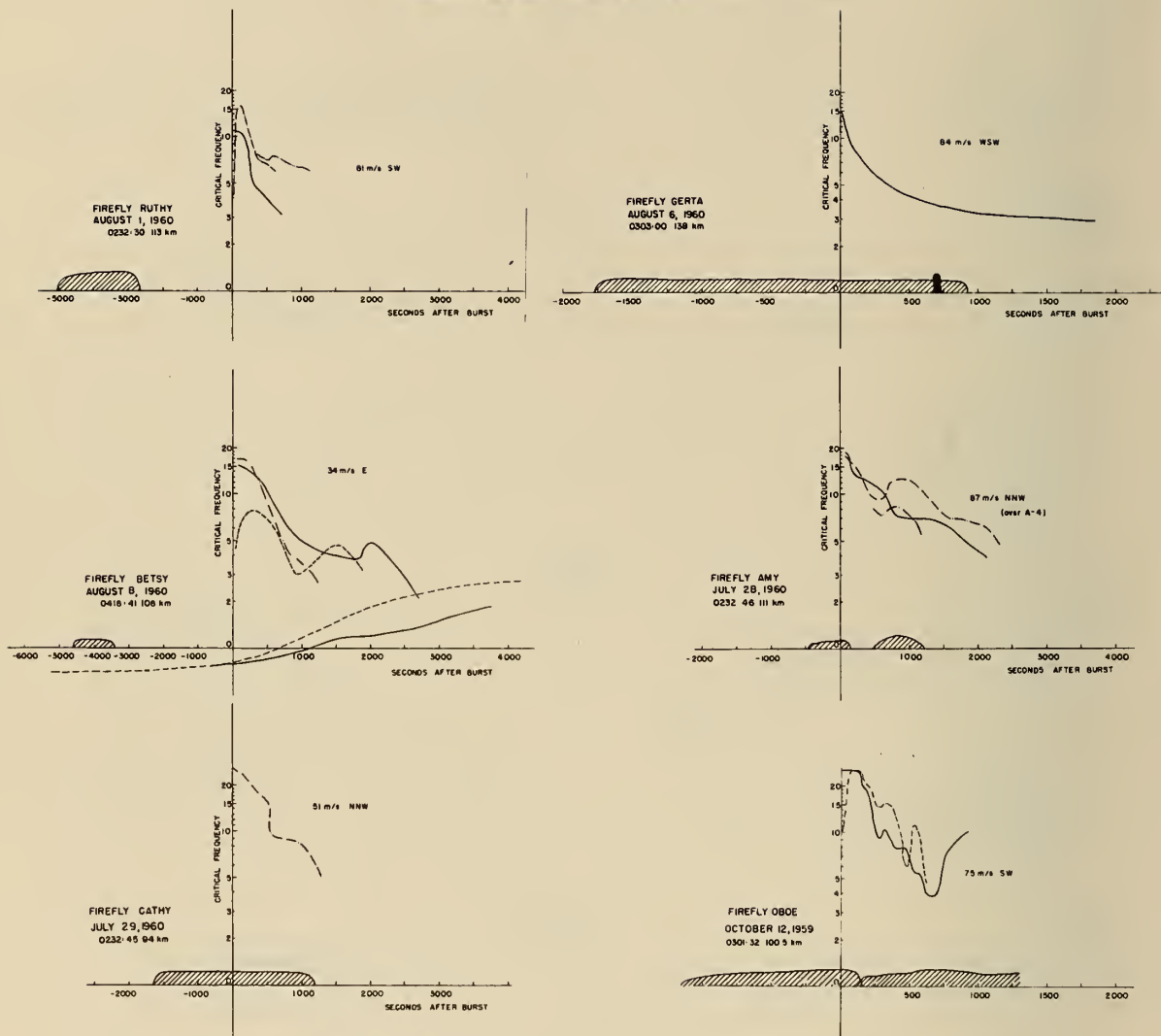


Figure 3: ELECTRON CLOUD CRITICAL FREQUENCIES VS TIME, FIREFLY 1959, 1960 NIGHT SERIES. STATION A-4, —; FIELD 1 OR WEAVER, - - - - -; BARIN FIELD - - - - -; TYNDALL - - -. HATCHED AREAS SHOW THE DURATION AND MAGNITUDE OF SOLAR FLARES OCCURRING DURING THE EXPERIMENT. VALUES OF AVERAGE f_{oE} (---) AND INSTANTANEOUS f_{oE} (—) AS INFERRED IN SECTION II C ARE ALSO SHOWN.

Figures 1, 2, and 3 showing the variation of maximum radio frequency (below 25 Mc) vs time, for each of the 1959, 1960 electron cloud experiments, are introduced immediately in order to establish the pertinence of the solar and ionospheric phenomena under discussion. In addition to the cloud critical frequency variations, these graphs show:

- (a) The expected ambient electron densities in comparison with the average (discussed in Section II A).
- (b) The occurrence of solar flares during the experiment (discussed below).
- (c) Annotations on the observed direction and speed of movement of the clouds.

A. SOLAR ACTIVITY

1. General Variations, 1959/1960

The graphs of Figure 4 show the variation of solar, geomagnetic, and ionospheric activity during both the 1959 and 1960 Firefly test periods. In each graph, the solid line gives the daily value of the parameter for July-August 1960, and the light dotted line gives the same information for the September-October 1959 period. At the top and bottom of the graphs, the dates and names of the 1959 and 1960 Firefly series, respectively, are indicated.

The Zurich daily sunspot numbers, and the 2800 Mc solar flux (in watts/cm²/cps bandwidth $\times 10^{-22}$), are measures of the sun's activity and are found to relate approximately to the daytime production of ionization in the lower ionosphere. This is further indicated by the graphs labeled "Noon foE" and "Noon f-min," which measure, respectively, the maximum electron density of the E layer at noon and the approximate level of noon-time D-region absorption. The values of foE and f-min were taken from observations at Cape Canaveral, Florida; they are seen to vary in the same general way as the solar radiation indices.

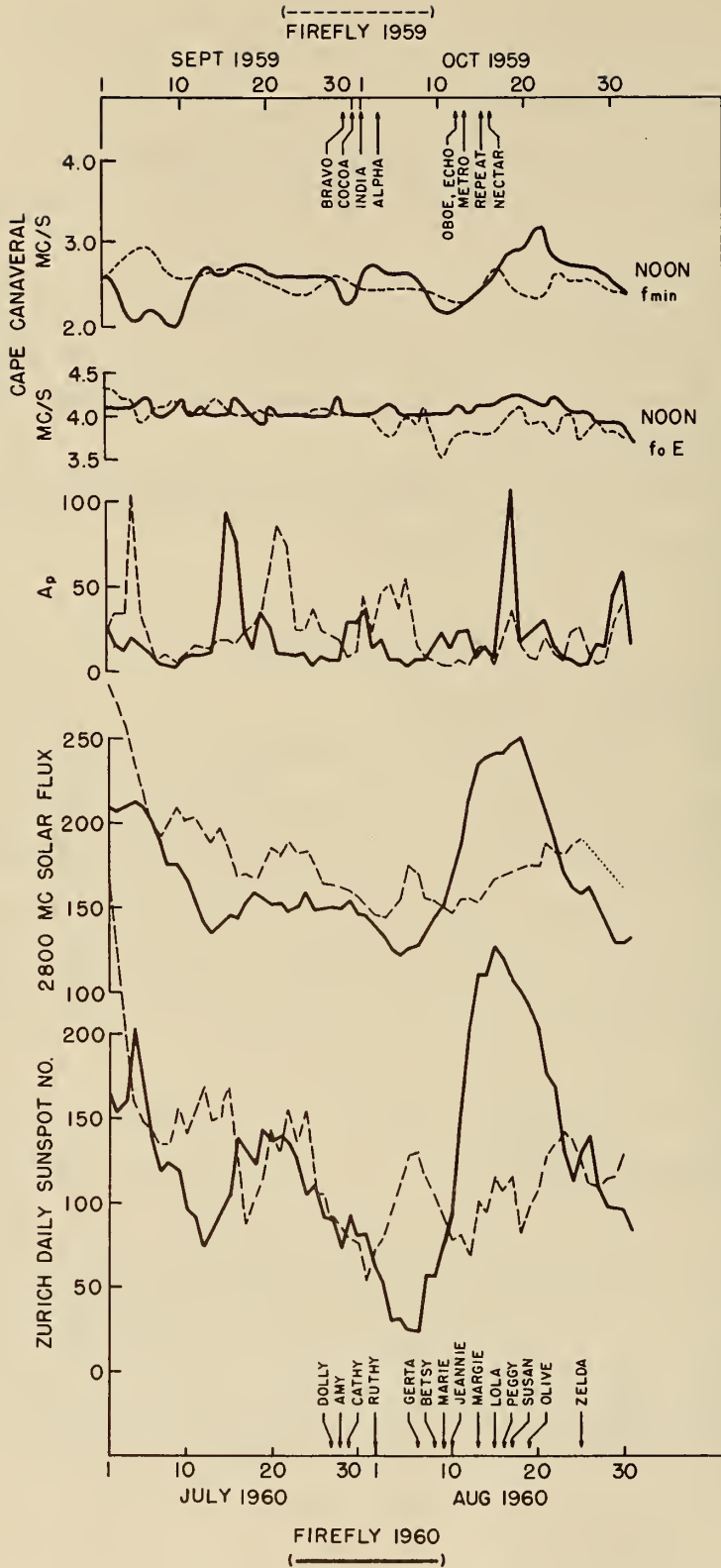


Figure 4: SOLAR, GEOMAGNETIC, AND IONOSPHERIC INDICES DURING FIREFLY SEPTEMBER, OCTOBER 1959 AND FIREFLY JULY, AUGUST 1960.

Because of the relatively gradual day-to-day variation in these solar parameters, they may be taken as an indicator of the relative ionizing effect of the sun near sunrise, the period of interest for many of the electron cloud experiments. They do not, however, give an indication of the nighttime E region electron densities, which are presumably under the influence of other factors, to be discussed below. The occurrence of sporadic enhancements of the ionization (sporadic E) is also ignored for the moment.

It is clear from these graphs that the early part of the 1959 and 1960 Firefly series (i.e., through Alpha (1959) and Ruthy (1960)) were in periods of approximately equal solar activity, with the 1959 levels slightly higher than 1960. Thus all of the 1960 nighttime clouds, and the dawn cloud Dolly, took place during a relative minimum of solar ionizing radiation. In 1959 only the night shot Oboe occurred at a similar level of daytime solar radiation.

The situation is different for the dawn experiments. During 1960, these (except for Dolly, already noted, and Zelda) took place during a relative maximum of solar ionizing radiation, considerably above the level for the 1959 series.

2. Solar Flare Effects

The best known effect of solar flares on the ionosphere is the "Dellinger effect," or short-wave fade-out which results from the sudden enhancement of solar radiation capable of producing a corresponding enhancement of ionization in the D -- or absorbing -- regions of the ionosphere. There is a small amount of evidence that corresponding enhancements of E layer ionization sometimes occur also.

Since most of the electron cloud experiments take place at a height above the probable level of maximum ionization enhancement during a flare, the (dawn) clouds are exposed to the full intensity of the enhanced radiations. It is therefore interesting to examine the cloud data for possible effects of flares.

In the graphs of Figures 1, 2, and 3, the maximum radio frequencies reflected by the dawn and night clouds, vs. time from burst, are shown for all observing stations together, for the 1959 and 1960 series. (The curves labeled "foE" are discussed in Section II C). Solar flares occurring in or near the observing period are indicated by the hatched areas extending from the observed onset to the cessation of the flare. The "importance" (magnitude) of the flare is shown on the conventional 1- through 3+ scale by the height of the hatched area.

There appears to be evidence from these graphs for flare enhancements of the cloud electron densities, as evidenced by increases in the cloud critical frequency from one or more stations during or shortly following an observed flare.

The most suggestive case is that of Peggy (1960), where several flares of importance 2 occurred during the lifetime of the cloud. Dolly and Olive (1960), Bravo, Echo and Alpha (1959) also give slight added support to the idea. There do not appear to be clear-cut negative cases, except perhaps Betsy (1960).

Thus it is possible that this effect may explain some of the critical frequency fluctuations observed during the electron cloud experiments; it would be quite interesting to pursue this hypothesis further, particularly since little is known about the ionizing radiation in solar flares.

Nevertheless, it would seem that the general level of solar activity, which was temporarily higher in the 1960 series than in 1959, cannot account directly for the great differences noted between 1959 and 1960 Firefly experiments.

B. GEOMAGNETIC ACTIVITY

The variation of the daily geomagnetic activity index A_p , through the 1959 and 1960 test periods, is also shown in Figure 4.

It is generally considered that values of A_p exceeding about 30 correspond to magnetically disturbed conditions; this usually is accompanied by greater nighttime absorptions, which implies an increase over the normal level of ionization in the lower ionosphere. We will find this expectation confirmed in Section II C, where we deal more specifically with ionization in the nighttime lower ionosphere.

From Figure 1 we see that Fireflies Alpha (1959), Susan, Peggy, and Cathy (1960) occurred on days of comparatively high geomagnetic activity, and that Oboe, Echo and Bravo (1959), and Dolly, Amy, and Gerta (1960), occurred on days that were magnetically quiet.

C. IONIZATION BELOW THE F-REGION AT NIGHT

As noted in the introduction to this section, the comparatively low electron densities of the nighttime E region are usually not directly measurable with conventional sounding techniques, except for sporadic E. Nevertheless, effects resulting from the presence of such ionization do appear on high frequency ionosphere soundings, and may be used to infer, in a semi-quantitative way, the amount of such ionization.

In Figure 5 is sketched part of the magnetoionic "ordinary" (O) and "extraordinary" (X) virtual height curves resulting from the conventional sweep-frequency sounding of the nighttime ionosphere.

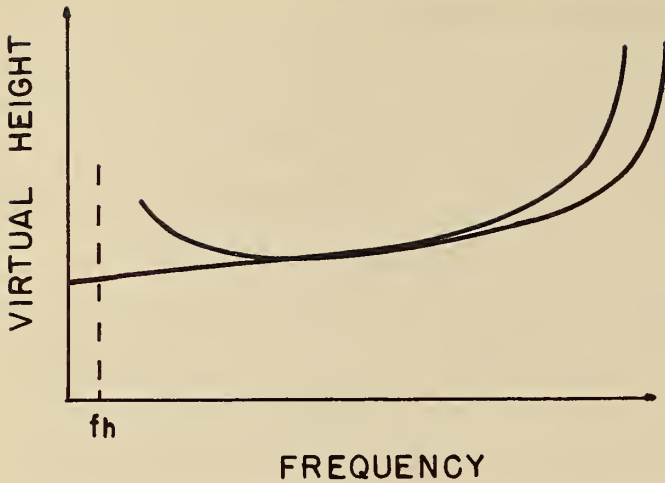


Figure 5: Typical nighttime virtual height curves from the F region, showing retardation of magnetoionic extraordinary component near the gyrofrequency due to underlying E ionization.

If the bottom of the F region proceeded to zero electron density suddenly, (i.e., with no tail, and with no nighttime E layer) the F region O and X virtual height curves would be similar in shape throughout; if the F region $N(h)$ gradient were large enough, they would actually be superimposed at the lower frequencies. This is frequently observed. If, however, the F region possesses a "tail," or a low density E region exists, the X virtual height curve is strongly retarded at frequencies near the frequency of electron gyro-resonance of the earth's magnetic field (f_H). This is at about 1.4 Mc, at Eglin AFB.

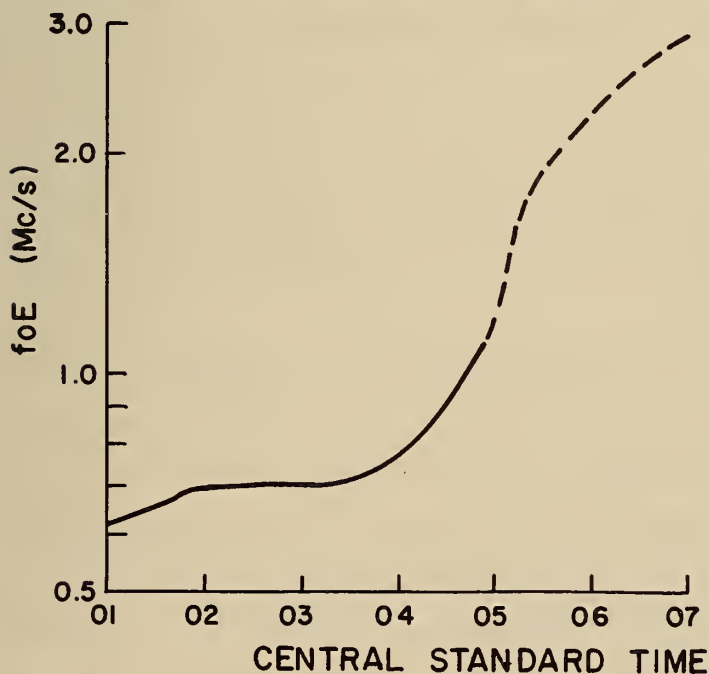
Now it may be shown (Titheridge, 1959) that this retardation, measured relative to the O-curve (which is unaffected near f_H), is to a good approximation a measure of the total electron content in the lower region.

Unfortunately, this method does not tell where (or whether) this ionization is localized, nor does it measure its maximum electron density. Other work (Watts and Brown, 1954) has shown that the nighttime E layer is remarkably constant, and often has a peak density corresponding to 0.5 - 0.8 Mc, and is localized above about 120 km. It is probable that such a layer accounts for most, if not all, of the ionization detectable by the method described above.

Studies of the magnitude of the retardation of the X-curve show that it also is frequently constant at night (about 30 km above the O-curve at 2 Mc), and increases rapidly at sunrise. If we assume this steady nighttime ionization to be contained in a parabolic distribution of semi-thickness $2H$ (where H is the scale height, about 7 km in the E region), and of peak density corresponding to 0.7 Mc, then we find that the nighttime X gyro-retardation of 30 km corresponds to a total electron content below the F region, of

$$\begin{aligned} N_T &= 4/3 N_{\max} (2H) \\ &= 1.2 \times 10^{10} \text{ electrons/cm}^2 \text{ column,} \\ &\text{where } N_{\max} = 0.62 \times 10^4 \text{ cm}^{-3}, \text{ corresponding to} \\ &\text{foE} = 0.7 \text{ Mc.} \end{aligned}$$

With this figure we can "calibrate" individual measurements of the X-gyro-retardation in terms of an equivalent N_{\max} . The values of foE at night deduced in this way, are shown in Figure 6 (solid line).



Also shown in Figure 6 (dashed line) is the average E layer critical frequency (foE) for the sunrise period. At about 0410, on the average in July-August 1960, foE attains the value 1.0 Mc, ($1.24 \times 10^4 \text{ cm}^{-3}$), or roughly twice the assumed nighttime value. At this time, the X gyro-retardation has also doubled from its nighttime value of 30 km, thus tending to confirm the method of

Figure 6: The deduced (—) and observed (----) average variation of night and dawn E layer critical frequency.

inference. It must be noted that the layer is assumed to be of constant thickness, and that no information is given regarding its height.

The nighttime E layer critical frequencies have been estimated in this way for each of the Electron Cloud experiments, and the results (in comparison with the average) appear on the graphs showing cloud "critical frequency" vs. time. In most cases, the E layer actually becomes visible in the late sunrise period; these values have been used wherever possible.

D. SPORADIC E

1. Occurrence by Type

From its appearance on the ionogram in moderate latitudes, sporadic E may be easily classified into one of several types. These types are essentially based upon the observed or inferrable height range in which the Es exist. The following are the conventional type designations and a short description of the four types commonly observed at moderate latitudes:

- f-"flat", the common type occurring at night;
- l-"low", sporadically reflecting strata below the daytime E layer (i.e., typically below 110 km);
- c-"cusp", a reflecting stratum embedded in the normal daytime E layer below the level h_{maxE} ;
- h-"high", a reflecting stratum embedded in the daytime E layer above the level h_{maxE} .

In this section, we shall discuss the frequency of occurrence of sporadic E expected at Eglin Air Force Base during the two Firefly series. Since the necessary control data do not exist for the Eglin area, our conclusions are based upon synoptic data obtained at White Sands, New Mexico and Cape Canaveral, Florida, the nearest and most regularly-operated station likely to be representative of conditions at Eglin Air Force Base.

Figures 7A, B, C, D, show the diurnal occurrence of the four Es types in July-August 1960 and September-October 1959 expressed as a simple count of occurrences on the quarter-hourly ionograms. (Percent occurrences are difficult to estimate because more than one type of Es frequently occurs simultaneously). White Sands and Cape Canaveral data are combined on the graphs, making a total of 248 possible cases per type, at each hour, on each graph.

In general, the curves indicate distinct diurnal patterns, and also a significant difference between the September-October 1959 and July-August 1960 periods. The seasonal variation of Es occurrences at these latitudes is well known. In all months there is clear evidence of solar control, giving maximum frequencies of occurrence in the daytime. In all cases, the extra daytime Es is of the c and h types but the greatest portion of it is Es-c. That is, most of the daytime Es occurs within the daytime E layer, but below the level $h_{max}E$ (about 125 km). Es occurring above this height (Es-h) is relatively insignificant, and does not appear to vary in abundance from month to month as much as the Es at lower levels. Es occurring at heights below the daytime E layer usually shows a morning and evening maximum; this is probably because the normal E layer rises at these times, revealing a larger range of heights within which Es-1 is defined.

The large differences between 1959 and 1960, in the occurrence of Es-f at night, are of great interest here. The reasons for this seasonal variation in nighttime Es occurrence are not known, but it appears reasonable to associate it with changes in the amount of nighttime atmospheric motions, since other evidence, to be discussed below, does not suggest corresponding seasonal variations in the mean amount of ionization in the nighttime E region.

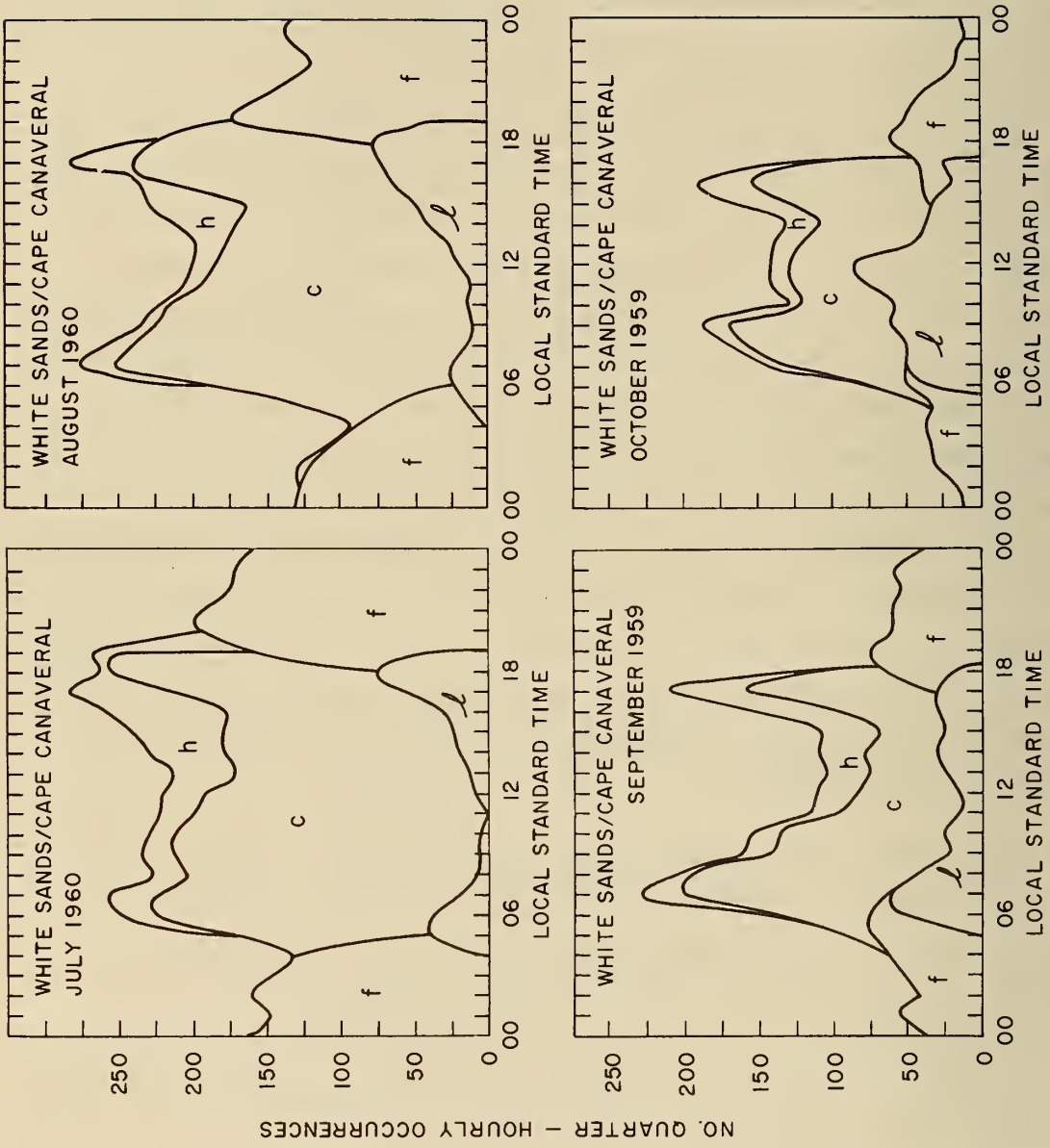


Figure 7 A,B,C,D: THE DIURNAL OCCURRENCE FREQUENCY OF SPORADIC E, BY TYPE OF Es, USING QUARTER-HOURLY DATA FROM WHITE SANDS AND CAPE CANAVERAL TOGETHER, JULY-AUGUST 1960 AND SEPTEMBER-OCTOBER 1959.

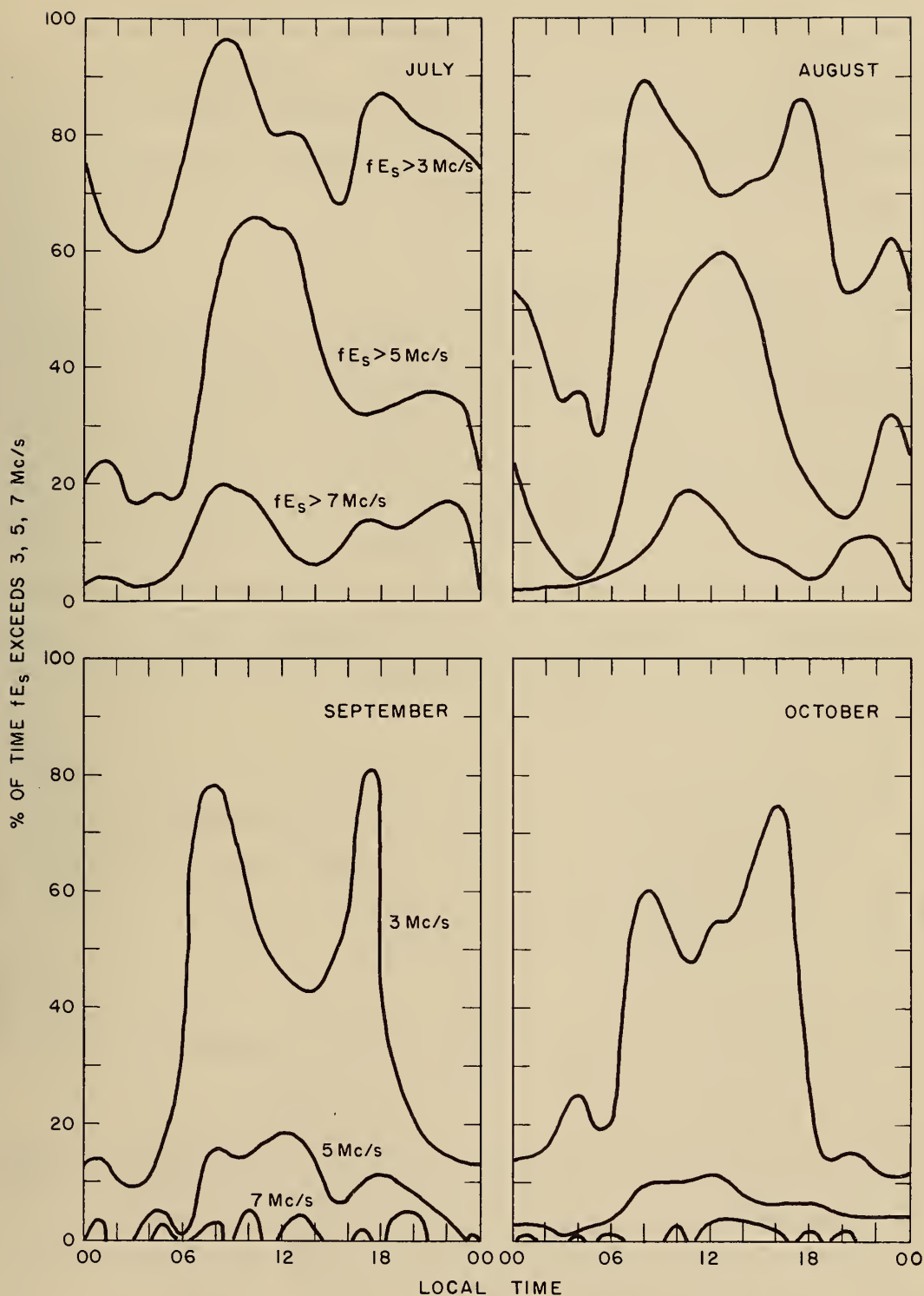


Figure 8 A,B,C,D: PERCENT OF TIME fE_s (ALL TYPES) EXCEEDS 3, 5 OR 7 MC, VS. LOCAL TIME OF DAY. DATA TAKEN FROM CAPE CANAVERAL, GRAND BAHAMA ISLAND, AND WHITE SANDS FOR 1958, 1959, 1960.

This behavior is perhaps related to the observed motions of electron clouds during Firefly 1959 and 1960. Although no clear drift patterns were established by either series of clouds, the 1960 clouds seemed to drift shorter distances, and in a wider variety of directions than those of the 1959 series.

2. Electron Densities in Sporadic E

It is customary to summarize the variation of the maximum vertical incidence reflection frequency of sporadic E (foEs) in terms of the percent of total time it exceeds certain levels, thus giving a more smoothly varying parameter than the median or mean value. As an example of what might be expected at Eglin Air Force Base during the 1960 Firefly series, we have constructed the graphs shown in Figure 8A, B, C, D, showing the percent total time foEs exceeds 3, 5, 7 Mc/s at Cape Canaveral, Grand Bahamas Islands, and White Sands for months July, August, September, October. The graphs represent averages of three years' data (1958, 1959, 1960).

There are clear seasonal variations showing in a higher occurrence of greater Es electron densities in July-August (i.e. Firefly 1960), than in September-October (Firefly 1959). Diurnally, there is a late morning and later evening maximum of the greater foEs values, with the morning values somewhat more common.

The seasonal variation is apparent, leading to lower foEs values in September-October than in July-August. Again, this is in contrast to the electron densities attained by artificial electron clouds in the two periods: in 1959, clouds of generally greater electron densities were produced. If these observations are related, it then seems that the factors leading to abundant and high Es electron densities (as in July-August) interfere with the effective production of electron clouds.

E. METEORIC INFLUX

Meteors entering the earth's upper atmosphere produce ionization which may be -- and is -- detected by much of the same radio instrumentation as is used to identify artificial electron cloud effects. For most methods of observation, the distinction between meteoric ionization and the electron cloud may be difficult to make, especially if the latter be short-lived, or the rate of the former be high. It is, therefore, useful to have some information concerning the occurrence of ionization-producing meteors. As will be seen below, the 1960 Firefly series took place during the seasonal maximum of meteoric activity, and most of the electron cloud experiments occurred during the diurnal maximum.

The height of maximum ionization production for an incoming meteor is at about 93 km; and the mean length of the trail, for radio purposes, is about 25 km (Manning and Eshleman, 1959).

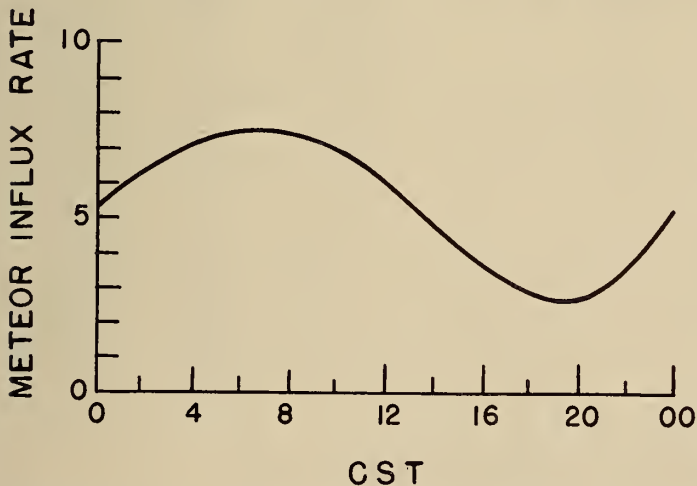


Figure 9: Mean diurnal variation of hourly meteoric influx rate, July-August.

in a collecting area of about 10^5 km^2 , at the ionizing altitude, and observed at a radio frequency of 72 Mc. It is evident from both of these figures that the 1960 Firefly series, and particularly the dawn electron cloud experiments, have been conducted during the peak in meteoric activity. In Figure 10, the echoes produced by recognized

The diurnal occurrence rate appropriate to 30°N geographic latitude, and the months of July and August, is given in Figure 9. The seasonal variation of occurrence rate is given in Figure 10. These figures, taken from the work of Hawkins (1956), express the rate of occurrence of meteors

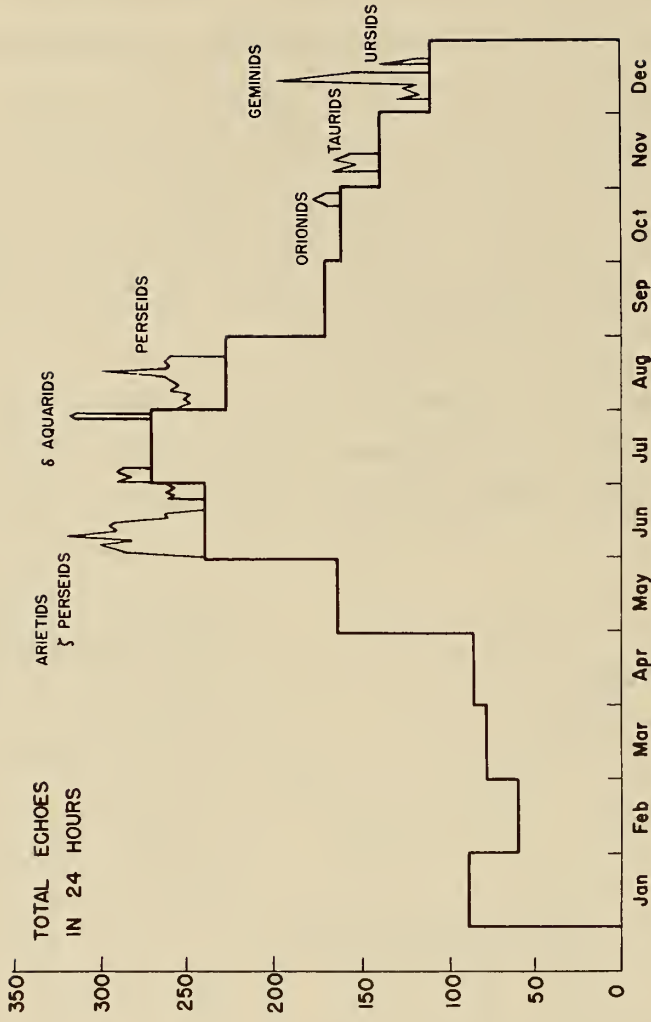


Figure 10: SEASONAL VARIATION OF METEORIC INFLUX.

meteor showers have been superimposed on the random influx rate. It should be noted that these showers, of visual magnitude ≤ 5 , negligibly increase the radar echo rate (Brown, et. al, 1956).

F. f-PLOTS FOR SELECTED SHOT DAYS

A succinct and lucid representation of many important features of a day's ionospheric soundings is afforded by the standard f-plot, a graph of frequency characteristics vs. time. f-plots were prepared at A-4 for each day of available complete (quarter-hourly) data during the 1960 Firefly series. A group of these are given in Figures 11 through 18, for the following dates:

- Figure 11 August 6, 1960 (Gerta)
- Figure 12 August 8, 1960 (Betsy)
- Figure 13 August 10, 1960 (Jeannie)
- Figure 14 August 13, 1960 (TP Annie, Norma; Margie)
- Figure 15 August 15, 1960 (Lola, Arlene)
- Figure 16 August 16, 1960 (Peggy)
- Figure 17 August 17, 1960 (Susan, Linda)
- Figure 18 August 19, 1960 (Olive, Rena).

Each graph shows the quarter-hourly values of a number of frequency parameters (in Mc/s), and the occurrence of sporadic E types. Starting at the bottom, (for example, in the daytime), the following data are recorded:

a. Occurrence of Sporadic E, by Type. The four "Es-types" occurring frequently at these latitudes designated f, l, c, h, have been described in Section II D. Occurrence of the various types are noted by small circles on the bottom graph of the f-plot.

b. f-min. The minimum frequency at which echoes can be observed, represented on the f-plot by lines extending upwards from the base line (1.0 Mc) to the value of f-min. In the daytime, and occasionally at night, f-min qualitatively indicates the level of absorption in the D-region. The constant value of 1.6 Mc at night is the result of broadcast interference.

c. foE. The critical frequency of the normal E layer, represented by small circles.

d. fbEs. The "blanketing frequencies" of the occurring Es types. This is often a measure of the maximum electron density of an Es stratum, indicating the lowest radio frequency that can penetrate it.

e. foF1. The critical frequency of occurring intermediate stratifications in the F region.

f. foF2 and fxF2. The ordinary and extraordinary critical frequencies of the F2 layer -- usually the highest critical frequencies observed.

In general, reliable values are indicated by o's (or x's), and doubtful values by filled circles. The letter C indicates loss of data through breakdown or off-time of the equipment. The above parameters have been identified on the f-plot for August 16 as an example.

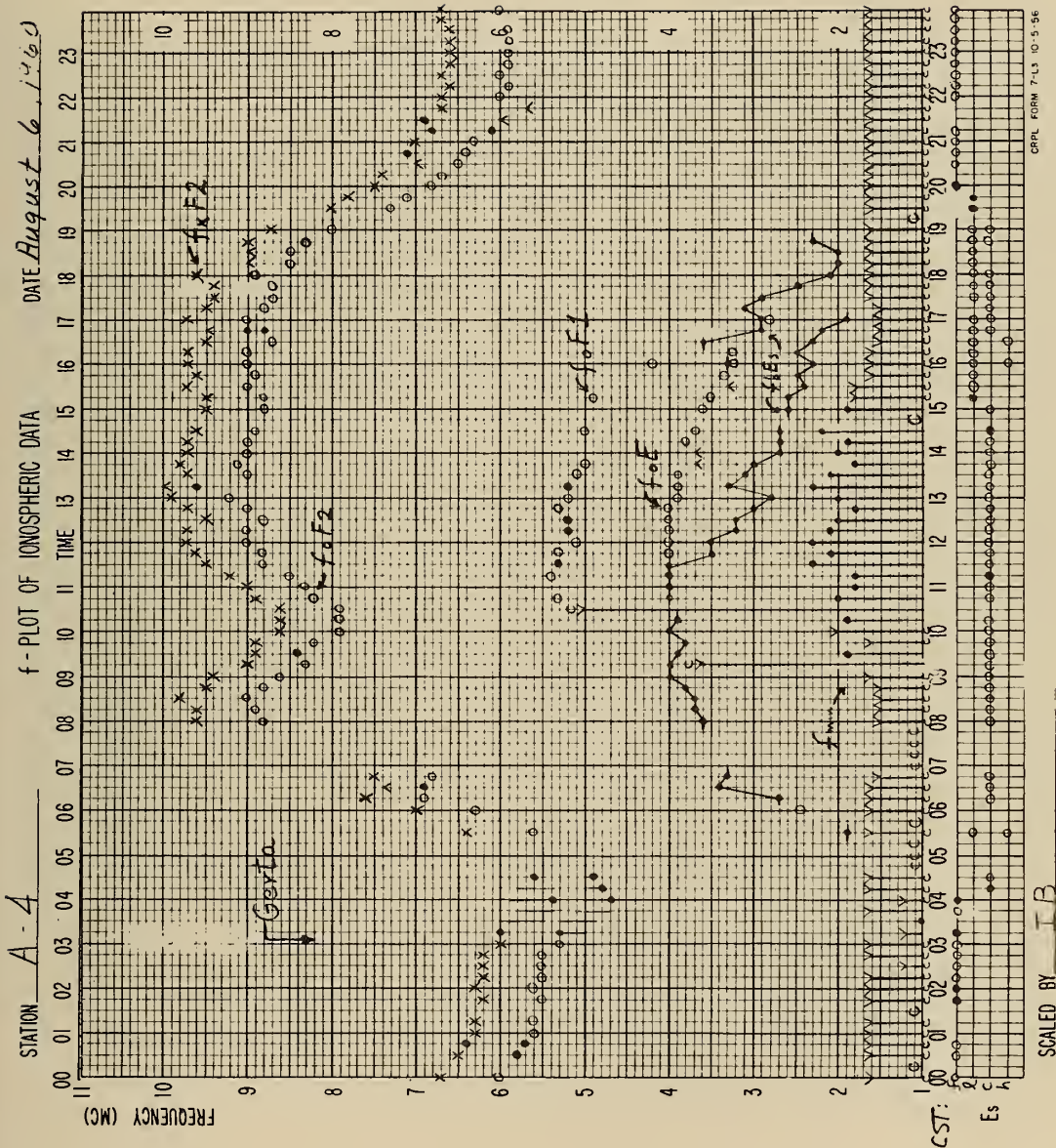


Figure 11: f PLOT FROM A-4 SITE, AUGUST 6, 1960.

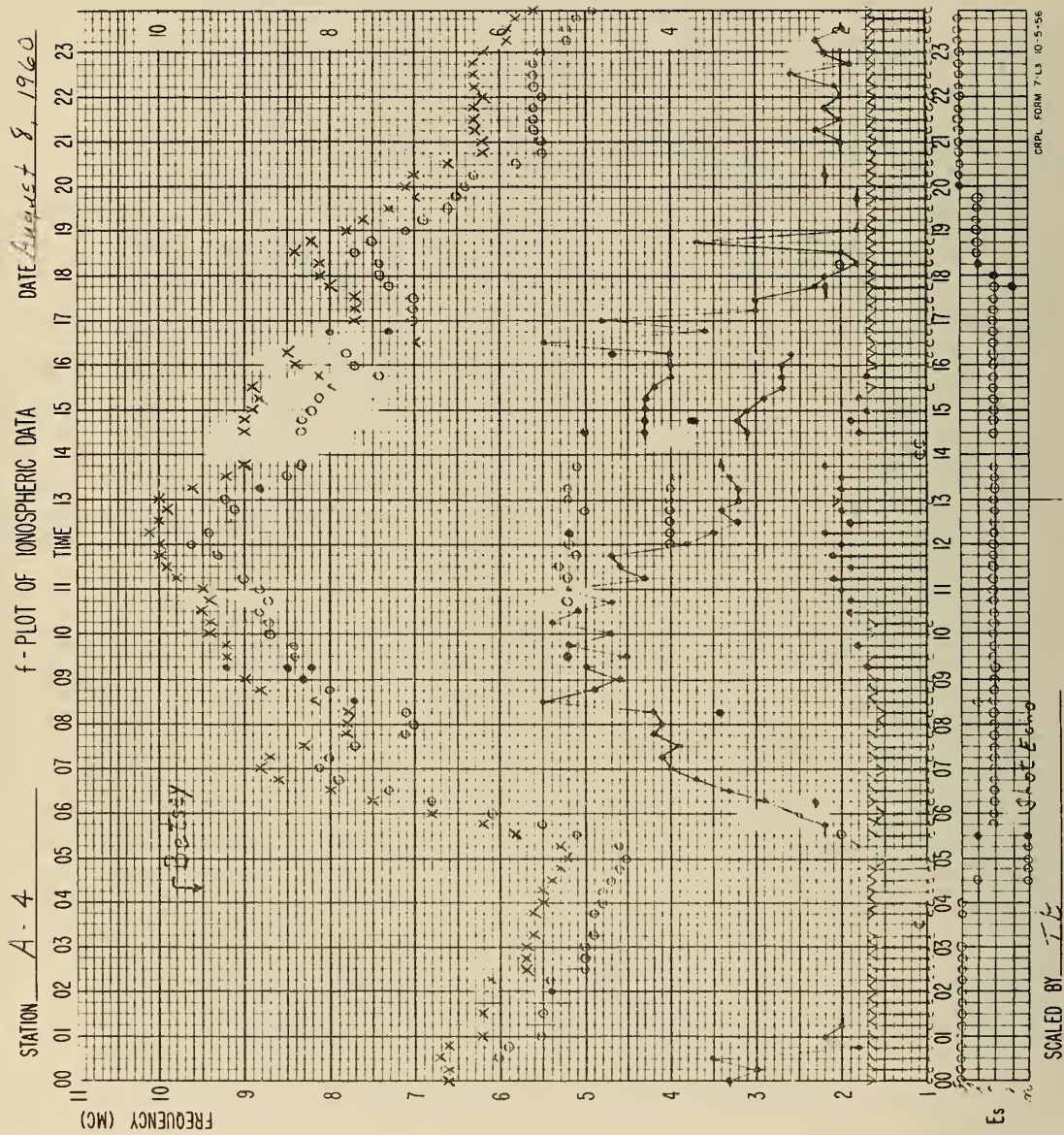


Figure 12: f PLOT FROM A-4 SITE, AUGUST 8, 1960.

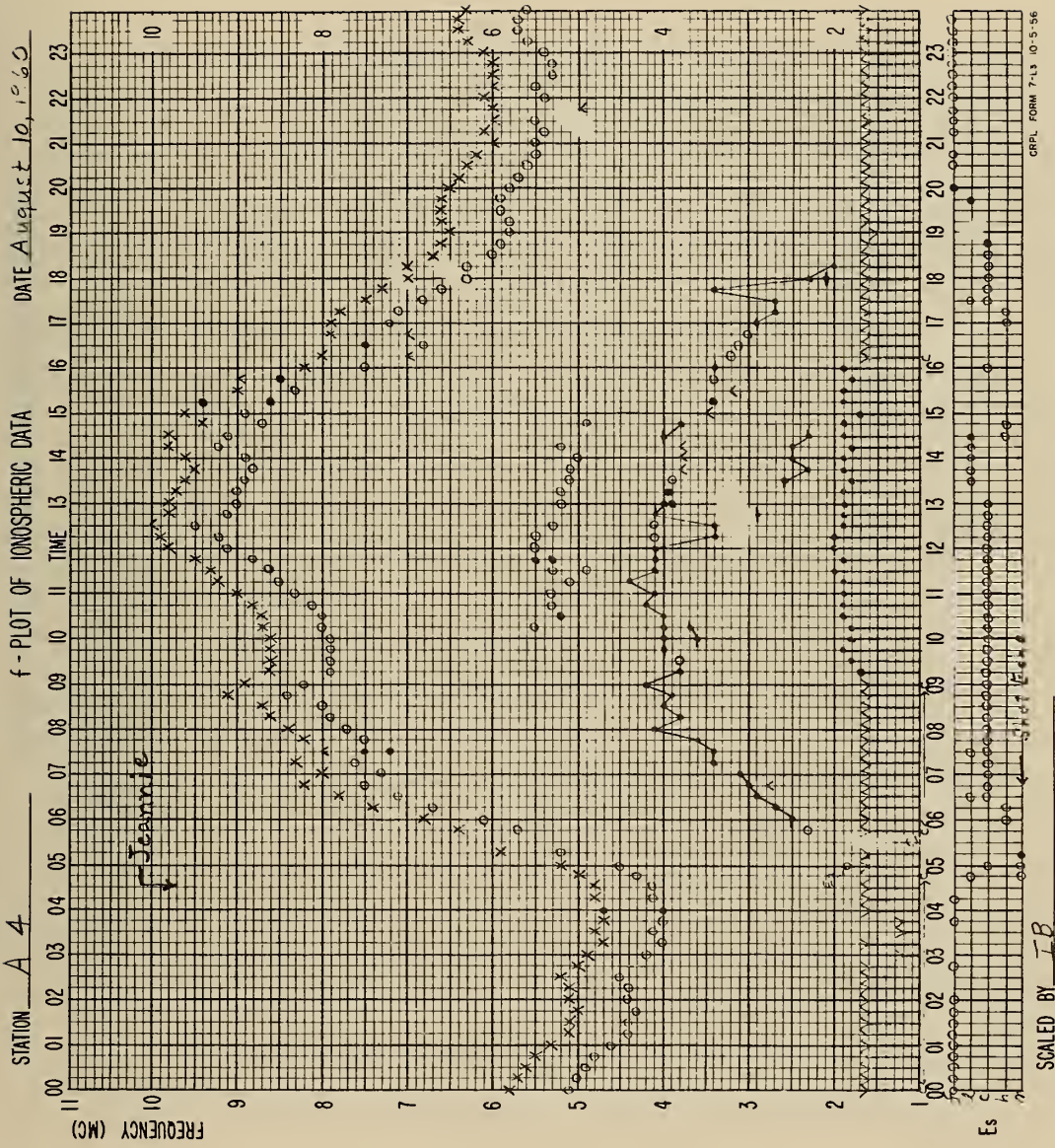


Figure 13: f PLOT FROM A-4 SITE, AUGUST 10, 1960.

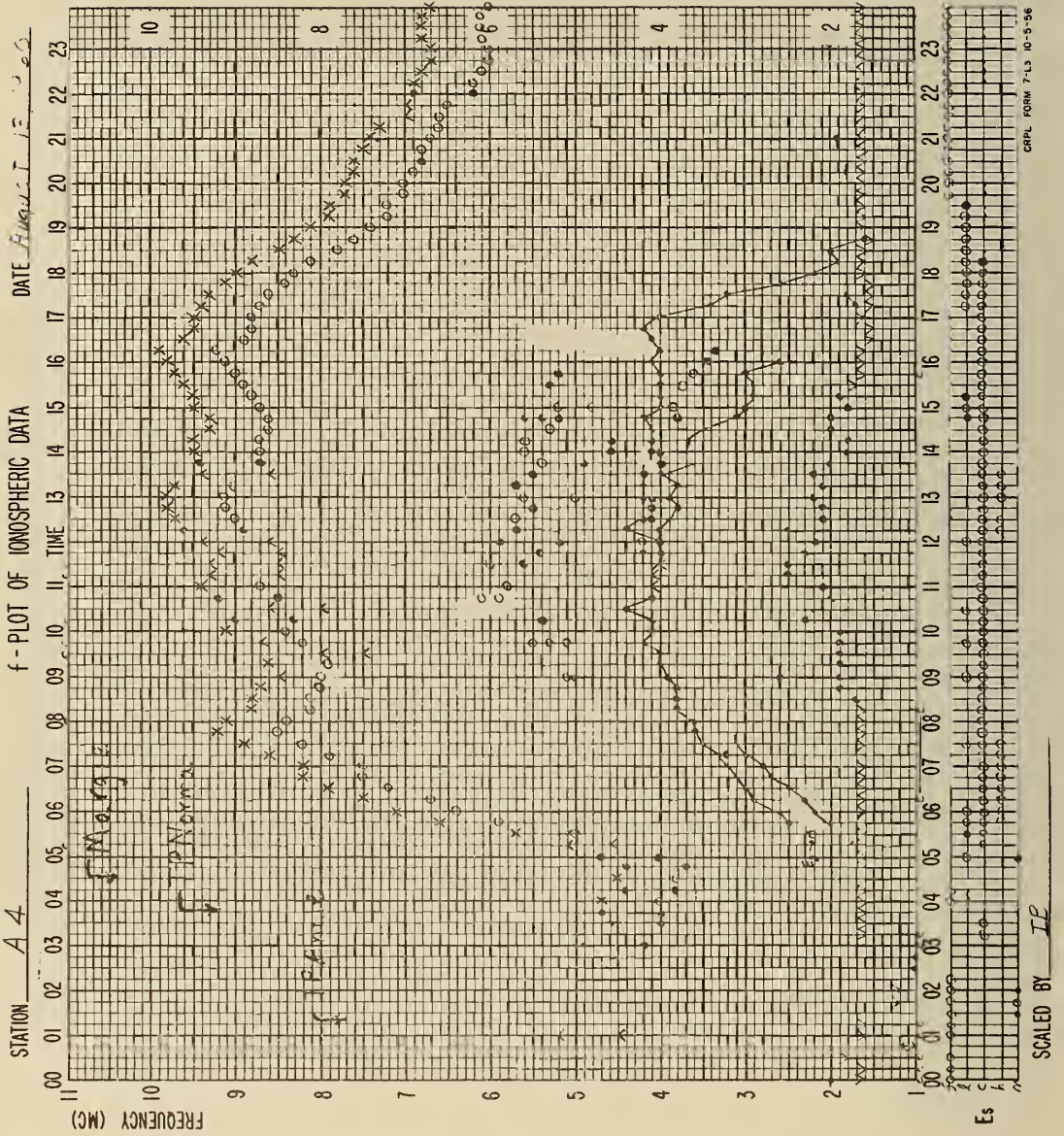


Figure 14: f PLOT FROM A-4 SITE, AUGUST 13, 1960.

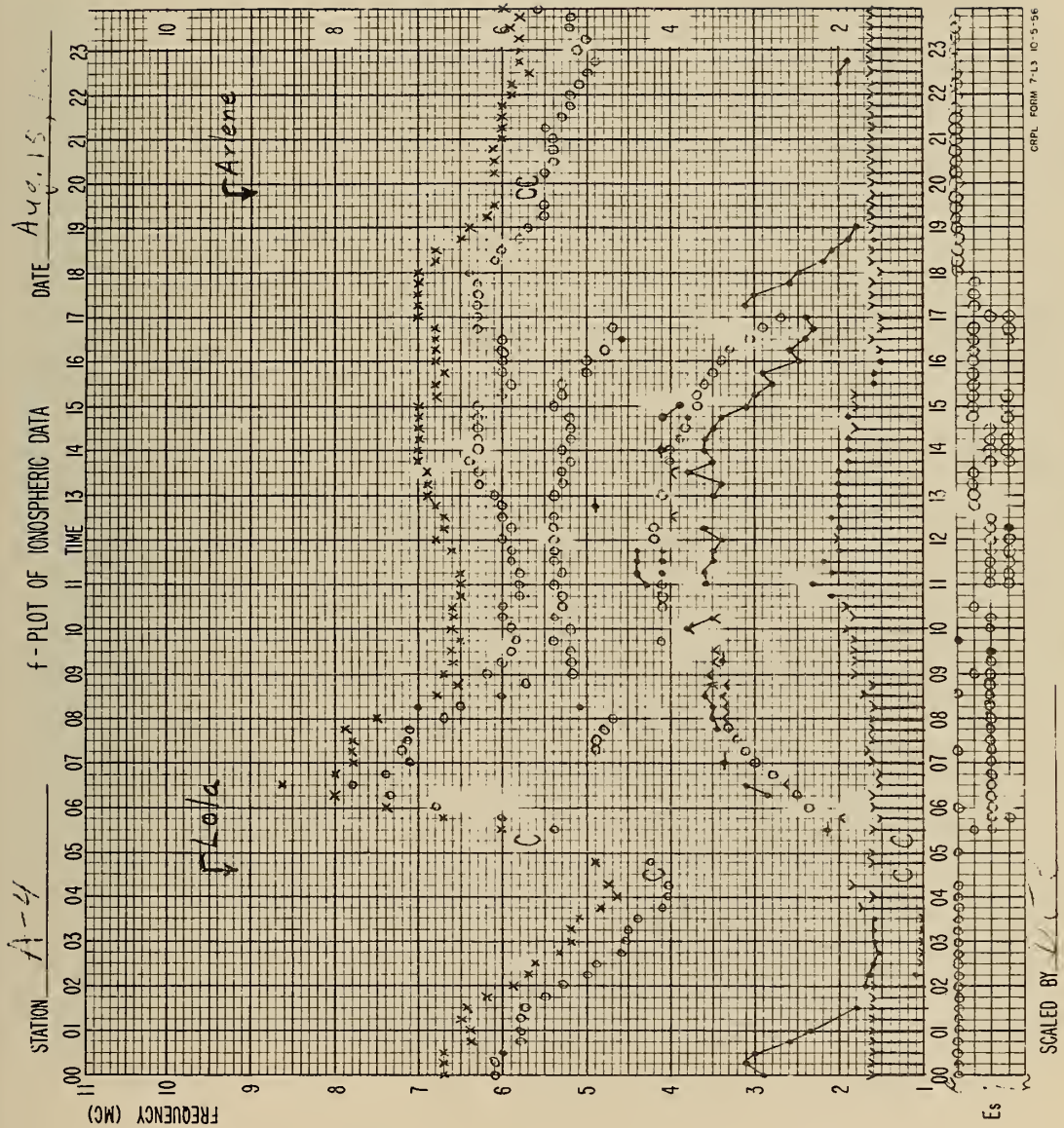


Figure 15: f PLOT FROM A-4 SITE, AUGUST 15, 1960.

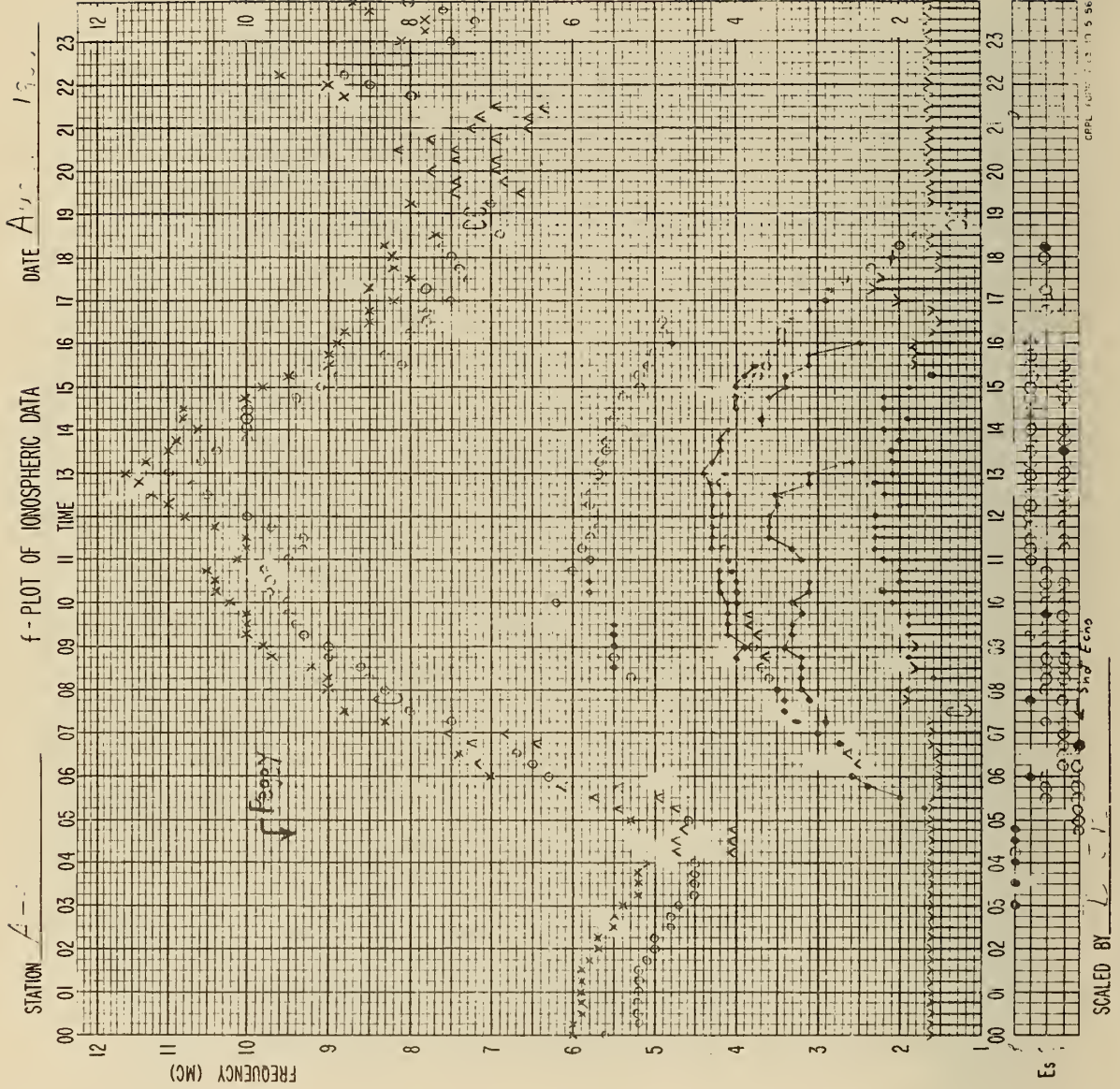


Figure 16: f PLOT FROM A-4 SITE, AUGUST 16, 1960.

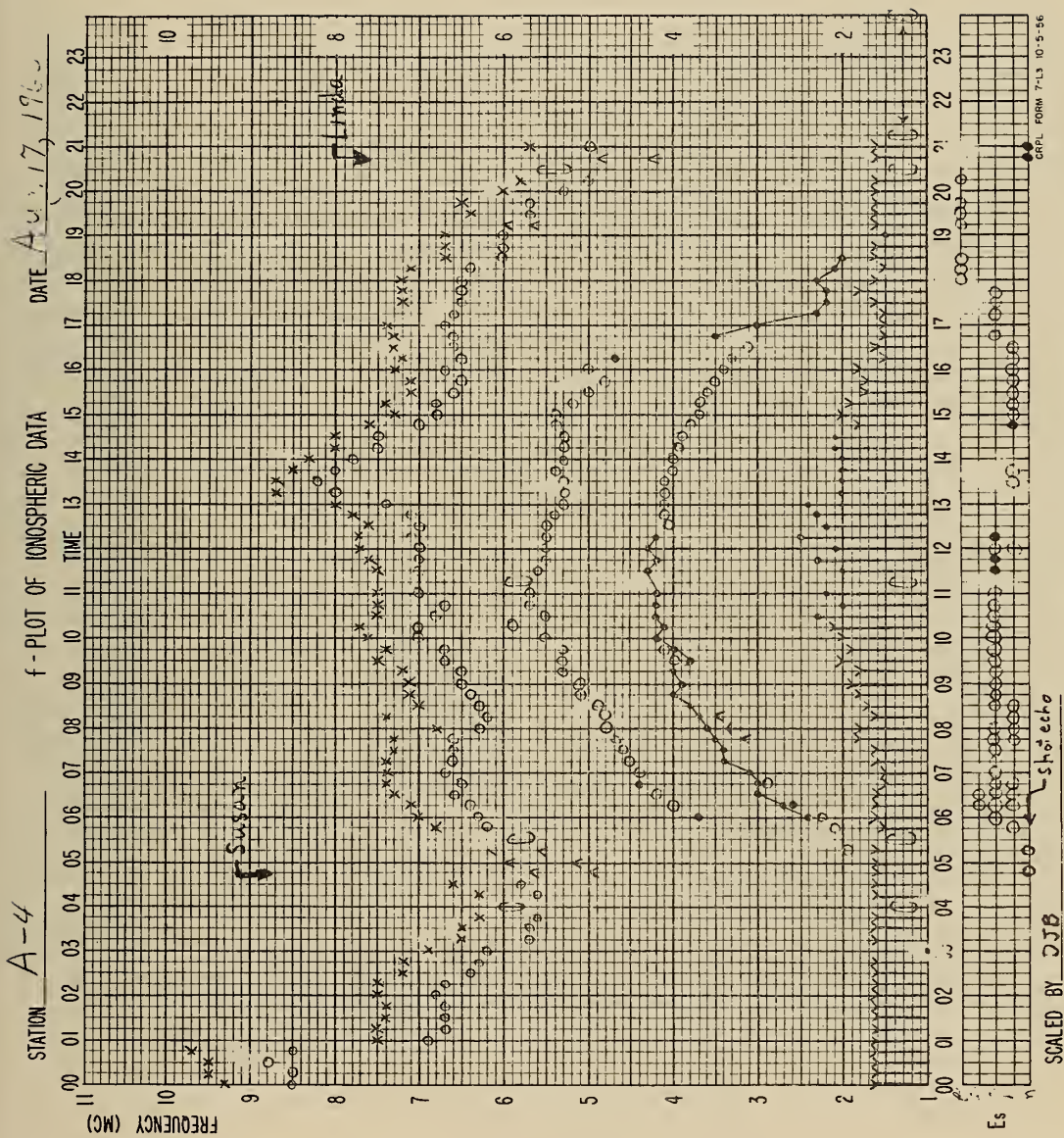


Figure 17: f PLOT FROM A-4 SITE, AUGUST 17, 1960.

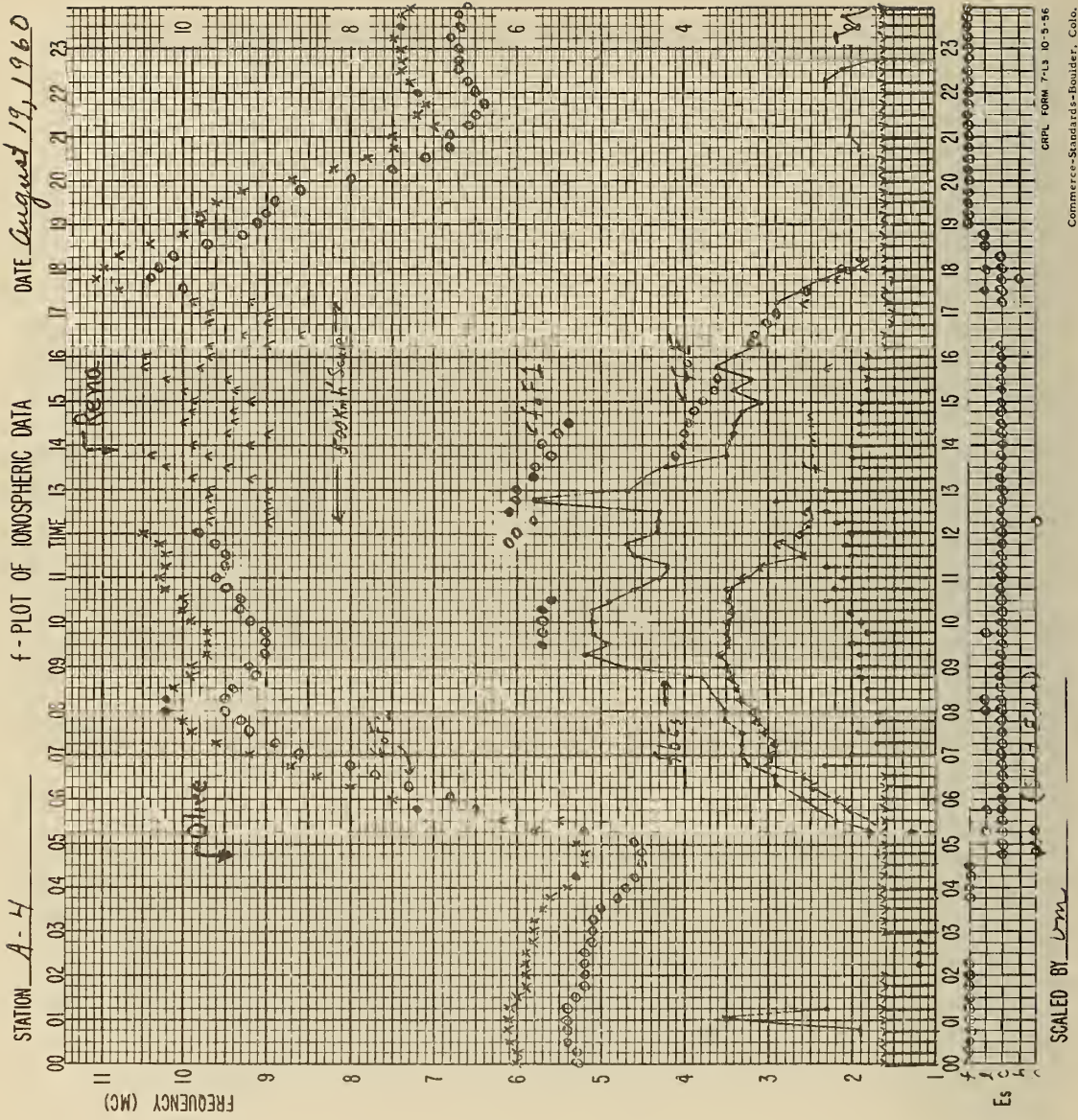


Figure 18: f PLOT FROM A-4 SITE, AUGUST 19, 1960.

III. DETAILS OF INDIVIDUAL EXPERIMENTS, FIREFLY 1960.

Most of the experiments conducted during Firefly 1960 were expected to give effects detectable by the extensive variety of radio techniques assembled. Not all of these would be expected to be observable by ionosondes; for example the highly transient ionization in the high-explosive shots has little chance of detection on ordinary ionograms. The group of experiments aimed at optical study of fine-particle light scattering, and those attempting to isolate rocket exhaust effects were not expected to have radio effects at all.

Nevertheless, the A-4 ionosonde (and, on some occasions, one or more of the other ionosondes) obtained observations during each of the experiments with a view to providing control data should they later prove useful.

The following sections contain a description of the ionospheric observations made during each experiment. In most cases the pertinent A-4 ionograms are shown and discussed. The reader is referred again to Figures 1, 2, 3 at the beginning of the report, which show the critical frequency variations vs. time for each of the electron cloud experiments, and to Table 1 at the beginning of this report for a summary of all ionosonde results.

A. Dawn Electron Clouds

The dawn series consisted of nine cesium payloads released at altitudes between 74 and 115 km. They are discussed below in the order of increasing altitude. Negative or doubtful results were obtained for the two lowest shots, and only Lola (83 km) with a large payload (80 kg) gave positively identifiable echoes at less than 100 km. This same

payload at 74 km (Margie) was probably not detectable at all. At greater heights positive results were obtained, in most cases, from all operating ionosondes.

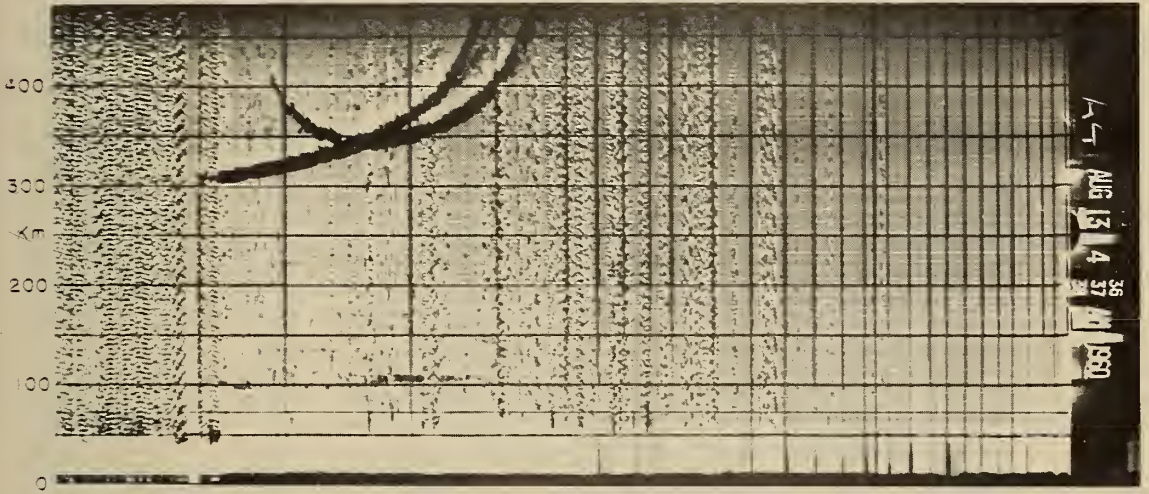
In the following discussions, times are given in seconds, measured from burst. Some indication is given of meteoric observations, when it is felt that this may be of use to other observers.

It should be noted here that Firefly Betsy, launched into the earth's shadow at 108 km, became solar-illuminated after 500 seconds. Its behavior after that time is characteristic of a dawn cloud. The discussion of Betsy is nevertheless included in Section B, with the night clouds.

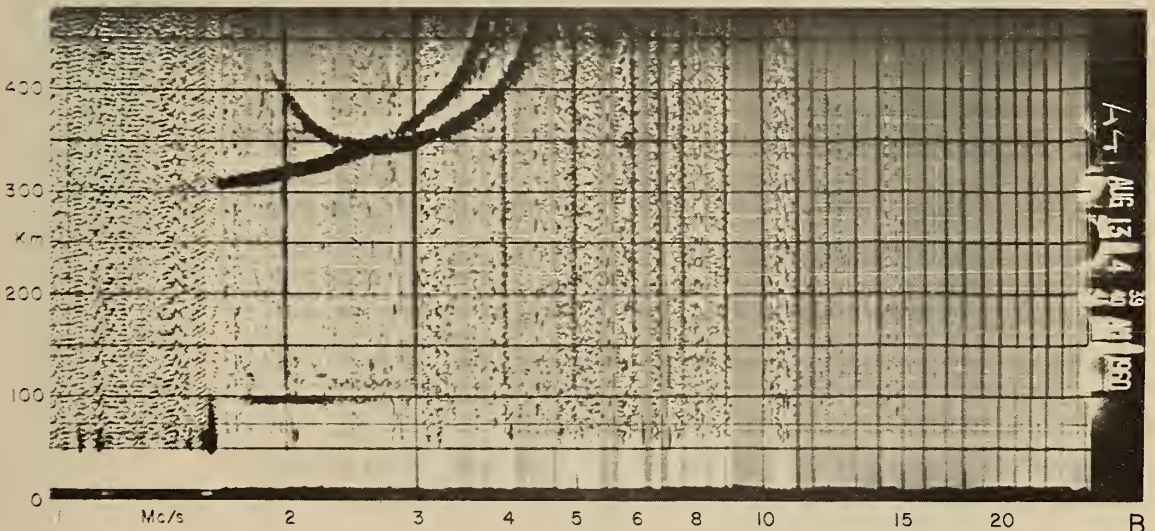
MARGIE

Margie (Burst 0437:00, August 13 at 74 km) was the lowest of the night series of Point Electron clouds. Tyndall was not operating for this experiment; Barin Field, with good observing conditions, saw no echo that could be attributed to the cloud. No sporadic E was observed during the experiment at Barin, Field-1 or A-4, except for a few short-lived echoes which were probably meteors.

The echo at A-4 attributed to the cloud is seen in Figure 19 A, B, at Burst and at B + 180. The observed range is 95 km (vs. 81.4 computed from optical data), possibly suggesting that the cloud was not observed at all. By B + 180, this echo is at 92 km. Just at Burst a meteor is seen (Figure 19 A, at 103 km); considering that Margie was inferior, at best, to this meteor as a producer of ionization, it is rather likely that signal enhancements of more than one second at VHF during Margie, are meteoric.



A



B

Figure 19: FIREFLY MARGIE, AUGUST 13 AT 74 KM: A-4
 IONOGRAMS AT BURST (A, 0437) AND AT B + 180 (B, 0440).

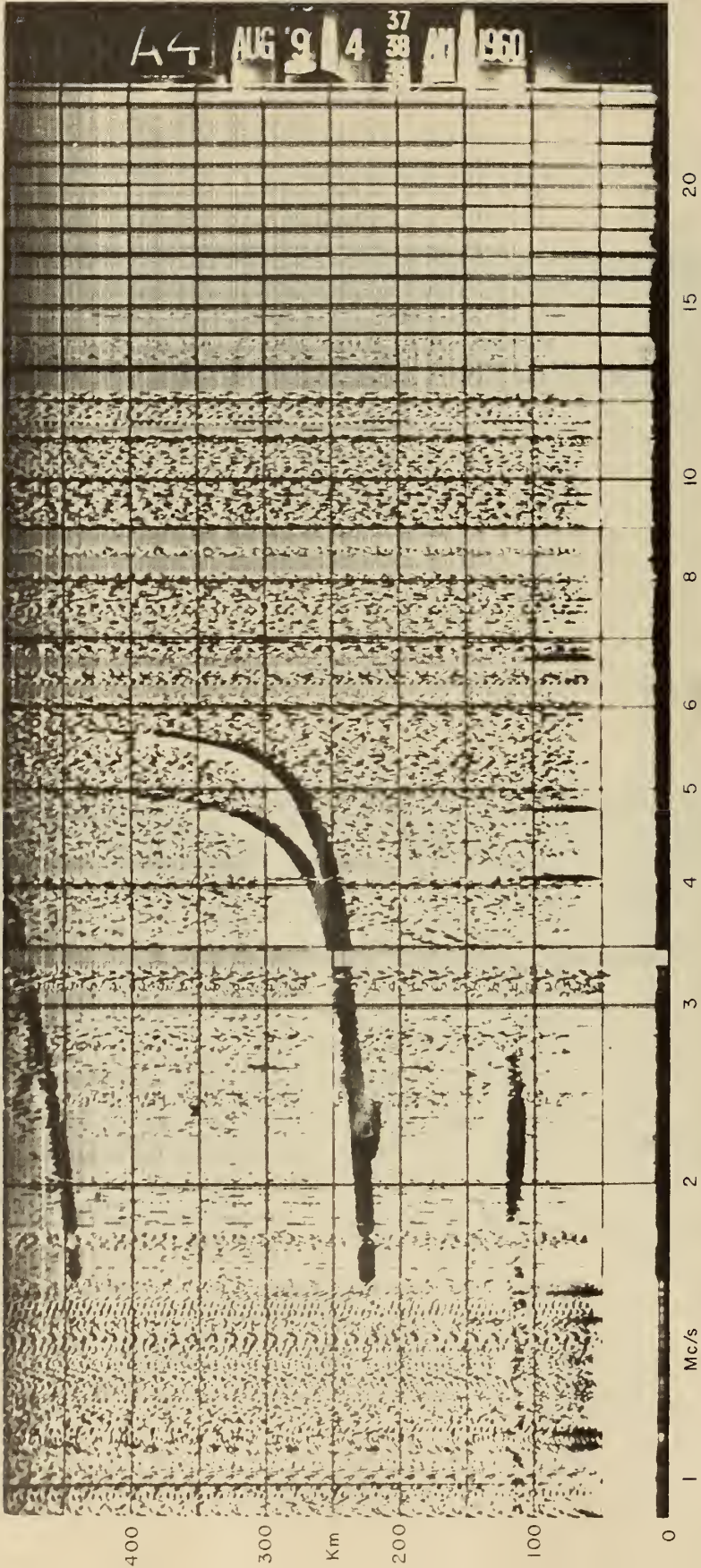


Figure 20: FIREFLY AURORA, AUGUST 9 AT 82 KM: A-4
 IONOGRAM AT BURST (0438).

At burst, Field-1 observed an echo for 90 seconds at a range of 105 km (vs. computed 103).

MARIE

Marie (Burst 0438:26, August 9 at 82 km) was one of two Point Electron cloud experiments launched to the same level, but with greatly different quantities of the same payload: Marie carried 18 kg. while Lola carried 80 kg.

No echoes were observed at any of the stations, which could be ascribed to the burst. (Field-1 was, however, not operating).

The ionogram from A-4 at the time of burst is shown in Figure 20. Sporadic E with a peak density of $3.4 \times 10^4 \text{ cm}^{-3}$ (fxEs = 2.5 mc) is found at a height of 106 km. There is evidence for considerable ambient ionization at lower altitudes (cf Section II C), with an inferred density of about $1.3 \times 10^4 \text{ cm}^{-3}$. At Barin, Es was at 114 km.

Meteor echoes were observed at

B + 23	(124 km slant range)	} same source
B + 75	(125 km)	
B + 100	(158 km and 123 km (new echo))	
B + 280	(131 km);	

these may be useful in eliminating spurious signals on other types of observations.

LOLA

Lola (Burst 0438:00, August 15 at 83 km) was a low-altitude Point Electron Cloud of large payload (80 Kg.). A definite cloud echo was observed at A-4 and at Field 1; the A-4 observations are illustrated at Burst and at B + 30 in Figure 21 A, B. The A-4 ranges agree exactly with those computed from the optical burst position. The Field 1 echo disappeared promptly; the A-4 echo persisted for only 270 seconds. The

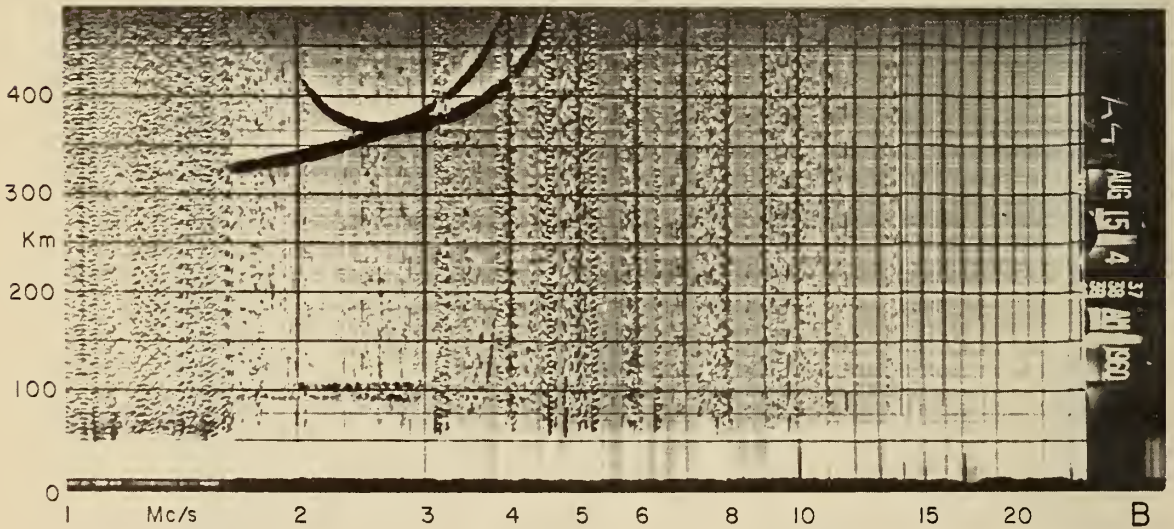
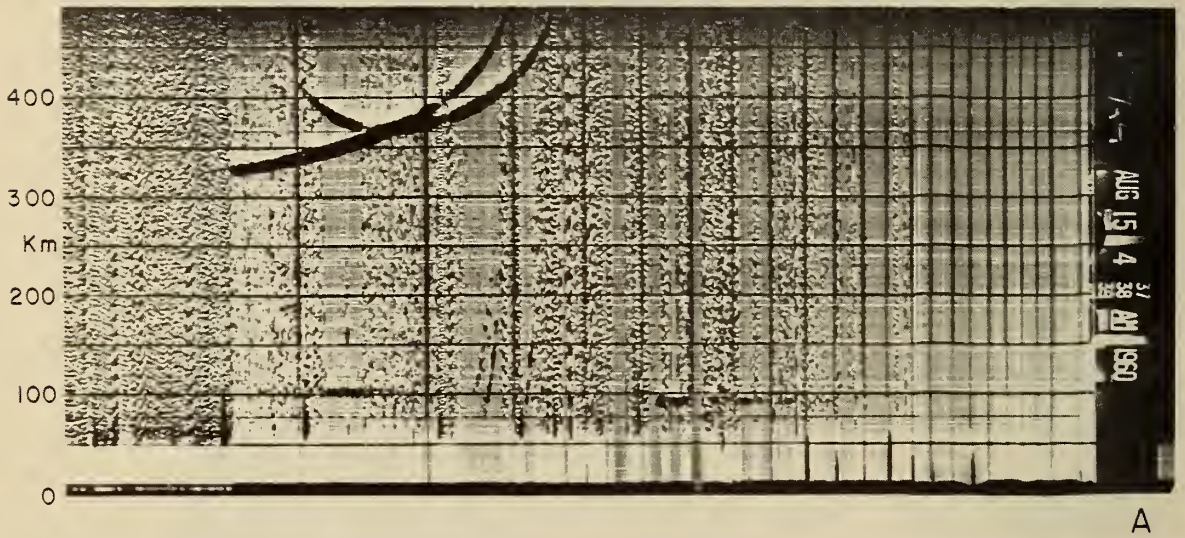


Figure 21: FIREFLY LOIA, AUGUST 15 AT 83 KM: A-4 IONOGRAMS AT BURST (A, 0438:00) AND AT B + 30 (B, 0438:30).

following table gives the variation of critical frequency and slant range during this time:

TIME	STATION	RANGE	"CRITICAL FREQ."
Burst, to + 10	A-4	86 Km	9.6 mc
	Field-1	106	6.0 mc
B + 30	A-4	88	3.6 mc

Ionograms obtained during this experiment show many meteor echoes, some of which are noted in the table below:

STATION	TIME (APPROX)	RANGE	REMARKS
A-4	B + 75	131 Km	
A-4	B + 210	193 Km	
Tyndall	B + 210	200 Km	Predicted range, Lola to Tyndall- 140.5 Km
A-4	B + 270	110 Km	
A-4	B + 300	110 Km	

At A-4, a strong echo began at B + 1110 at 75 km, and lasted until B + 1400 (at 109 km). Similar echoes were simultaneously also seen by Field-1 (112 km) and Barin (108 km). These ranges are consistent with a reflecting cloud at a position approximately 30.68°N , 86.95°W , assumed at the same height as Lola's observed cloud. Although there is every likelihood that this is an Es patch entirely separate from the artificial electron cloud, it seems worthwhile to record the possibility that this may be a second view of the cloud. If so, it implies a drift speed of 29.7 m/s heading 265° .

ZELDA

Zelda (Burst 0830:40, August 25 at 102 km) was a medium large payload (49.5 kg) release into the daytime E region. The A-4 ionograms at B - 60, Burst and B + 810 are shown in Figure 22 A, B, C. A strong echo was observed at A-4 at burst (at 102 km) definitely at a shorter slant range than predicted (105 km). There was strong, blanketing Es overhead before and during the experiment, at an altitude of 104.5 km.

At Field-1, this Es was also seen at 104 km; at Tyndall it was at 107 km. At Barin Field, the Es was at 104 km, but the quality of the records does not permit reliable analysis.

In any case, it appears that a strong Es layer existed just above the cloud, and that by B + 720 the cloud had risen to the point of being obscured by this Es -- at least from the point of view of A-4 and Field-1.

In this early period, when the cloud is seen by only A-4 and Barin, an ambiguity of radio position and drift exists consisting of two possible paths on either side of the line between these two stations. Both of these are shown on the map of Figure 23. The predicted burst position is also shown, and does not agree well with the observed radio ranges at B + 210, assuming the predicted burst height to be approximately correct. During the first 720 seconds, the data give a drift speed of 61 m/s heading either 119° or 310° .

At B + 1140 an echo was observed at Tyndall at 109 km slant range which rapidly moved overhead to 100 km, between B + 1740 and B + 2700. It is shown in Figure 22 D at B + 1290. Previous to this, there had been an Es layer at about 107 km, as has already been noted. The ionogram of Figure 22 D gives evidence of the superposition (in range) of

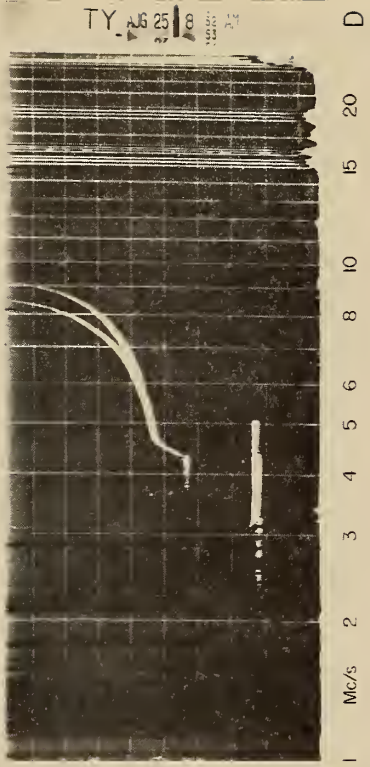
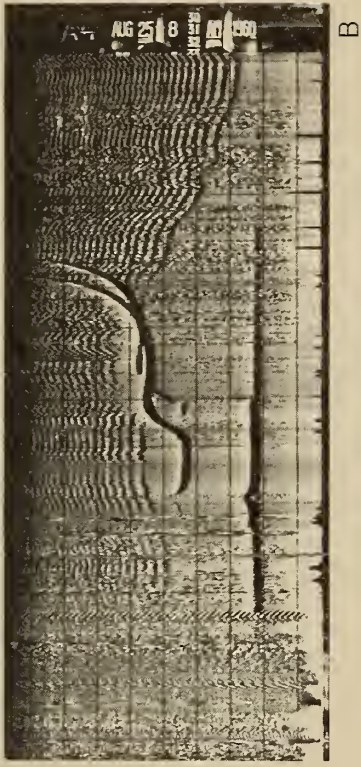
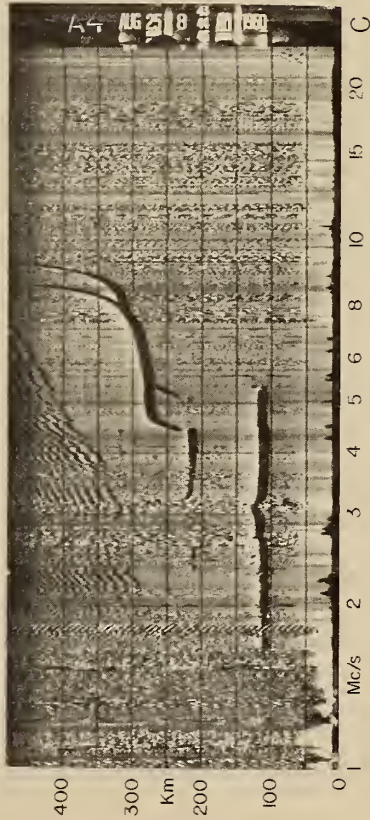
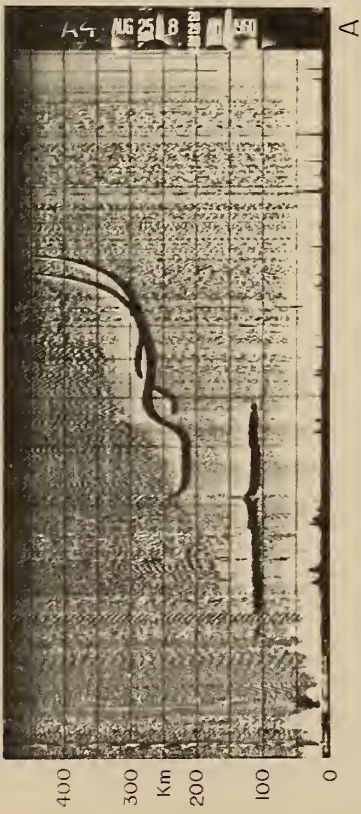


Figure 22: FIREFLY ZELDA, AUGUST 25 AT 102 KM: A-4
 IONOGRAMS AT B - 60 (A, 0829), AT BURST (B, 0831) AND
 AT B + 810 (C, 0844). TYNDALL IONOGRAM AT B + 1290
 (D, 0852).

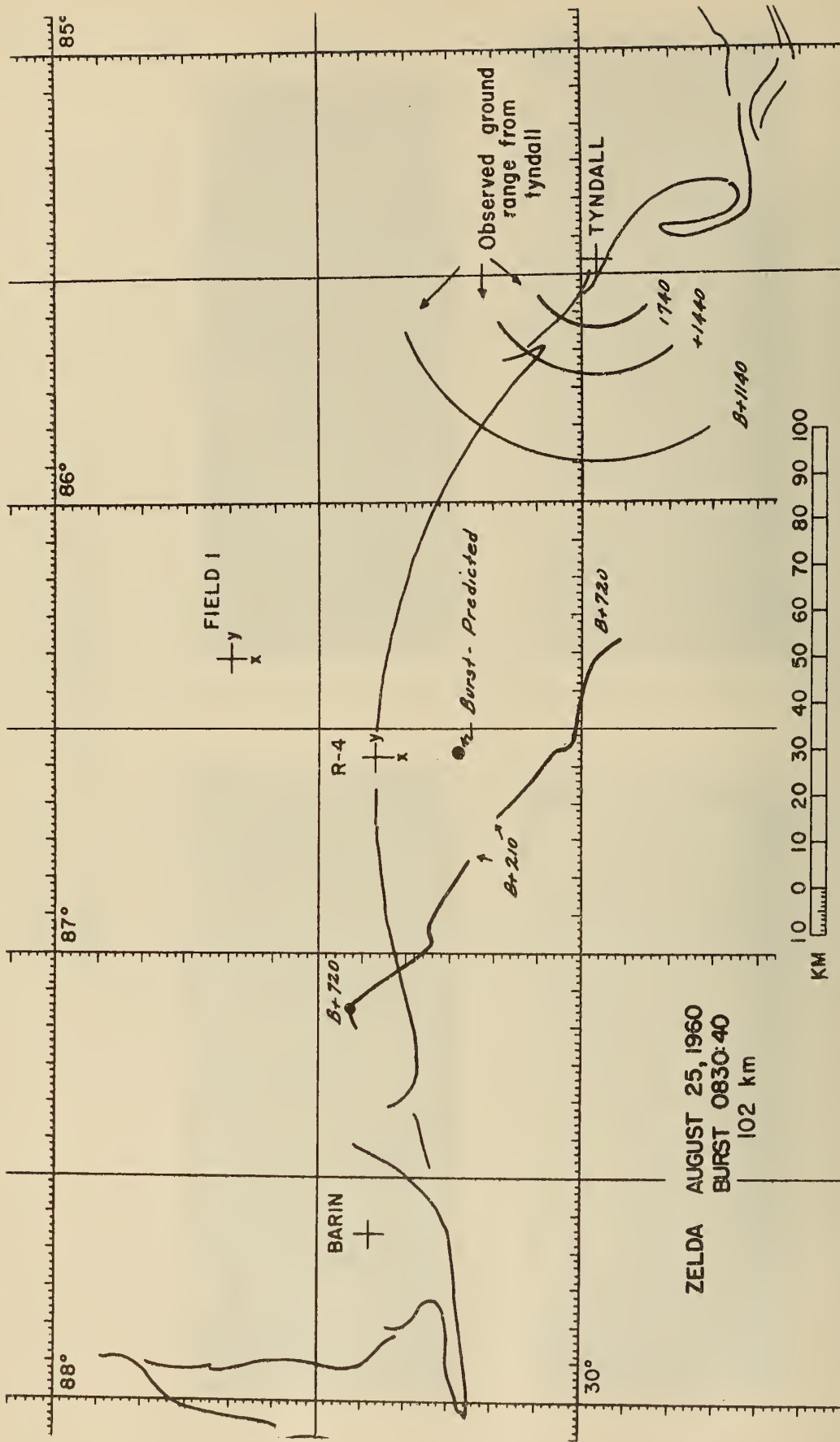


Figure 23: FIREFLY ZELDA LOCUS DEDUCED FROM IONOSONDE DATA.

these echoes by the faintly rhythmic oscillation of the Es echo -- the result of beats between the two nearly superposed echoes as the frequency is varied. This echo was present at Tyndall until the station abandoned observations at B + 4500.

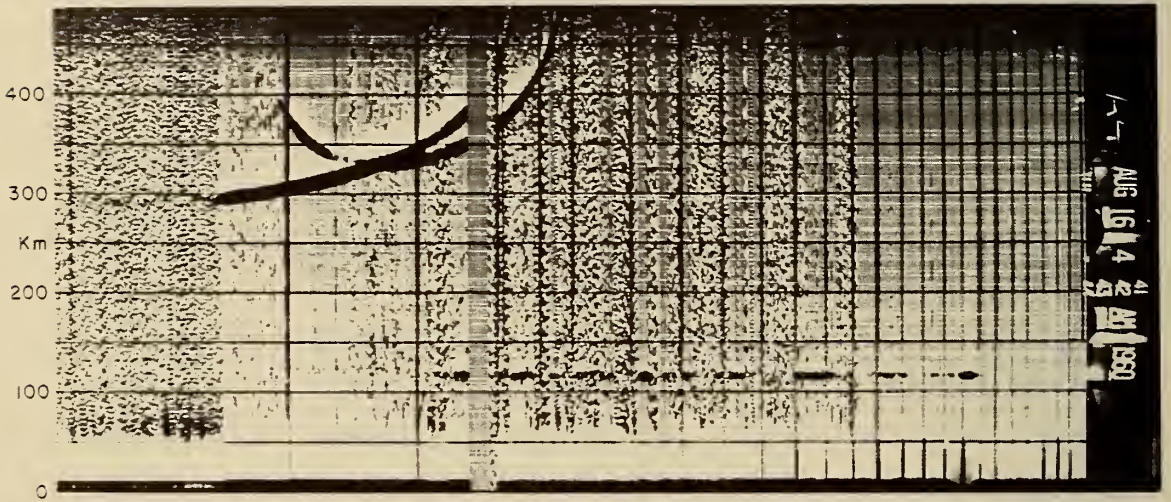
We may conclude from the above that the heading 119° is more probable for the cloud drift; this gives an average drift speed over the entire period (to B + 1740) of 59 m/s, in fairly good agreement with the value deduced above for the first 720 seconds.

At Barin Field, there is also a sudden appearance of a reflecting layer at 107 km slant range. This is, however, inconsistent with either heading and position and hence is probably sporadic E.

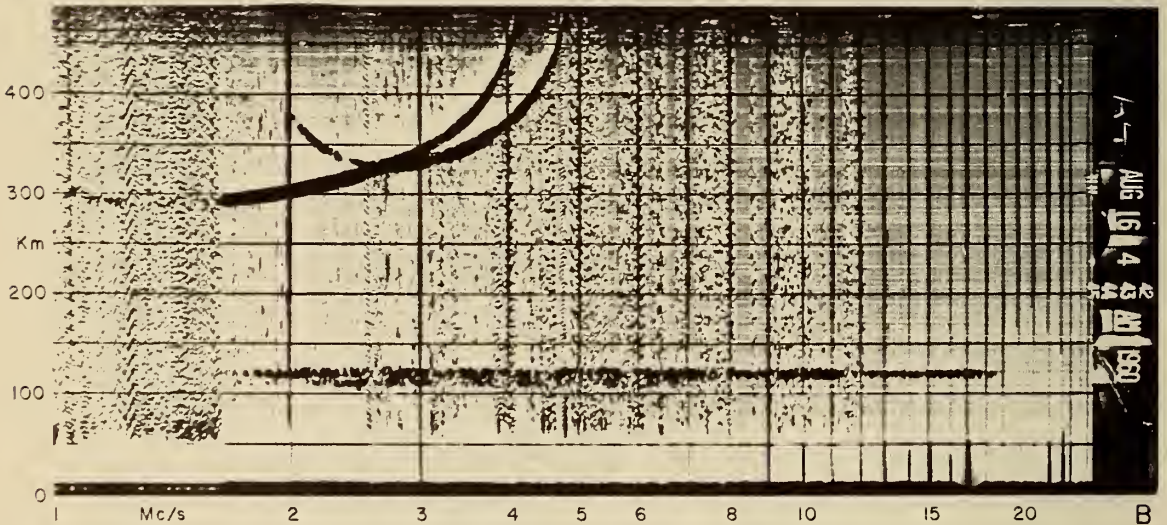
We conclude with caution that Zelda persisted for at least 4500 seconds and shortly afterwards, dispersed to the point of undetectability at our radio frequencies at a point near Tyndall. It drifted to this position with a mean speed 59 m/s, mean heading 109° .

PEGGY

Peggy (Burst 0441:50, August 16 at 103 km) was apparently one of the longest-lived clouds of the present series. Echoes were seen promptly at burst by all stations except Barin, where the echo first appeared at B + 360. Figure 24 illustrates the appearance of the echo at A-4 at Burst and B + 60. From burst through B + 360, the cloud position and movement as given by the ionosonde data are consistent with the available optical results. From B + 360 through B + 7050 seconds we deduce the curved path shown on the map of Figure 25. The total eastward displacement, ignoring irregular motions, corresponds to a drift speed of only 16.6 m/s heading 274° . It is possible that this represents mostly growth of the cloud rather than actual movement, considering its optical dimensions at B + 360. Thus the cloud appeared to be nearly overhead at A-4 at B + 840 and B + 330, at Barin Field at B + 4560, and nearly overhead at Tyndall



A



B

Figure 24: FIREFLY PEGGY, AUGUST 16 AT 103 KM: A-4
 IONOGRAMS AT BURST (A, 0442) AND AT B + 60 (B, 0443).

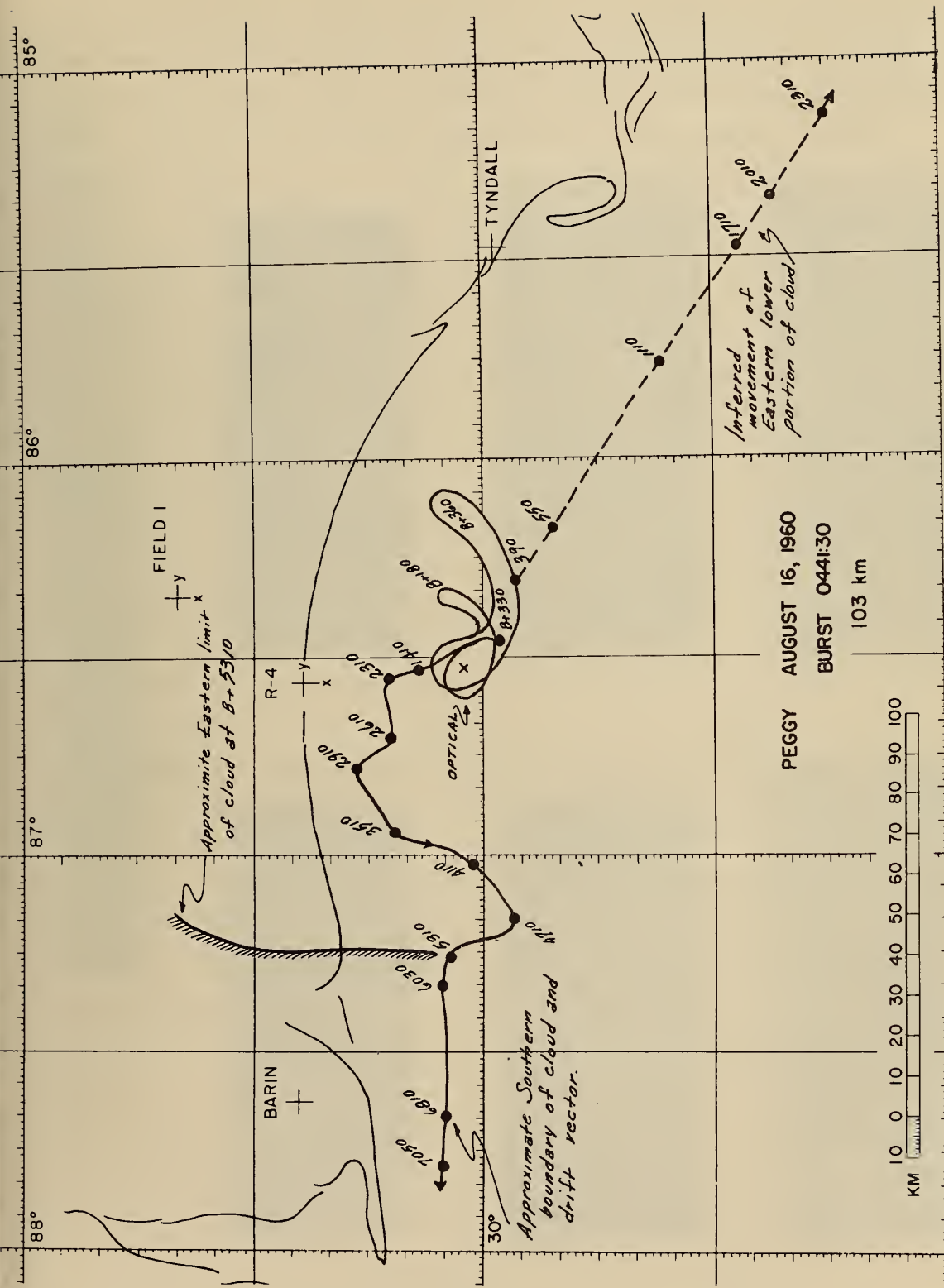


Figure 25: FIREFLY PEGGY LOCUS DEDUCED FROM IONOSONDE DATA, ALSO SHOWING OPTICAL DATA AT B + 1.80 AND B + 3.60 SECONDS.

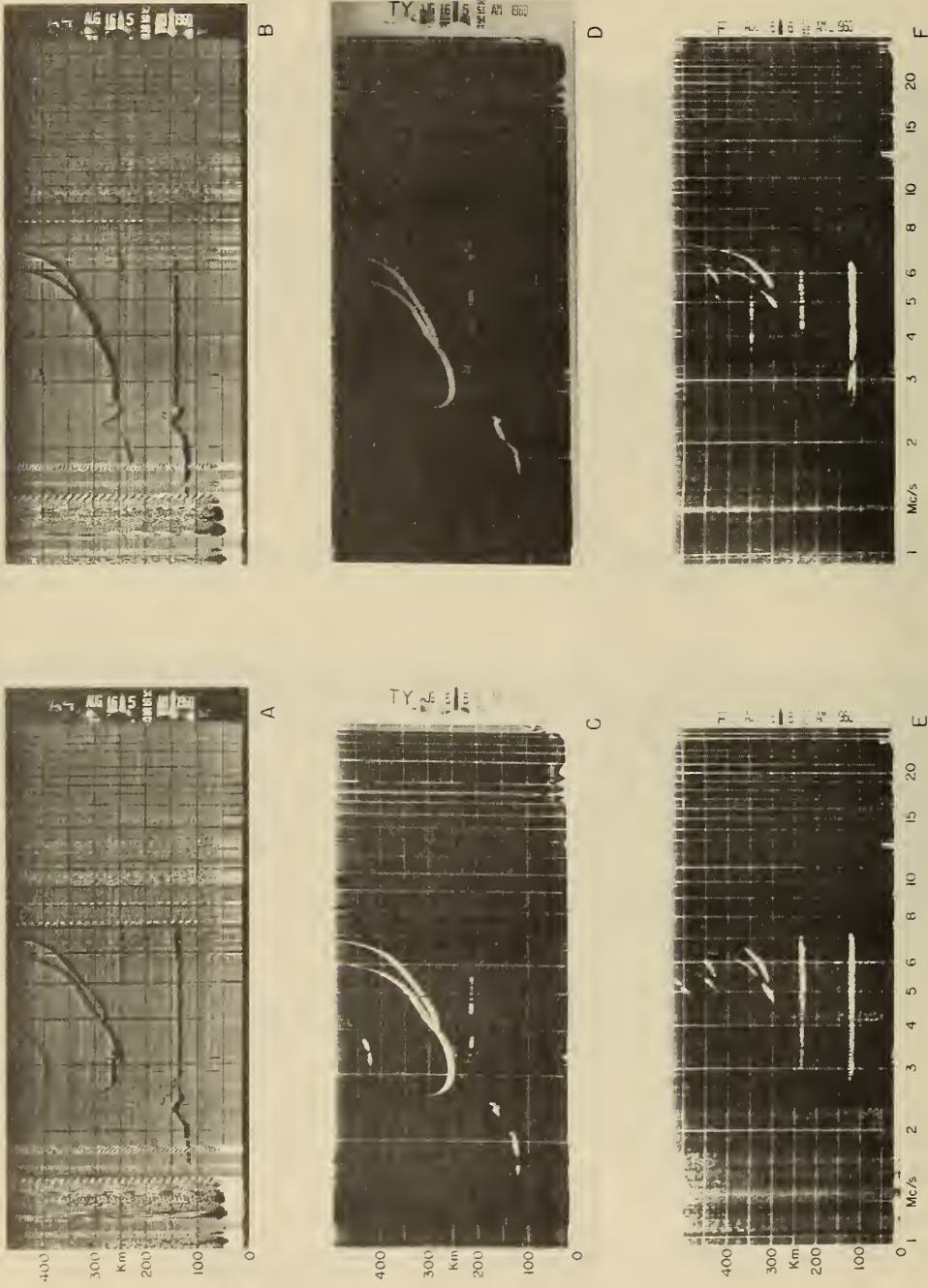


Figure 26: FIREFLY PEGGY, AUGUST 16 AT 103 KM:
 APPEARANCE OF ELECTRON CLOUD IN DAYTIME E LAYER AFTER
 ABOUT B + 4000 AT A-4 (A, 0555; B, 0558), TINDALL
 (C, 0551; D, 0553) AND AT BARIN (E, 0621; F, 0629).

at B + 1110. This appearance at (or near) Tyndall deserves further comment: optically, the cloud was observed to produce an eastward moving tail (at B + 360), yet our radio data show rather conclusively that a major part of it later moved to the west, with the above-mentioned speed of 16.6 m/s. Now the optical results show this "head" of the cloud to be between 105 and 109 km altitude, while the tail, distended towards Tyndall is at altitudes between 97-98 km, and perhaps lower. The appearance of a nearly-overhead cloud at Tyndall at B + 1110 suggests that this lower tail continued its movement eastward at a mean speed of 82 m/s (heading 124°) while the higher portions of the cloud were transported to the west. Our deductions about the eastern portion of the cloud are based only upon Tyndall data, and are very tentative regarding speed and direction. Nevertheless our deduced speed of 82 m/s is not in bad agreement with the value of 116 m/s which may be obtained from the optical data for the first 360 seconds.

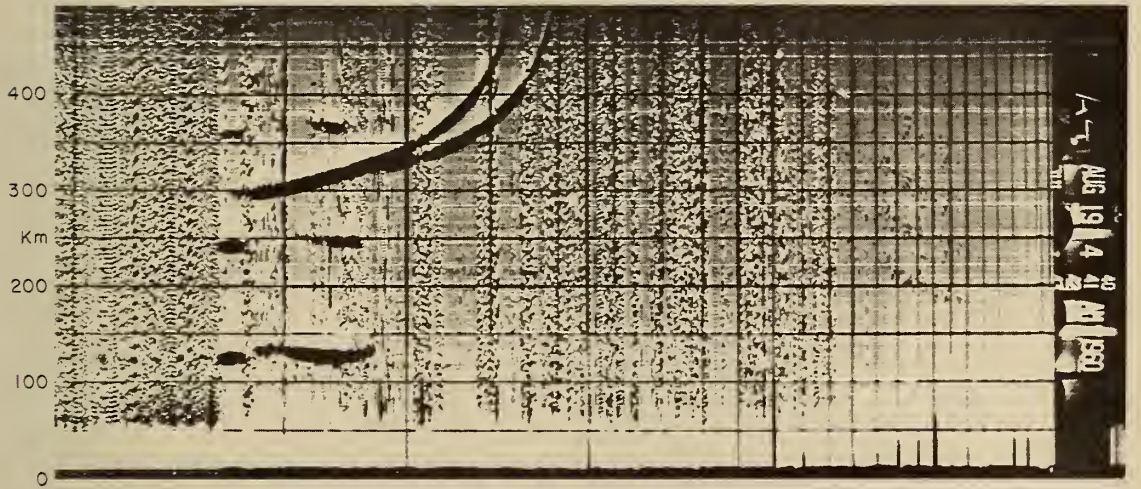
Following the development of the normal E layer after sunrise, remarkable effects were observed at all stations (except Field 1, where the ionograms are too poor for study). Figures 26 A-F, illustrate the appearance of the cloud echo after about B + 4000 at A-4, Tyndall, and at Barin, when the normal E layer critical frequency was about 2.5 mc. Note that the cloud echo is strongly retarded near foE at Tyndall and Barin, but not at A-4. From the multiple echo, it appears to be overhead at Barin. From the observed ranges to A-4 and Tyndall, we deduce an eastern limit to the cloud at B + 5310, as shown on the map of Figure 25. We would speculate that the cloud became embedded in the E layer at an altitude favorable to the formation of the so-called "cusp" type sporadic E; that the favorable conditions abundance of ionizable material, combined with unusually low drift speeds, resulted in an ionized cloud of unusually long life.

It was still observable at Barin at 0707 CST (B + 8670) when the station unfortunately ceased observations.

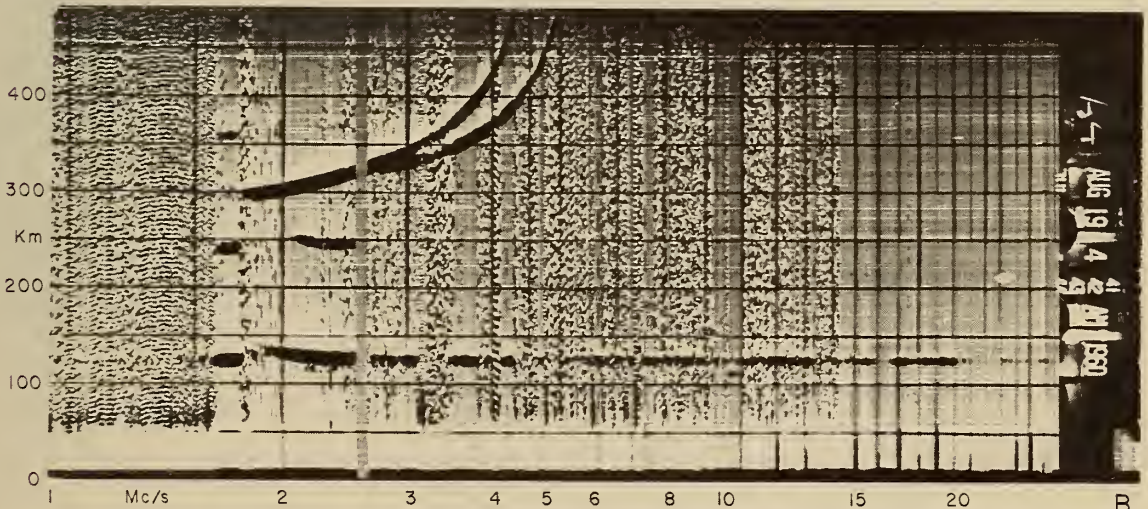
OLIVE

Olive (Burst 0441:50, August 19, 1960 at 106 km) was observed promptly at burst by A-4, Barin Field, and Tyndall; Field-1 was not operating during this experiment. Figures 27 A, B, show the A-4 ionograms obtained just prior to, and at Burst, respectively. There was evidently an E layer of critical frequency 1.1 mc, with "blanketing" (i.e., totally reflecting) sporadic E of foEs = 1.8 Mc embedded in it at 120 km. This is a comparatively large amount of ionization in the lower ionosphere for this time of the morning.

In this case, the configuration Barin Field - A-4 - cloud - Tyndall gave a nearly ambiguous and highly erratic cloud motion, when an attempt was made to solve simultaneously for cloud height and movement using these three stations' data. Much more satisfactory results were obtained by assuming the cloud height, and then using the stations in pairs to obtain its movement. The map of Figure 28 shows the trajectories deduced in this manner from the A-4 - Tyndall, A-4 - Barin, and Tyndall - Barin combinations assuming a cloud altitude of 106 km. Also shown on the map is the optical cloud configuration at B + 60, B + 300, and B + 420 records. Excellent agreement with the optical data is obtained over this period. It is evident, for example, that the A-4 - Barin data are consistent with reflections from the "head" of the loop until B + 420 seconds, whereupon the main reflection shifted to the western tail of the loop. In this transition, a split echo was observed at A-4, the two reflections agreeing excellently with these parts of the cloud. It would appear that as the main body of the cloud moved east (heading 108° with a deduced mean speed of 43 m/s) the western tail remained fixed, and perhaps actually moved southwestward. The



A



B

Figure 27: FIREFLY OLIVE, AUGUST 19 AT 106 KM: A-4
 IONOGRAMS PRIOR TO BURST (A, 0441:00) AND AT BURST
 (B, 0441:50).

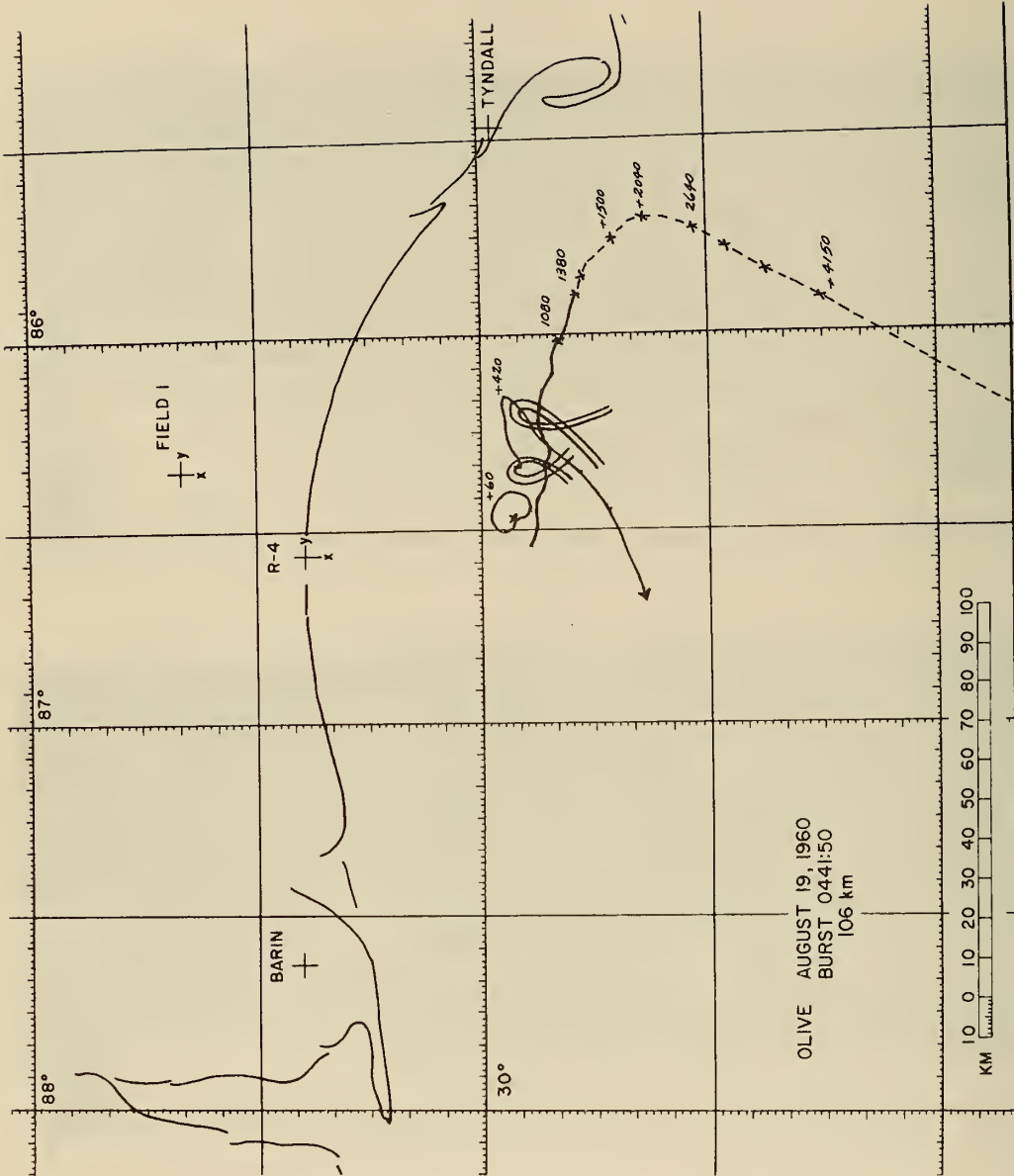


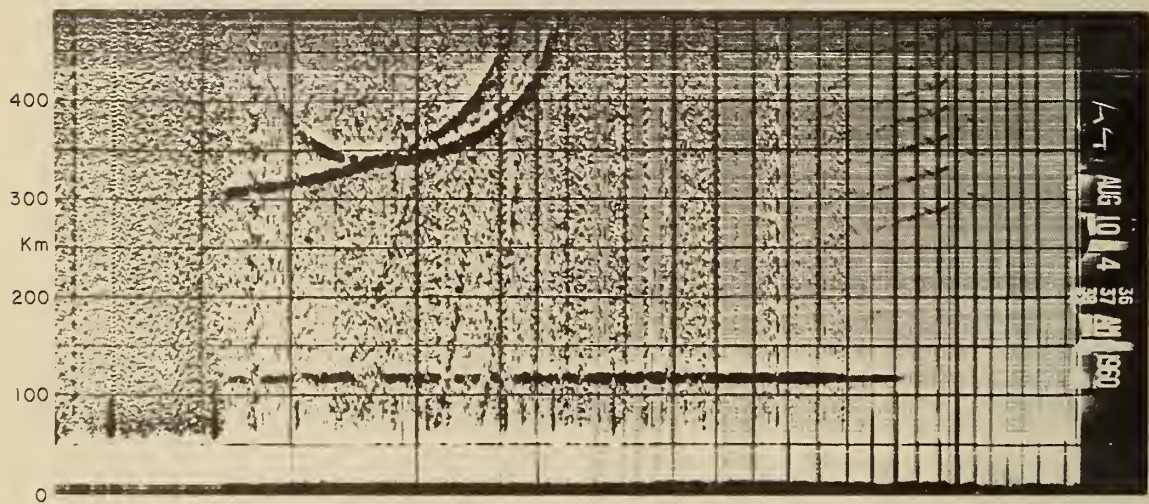
Figure 28: FIREFLY OLIVE LOCUS DEDUCED FROM IONOSONDE DATA, ALSO SHOWING OPTICAL DATA AT B + 60, B + 300 AND B + 420 SECONDS.

optical data show it at a somewhat higher altitude (110 km) than the eastern part of the cloud (103 km). At B + 2040, the A-4 - Tyndall data seem definitely to indicate that the cloud (or the main reflecting portion of it) turned approximately 90° , and moved in a direction parallel with the earlier western tail of the cloud. Shortly after this (B + 2640), A-4 ceased to receive echoes from the cloud; Tyndall, however, observed it continuously until B + 4680 (0600 CST), at a slant range of 198 km. Assuming no further change of direction, the cloud motion is shown on the map. This motion is appropriate to a speed of 54 m/s (between B + 2640 and B + 4680) heading 210° .

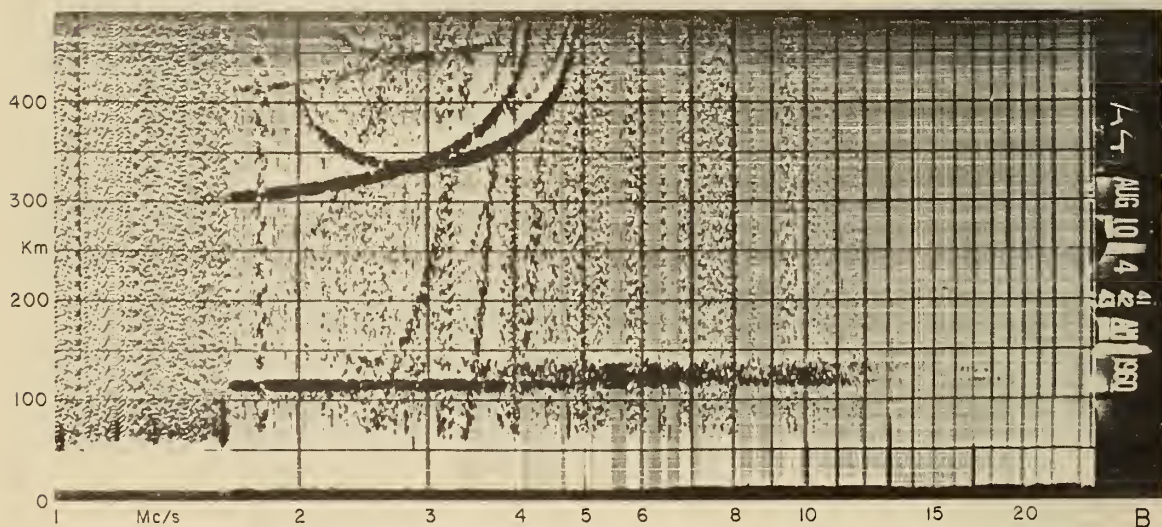
JEANNIE

Jeannie (Burst 0436:41, August 10 at 109 km) was observed promptly at burst at all four stations. Position deductions are, however, handicapped by poor data from Field-1, and from the fact that at B + 360 a very strong sporadic E layer appeared at A-4. This is illustrated in Figure 29, showing (A) the cloud echo at B + 15 with no sporadic E and (B) the cloud echo at 110-125 km with the sporadic E (below 4 mc) at 109 km. At B + 1380, when both Es and cloud echoes had disappeared, a new Es layer occurred, lasting for only a few minutes.

Burst position and height data from the four stations agree fairly well out to B + 120. We conclude that the cloud moved almost due south (heading 177°) at a speed of 96 m/s, through B + 780 as shown in Figure 30. Only crude evidence is given from our data regarding cloud growth, but characteristic dimensions of 20 and 40 km at B + 480 and B + 780 are suggested.



A



B

Figure 29: FIREFLY JEANNIE, AUGUST 10 AT 109 KM: A-4
 IONOGRAMS AT B + 15 (A, 0437) AND AT B + 315 (B, 0442).

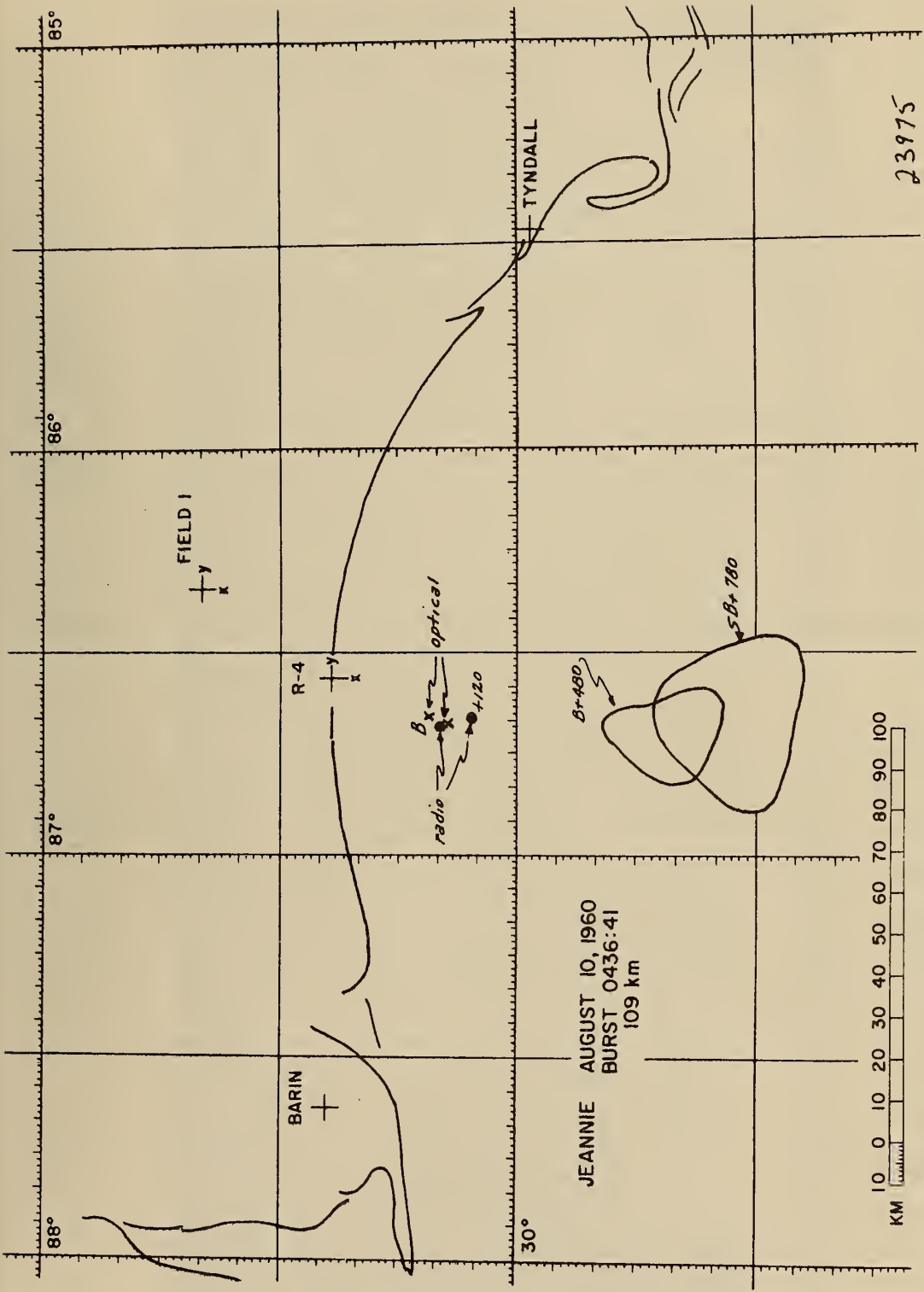


Figure 30: FIREFLY JEANNIE LOCUS DEDUCED FROM IONOSONDE DATA.

SUSAN

Susan (Burst 0443:50, August 17 at 114 km) has the most rapid, consistent movement, observed over the greatest distance, with the best early position agreement (with optical data) of all the experiments in this series. Echoes appeared promptly at burst at all stations; at Field-1 and Tyndall, they persisted, with systematic increase in range, for almost equal times -- to about B + 500. At A-4, a weakly ionized Es layer (estimated $N_{max} = 1.2 \times 10^4 \text{ cm}^{-3}$) was observed before and after burst at an altitude of 119 km. Only its extraordinary component shows on the ionogram of Figure 31, at about 2.0 Mc. The slight retardation of this Es at lower frequencies is evidence for a considerable quantity of ionization at still lower heights (i.e., below 119 km). It is thus likely that Susan was launched into an already well ionized medium.

At Barin Field, the cloud echo disappeared within 30 seconds of burst, then re-appeared at B + 180 with two components approximately 10 km apart. A-4 also showed a "split" echo from B + 600 to B + 900. This latter echo was observed first at higher radio frequencies (> 12 mc) and was the dominant echo out to B + 1380, when the cloud was finally lost. From B + 1380 the locus of the cloud shown on the map of Figure 32 was computed assuming constant cloud height of 118 km. The average drift speed -- remarkably constant within sub-intervals of the locus -- was 145 m/s, heading 230° . There is some evidence for sunrise effects on Susan similar to those discussed under Peggy, Dolly and Betsy, but the effects develop too near the last appearance of the cloud, and too far away for thorough observation. It is interesting to note that Susan was launched during a period of severe magnetic disturbance. The evidence from the ionogram of Figure 31 and the estimates discussed in Section II C of nighttime E region ionization, have already been mentioned. It seems probable that the very large drift speed noted

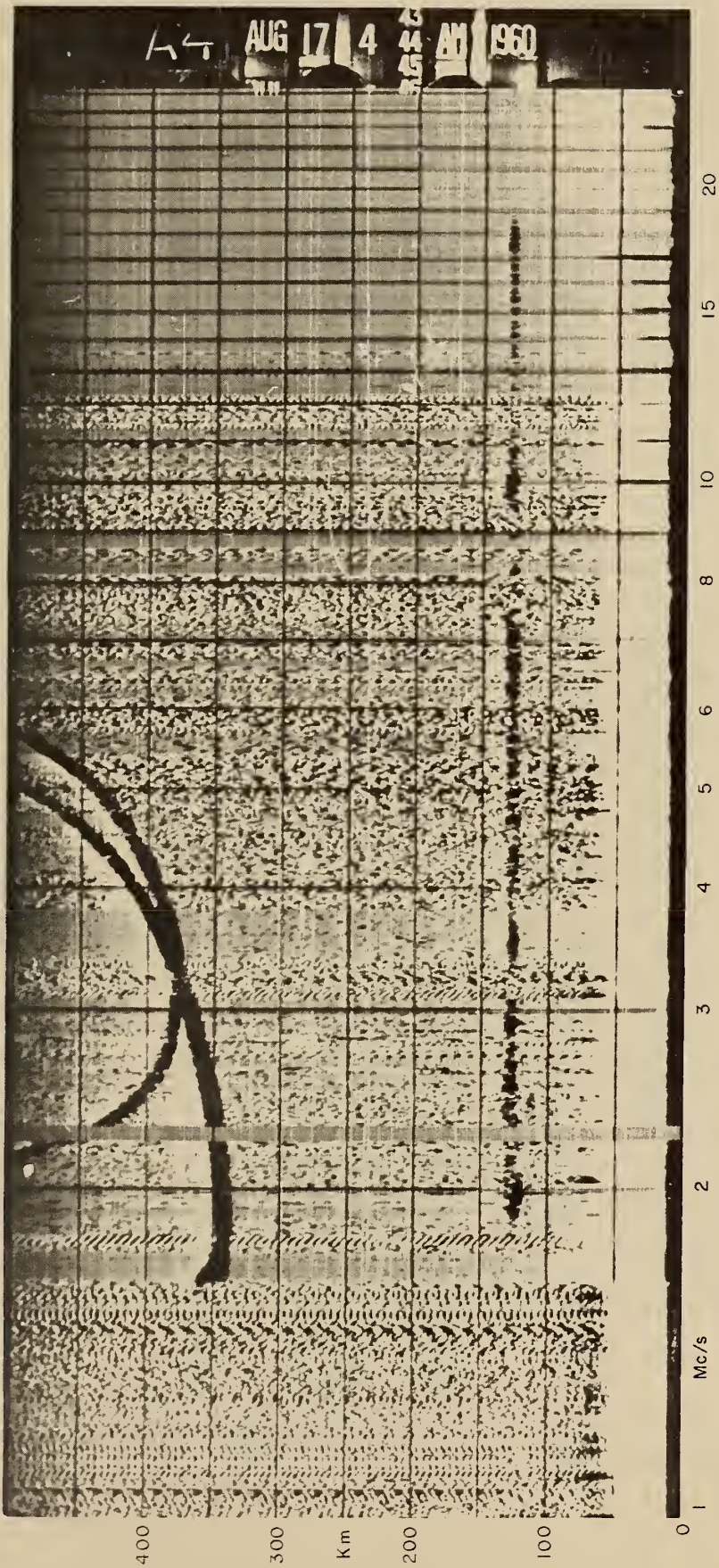


Figure 31: FIREFLY SUSAN, AUGUST 17 AT 114 KM: A-4
 IONOGRAM AT BURST (0444).

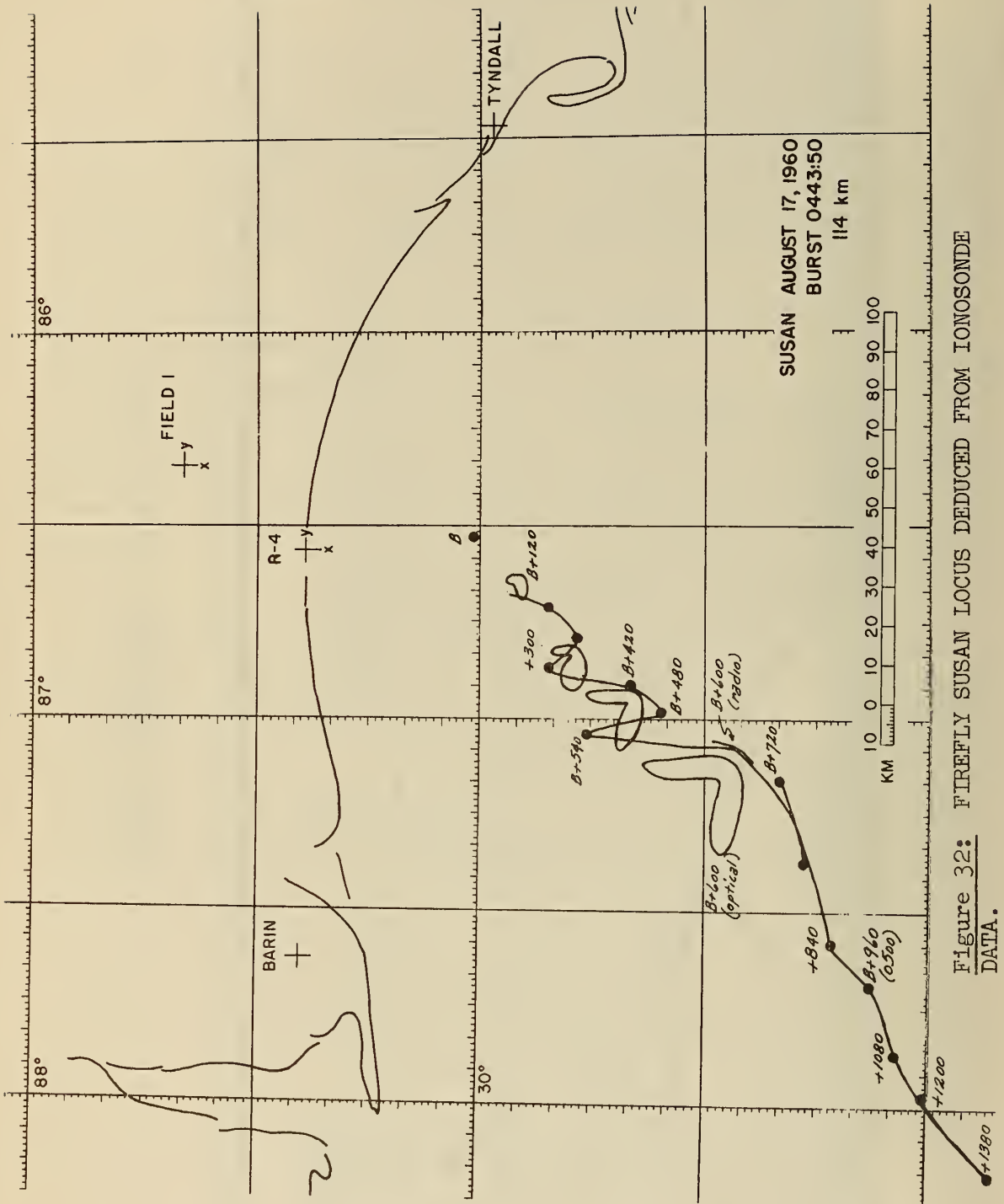


Figure 32: FIREFLY SUSAN LOCUS DEDUCED FROM IONOSONDE DATA.

in this case is genuine and is the result of the magnetic storm; E region drifts are known to increase during the larger magnetic disturbances.

However, it should be noted that Susan was the one electron cloud of the 1960 series using the same composition as used in 1959. In view of the geomagnetic and low-density ionization data referred to above, it is not clear that proper comparison can be made between Susan and the 1959 results.

DOLLY

Dolly (Burst 0421:46, July 27, 1960, at 115 km) was the highest dawn release of the 1960 series. Echoes were seen at burst at all stations. Figure 33 A, B shows the ionograms at A-4 at B + 1560. For the first 660 sec, good agreement is obtained with the available optical data regarding position and drift (see Figure 34). A consistent drift pattern is followed by the cloud until B + 2400, giving a mean drift for this period of 45 m/s heading 332° .

It is clear from the first 600 seconds of optical data, that the cloud grows to considerable dimensions. This is confirmed in the ionosonde data in two ways, both of which will require more study: the echoes are frequently observed to "split," components of the echo separated as much as 50 km in range being not uncommon; and, using data from three stations at a time, it is quite difficult to obtain time-consistent changes in position. It is possible that the cloud attains a size exceeding the distance between our stations (typically 100 km) and that our reflections came from changing portions of the cloud as time proceeds.

This happens in a dramatic way at about B + 2400: a new echo appears at all stations at higher frequencies and greater ranges.

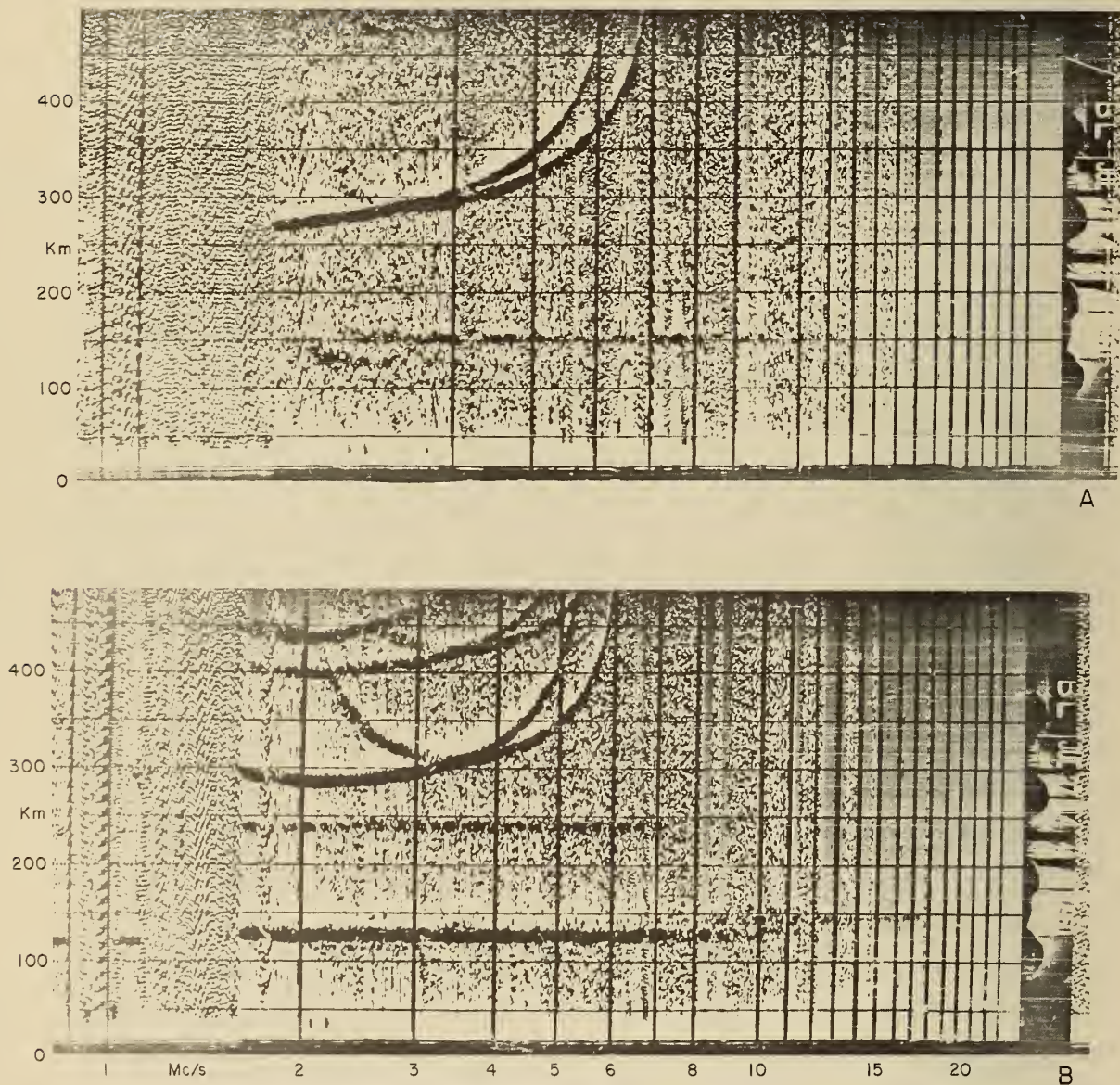


Figure 33: FIREFLY DOLLY, JULY 27 AT 115 KM: A-4
 IONOGRAMS AT B + 15 (A, 0421:45) AND AT B + 1560
 (B, 0448:30).

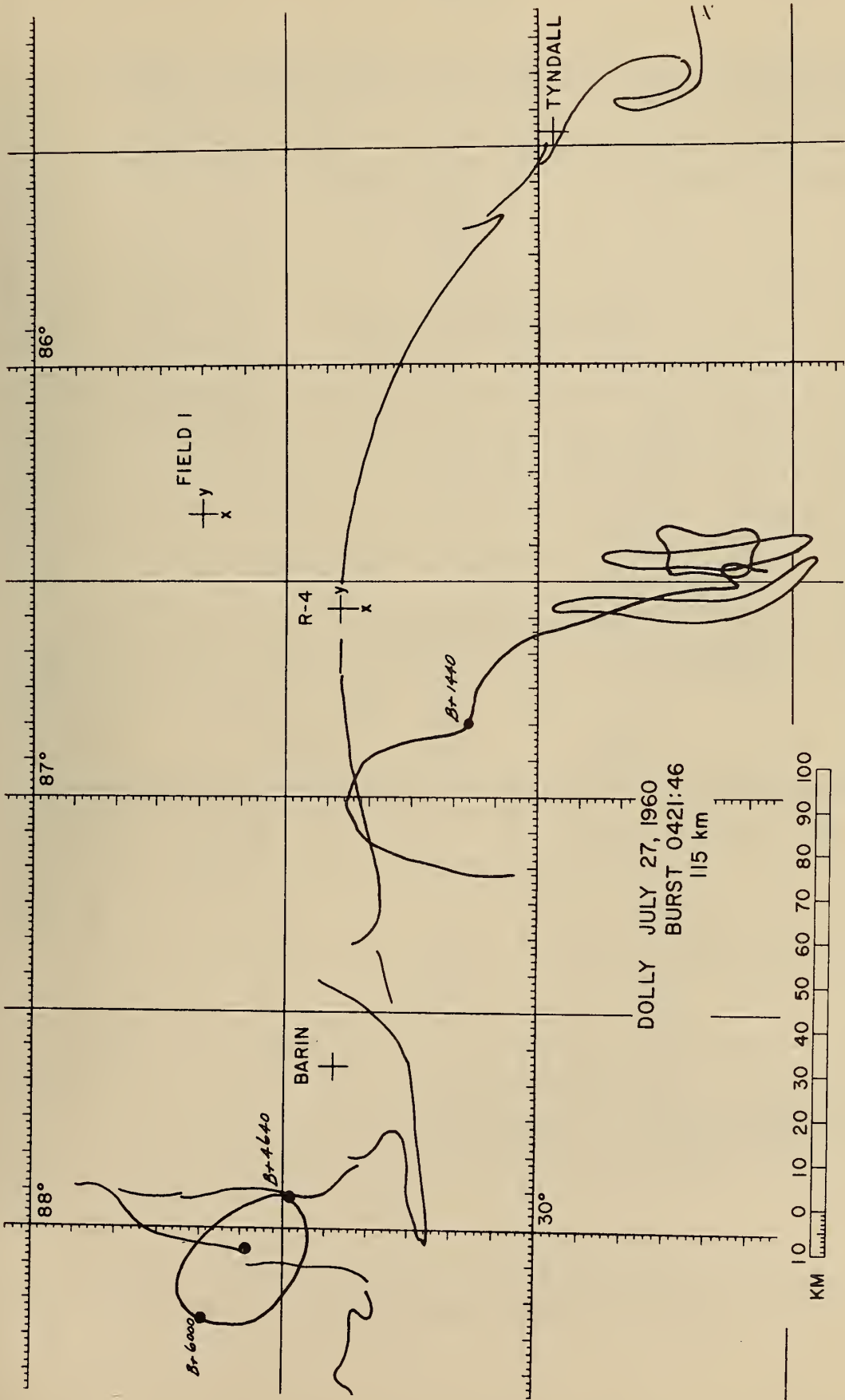


Figure 34: FIREFLY DOLLY LOCUS AS DEDUCED FROM IONO-SONDE DATA, ALSO SHOWING OPTICAL DATA THROUGH B + 660.

Triangulation places this at a point west of Barin roughly over Mobile, Alabama, where it appears to remain for nearly one hour until $B + 6000$ seconds. At sunrise the development of the normal E layer occults this cloud before its electron density has decayed to negligible values.

B. Night Electron Clouds

Five launchings to altitudes between 94 and 138 km comprised the 1960 Firefly night series; all used identical payloads. They are discussed below in the order of increasing height. Note that Firefly Betsy is included in the present discussion, although throughout all but the first 520 seconds of its life, it was a sunlit dawn cloud.

Definite ionosonde echoes were observed for all night clouds, although equipment malfunction resulted in a very regrettable loss of data in several cases.

Movement of the night clouds was difficult to deduce because of the short lifetime of these clouds at the outlying stations. The drift results are summarized on a single map, Figure 35.

CATHY

Cathy (Burst 0232:45, July 29 at 94 km) was at the lowest burst altitude of the night series of Point Electron Clouds. It was not observed at sites A-4 and Barin Field, because of equipment malfunction. However, echoes were observed from the Field-1 and Tyndall sites which may be attributable to the clouds.

At Tyndall, a faint echo appeared at burst between 16-17 mc and 142 km range (computed range at burst, 136 km) which by $B + 300$ was at

139 km. The echo was followed until B + 780 at 141 km slant range.

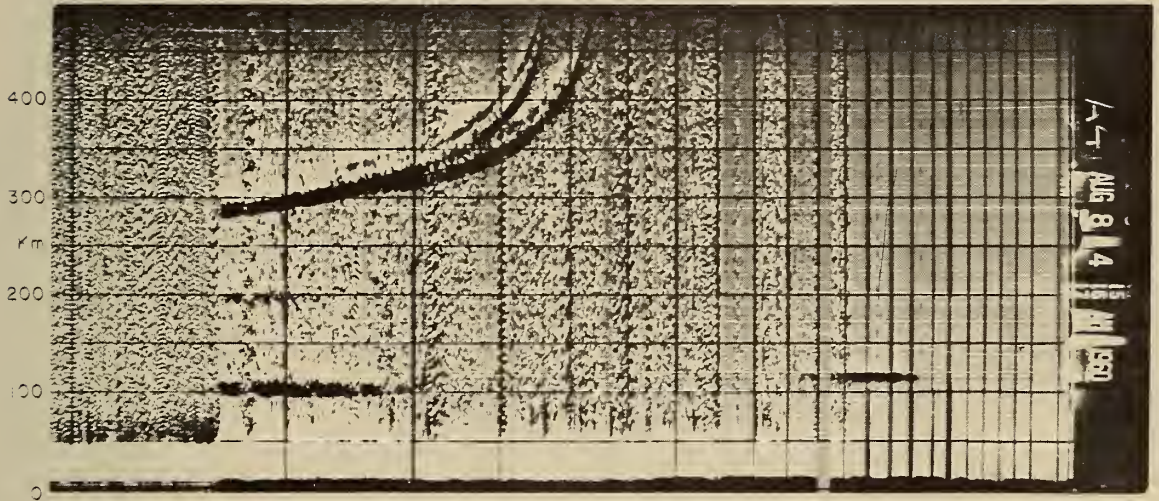
At Field-1 the echo appeared promptly at burst, and at 149 km range (computed range 142 km); it dropped rapidly in range, being found at 114 km by B + 1200. By B + 1680, this echo was at 105 km range, then faded out by B + 1980.

Assuming a negligible change in the height of the cloud, the above data are consistent with a velocity 51 m/s heading 330° . This was deduced supposing the cloud motion not to have been in the direction of Tyndall and assuming that at B + 1680 it had reached its closest approach to Field-1.

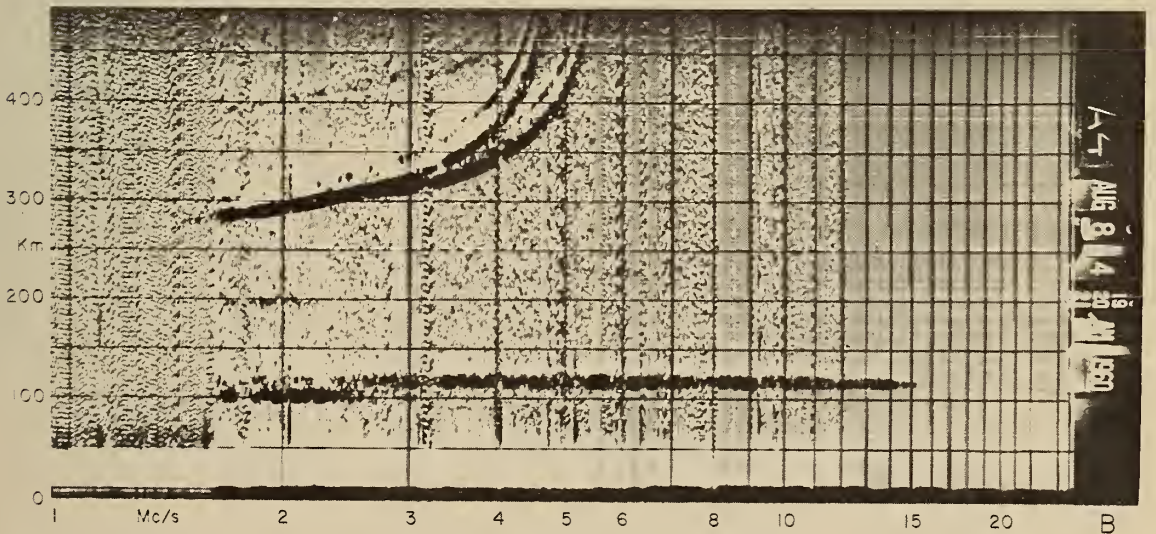
BETSY

Betsy (Burst 0416:41, August 8 at 108 km) was launched at a time when the earth's shadow was at 123 km; for the first 500 seconds the cloud was not illuminated by sunlight.

A fairly consistent and simple behavior was given by the ionosonde data for the position and drift of Betsy throughout the period B to B + 2580. A-4 ionograms at burst and at B + 240 are shown in Figure 36 A, B. Note the extraordinary component of a dense Es layer at 94 km, which was present before burst. Burst positions and altitudes agree fairly well with the optical data out to B + 540. However, a curious behavior is noted at later times. The optical data available at this writing show the cloud greatly distended at B + 360 through B + 720. Our radio data are consistent with northeasterly movement of the northeastern half of this distended cloud, as shown on the map of Figure 37. It would appear that at no time did we observe reflections from the southwestern portion of the cloud. Our data give a mean speed of 34 m/s, heading 88° through B + 2580 shortly after which all stations ceased to observe simple echoes from the cloud.



A



B

Figure 36: FIREFLY BETSY, AUGUST 8 AT 108 KM:
 A-4 IONOGRAMS AT BURST (A, 0416) AND AT B + 240
 (B, 0420).

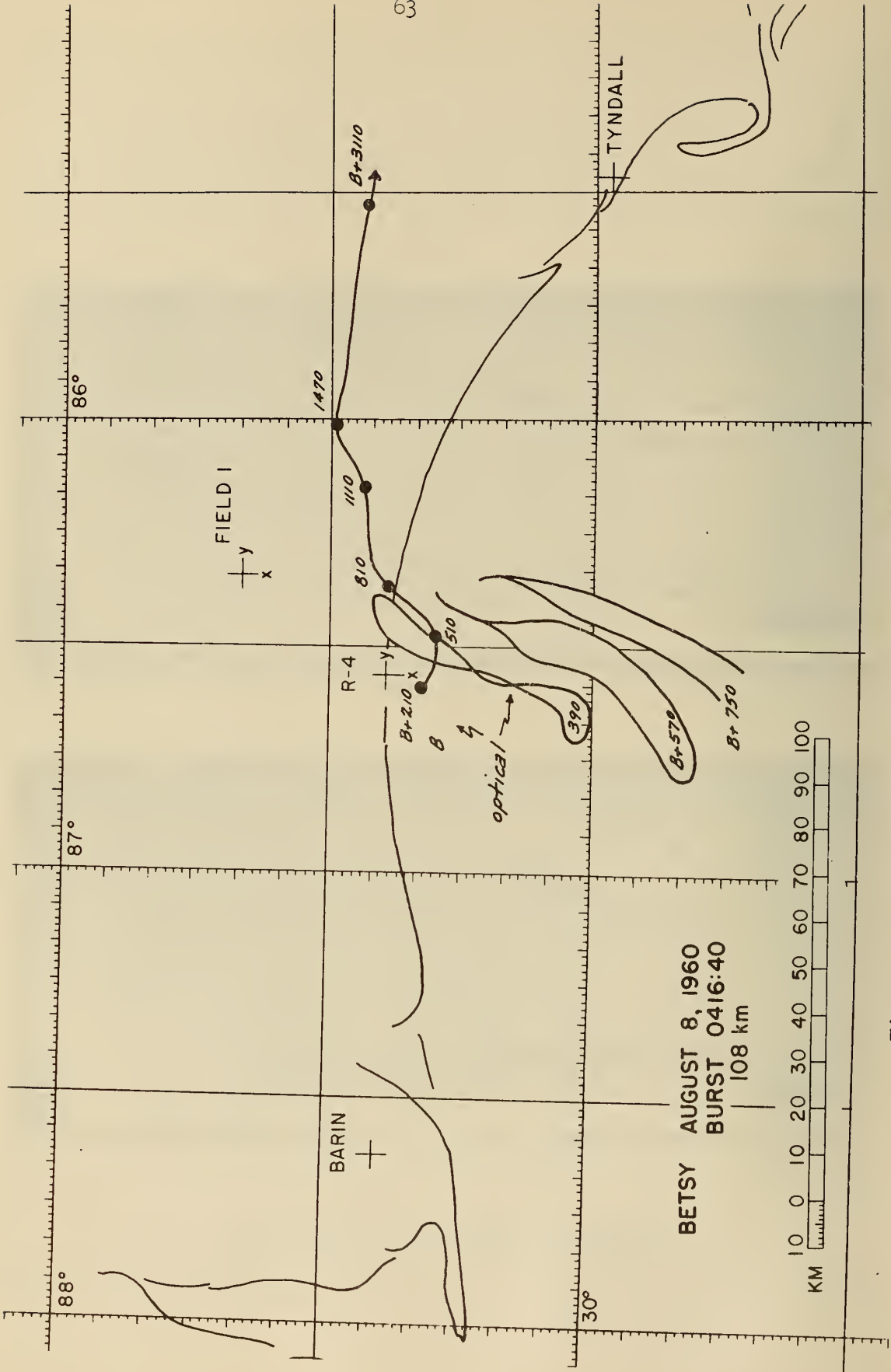


Figure 37: FIREFLY BETSY LOCUS DEDUCED FROM IONOSONDE DATA; OPTICAL POSITION AND SHAPE DATA ARE ALSO SHOWN THROUGH B + 720.

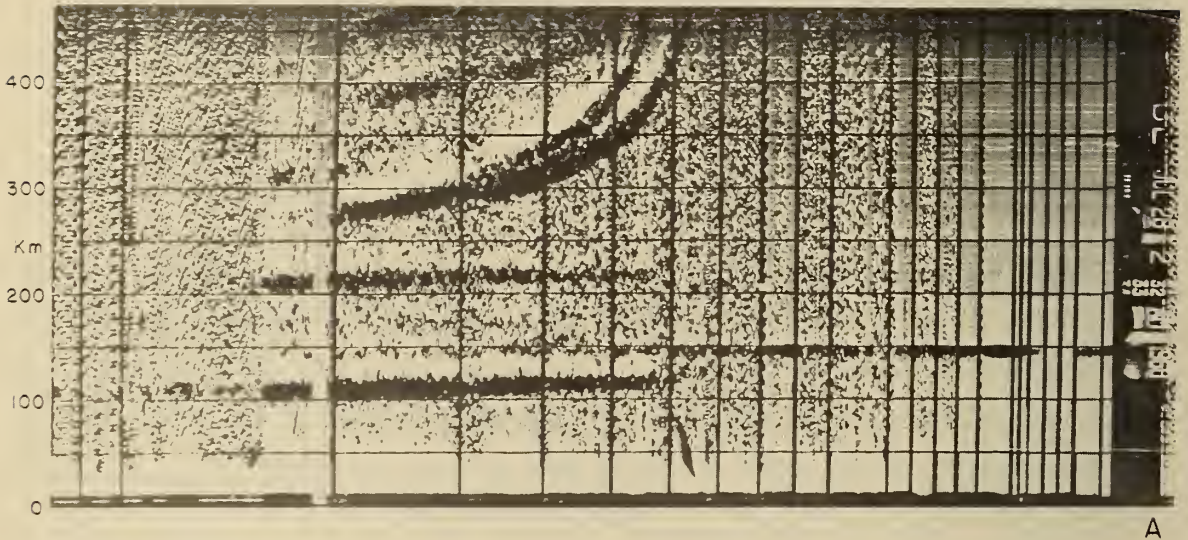
It would appear that after B + 2580 (0500), as the normal daytime E layer formed, the cloud became imbedded in it. A-4 (at a range of 173 km) and Tyndall (119 km) both observed a strong reflection from a layer well inside a retarding E layer. It was apparently localized to the east, as it disappeared rapidly from view at A-4 at B + 3750 (0519), but was quite strong at Tyndall by B + 3840 (0520) when the station ceased observation.

AMY

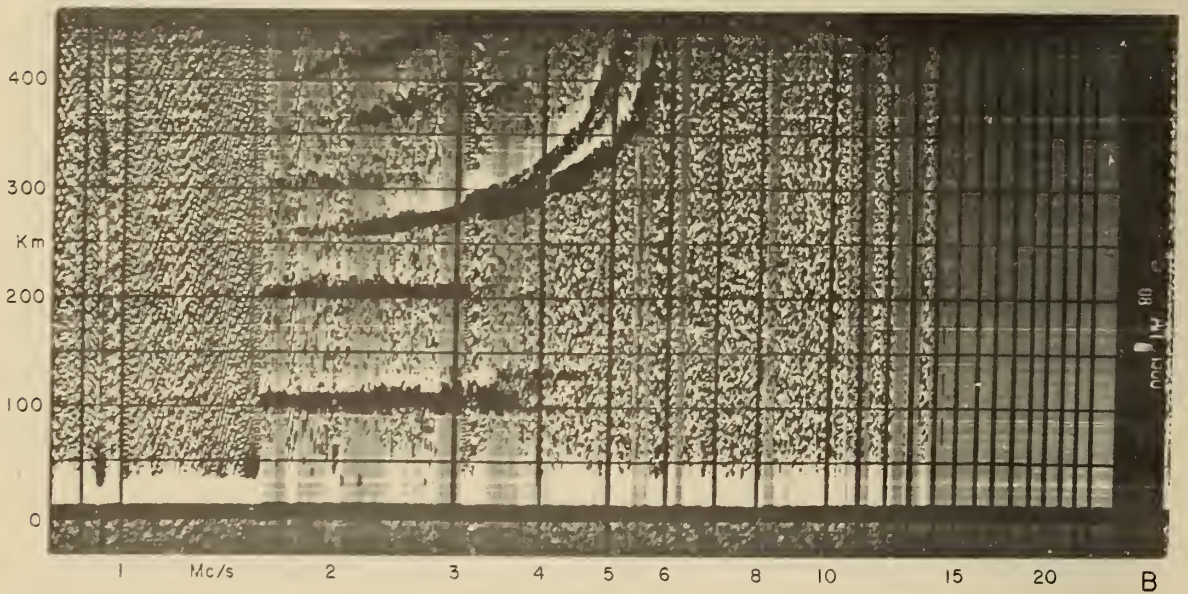
Amy (Burst 0232:45, July 28 at 111 km) was launched in the presence of intense Es at a level of 100 km. The cloud echo was seen immediately to frequencies above 25 Mc at A-4. However, the cloud echo dropped in range and frequency was soon lost in the Es. Figure 38 A, B illustrates the appearance of the echo at burst and at 0307 (B + 2040).

Barin Field did not observe an echo until B + 420. This is one of several unexplained instances of delayed appearance of cloud echoes at Barin. During the short period of detection (until B + 720), the echo dropped in range. Tyndall, unfortunately, was not observing until B + 2280; no echoes were observed that could be positively attributed to the cloud.

Field-1 observed two cloud echoes at burst (ranges 166 and 135 km) (computed range to Field-1 162 km). The second echo soon disappeared, and the cloud dropped in range until B + 1320, where the range began to increase again. With only this information it is necessary to assume a constant cloud height to infer the bearing and speed (Figure 35). Values of 87 m/sec and 350° are found. The speed is probably over-estimated, since the early Field-1 ranges do not change in a uniform manner.

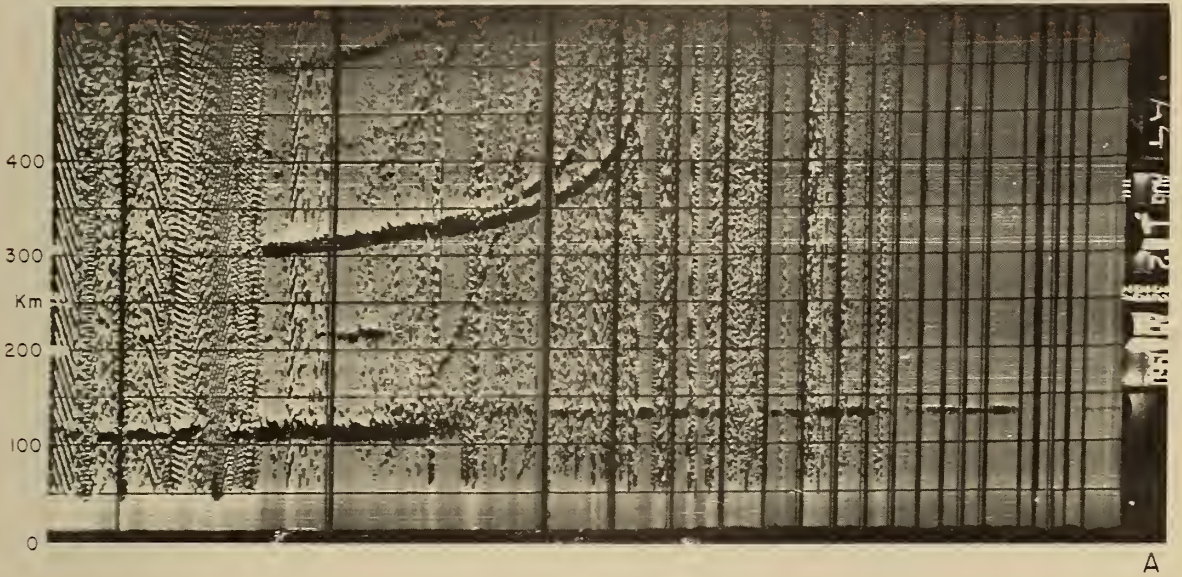


A

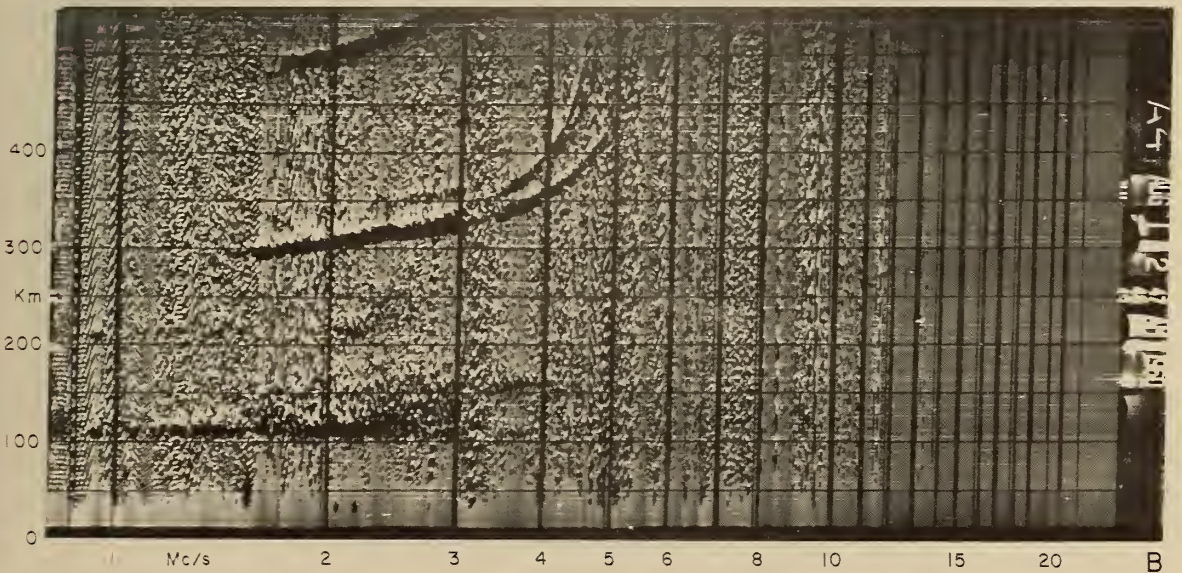


B

Figure 38: FIREFLY AMY, JULY 28 AT 111 KM: A-4 IONOGRAMA
 AT BURST (A, 0232:45) AND AT B + 2040 (B, 0307).



A



B

Figure 39: FIREFLY RUTHY, AUGUST 1 AT 113 KM: A-4
 IONOGRAMS AT BURST (A, 0232:30) AND AT B + 840
 (B, 0247).

RUTHY

Ruthy (Burst 0232:30, August 1 at 113 km) was launched, like Amy, in the presence of intense Es. Figure 39 A, B shows the appearance of the echo at A-4, at burst and at B + 840. At Tyndall and at Field-1, the echo was seen promptly at burst, over a wide range of frequencies to 25 Mc at Field-1, but only at high frequencies and very faintly at Tyndall. It is suggested that the reason for Tyndall's faint echo observed only at high frequencies, is that it was occulted by the intense Es patch which must have been nearly overhead at the burst position, covering a wide area to the north and west.

At Barin Field the echo did not appear until B + 420 and even then was apparently not a direct reflection from the cloud, since it is inconsistent with the (more reasonable) cloud position deduced from the other stations.

Good agreement with the optical data is obtained on position and altitude (113 km from our data) at B + 60 (see Figure 35). Cloud position could be determined out to B + 810, giving a drift measurement of 81 m/sec heading 229°.

GERTA

Gerta (Burst 0303:00, August 6 at 138 km) was the highest of the night series of Point Electron clouds. Unfortunately, Field-1 was not operating for this experiment; Barin and Tyndall observed the cloud at only 180 and 40, respectively, with a second Barin appearance at B + 720s (at 168 km range). A-4, on the other hand, observed the cloud continuously until B + 1920. See Figure 40 A, B showing the appearance of the echo at burst and at B + 840. The absence of Field-1 data makes

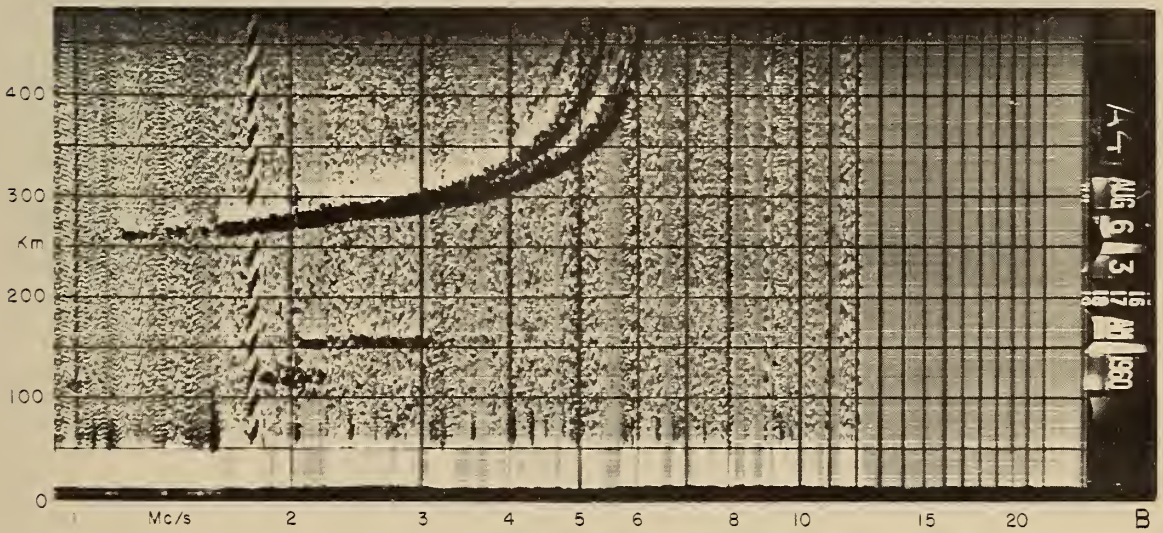
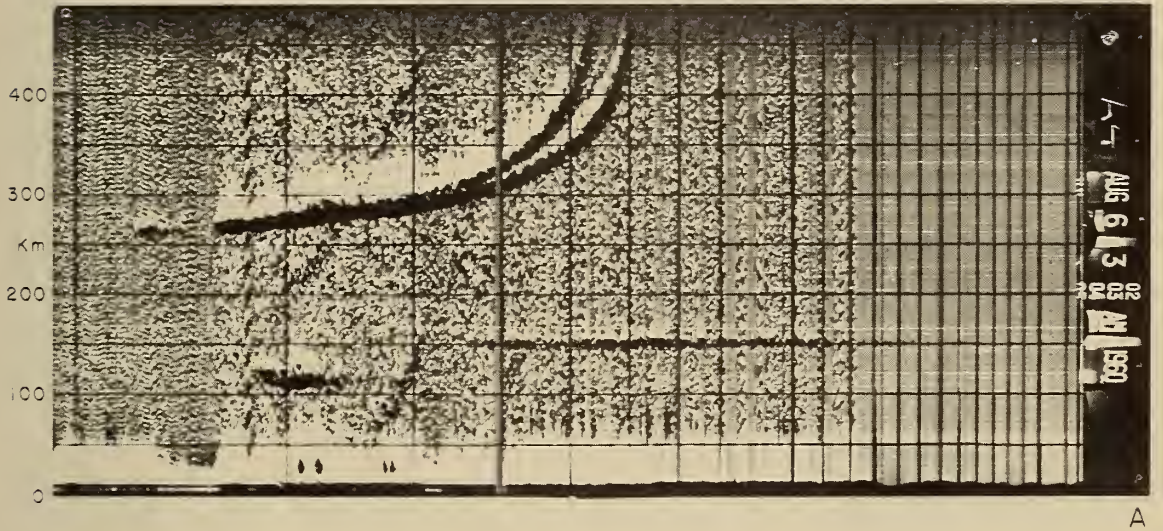


Figure 40: FIREFLY GERTIA, AUGUST 6 AT 138 KM: A-4
IONOGRAMS AT BURST (A, 0303) AND AT B + 840 (B, 0317:45).

it impossible to determine radio position data, since the Tyndall -- A-4 -- Cloud -- Barin Field deployment leads to an indeterminate problem.

However, one may conclude from the A-4 range data (Figure 41) that Gerta had a negligible component of motion radial to A-4 and that, therefore, it was moving in a heading roughly either 78° or 258° from its optical burst position. The heading 78° would carry the cloud towards Tyndall (which saw the cloud only at burst), while 258° would carry it only slightly toward Barin Field (which saw the cloud only momentarily at B + 270). At B + 270 Barin's range agrees with the cloud still in its burst position.

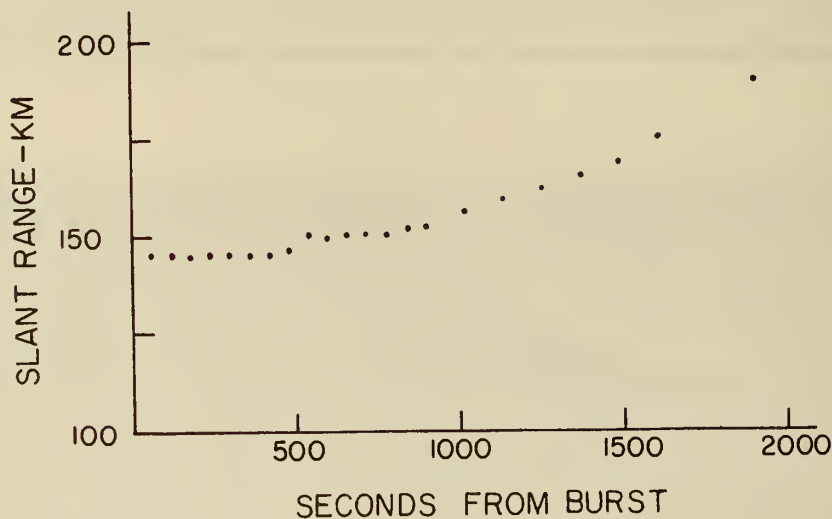


Figure 41: Firefly Gerta range vs. time data observed at station A-4.

The second appearance of the echo at Barin at B + 720, is consistent with motion of the cloud in the heading 258° and then at position $29^{\circ}57'30''\text{N}$, $86^{\circ}50'$ west, with a characteristic dimension of 13 km. Its motion to this position after B + 270s would imply a speed of drift of 84 m/sec, assuming horizontal motion (see Figure 35).

C. Trail Electron Clouds

JANET

Janet (Burst 0419:30, July 26 at 119 km) had a payload of 16 kg. This was an attempt to produce a trail electron cloud by the gradual release of payload.

The A-4 ionogram of Figure 42 A depicts the condition of the ionosphere at the time of release. Es at 112 km, with a peak density of $3.6 \times 10^4 \text{ cm}^{-3}$ (to 7 Mc) was present before and throughout the experiment. While there is a very weak echo at the predicted range (135 km), it is not considered probable that this is the result of the electron cloud. Figure 42 B is a range vs. time observation at 2.0 Mc, covering a period of about 15 seconds immediately prior to the time of launch (0417). Within this period three separate reflections occurred at this same range, presumably due to meteors or sporadic E, suggesting that the weak echo indicated in Figure 42 A has a similar origin.

HILDA

Hilda (Burst 0425:30, August 1 at 126 km) was the higher of the two trail (slow-release) electron cloud experiments. No echoes were observed at any of the sites, that could be attributed to the cloud.

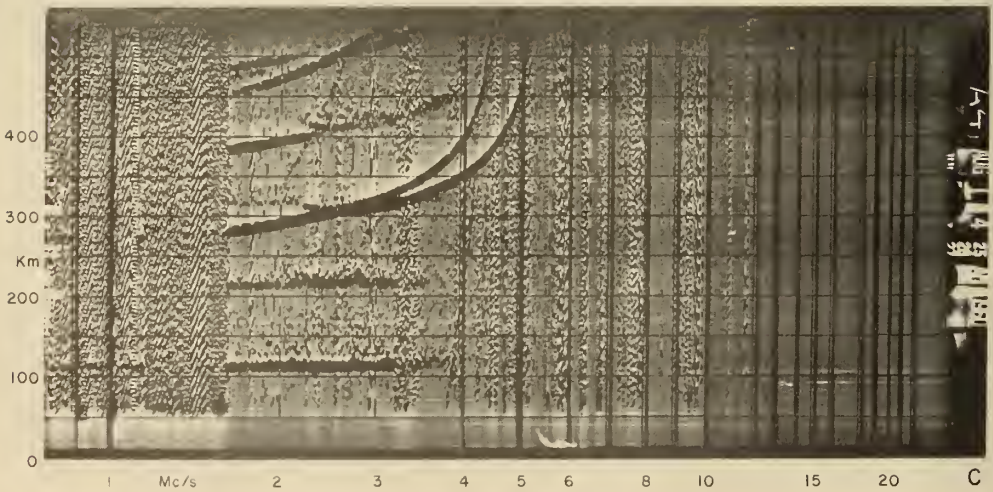
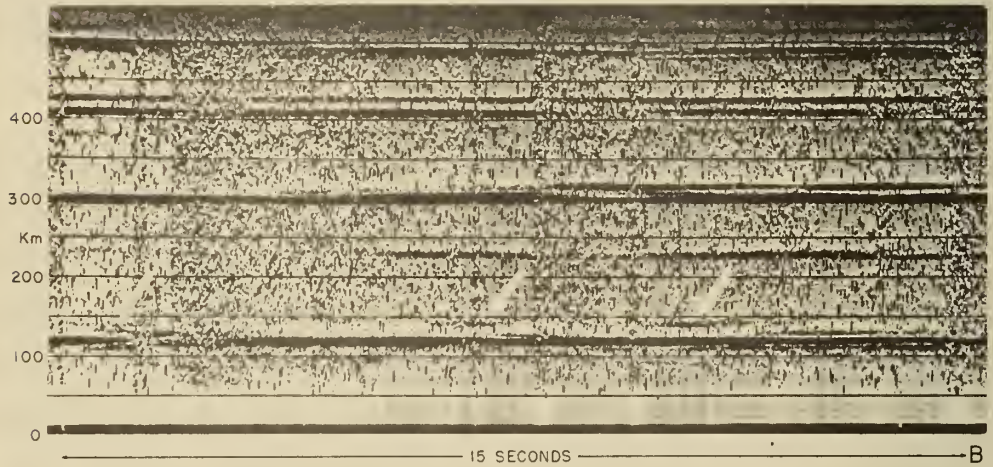
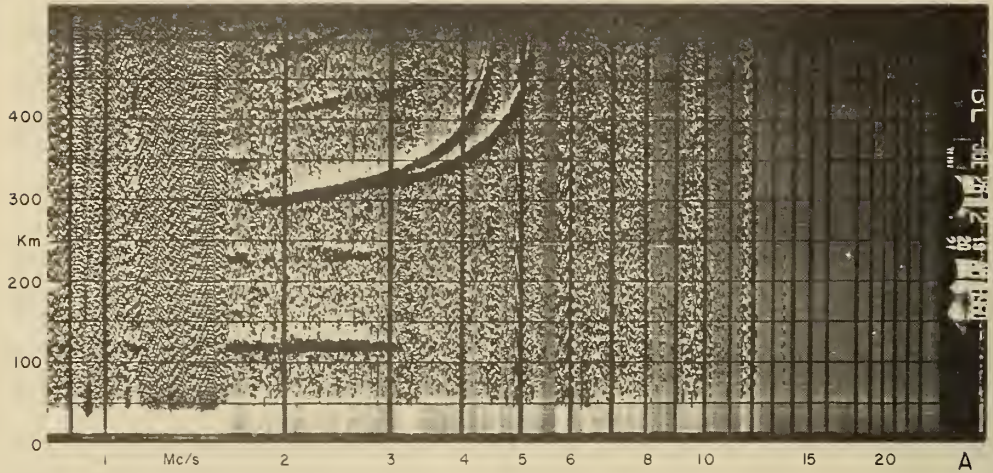


Figure 42: FIREFLY JANET AND HILDA, TRAIL ELECTRON CLOUDS. JANET: A-4 IONOGRAM AT RELEASE (A, 0419:30; RECORD TIME IS TWO HOURS SLOW). (B) HEIGHT VS TIME SEQUENCE AT 2.0 MC PRIOR TO RELEASE OF JANET, ILLUSTRATING SEVERAL ECHOES SIMILAR TO "JANET" ECHO ON IONOGRAM A. HILDA: A-4 IONOGRAM AT BURST, 0425.

Figure 42 C shows the A-4 ionogram at the time B + 30 and illustrates an important point; there is strong Es at 106 km overhead (or nearly so), which, while not "blanketing" the F region, is sufficiently "dense" to give strong multiple echoes. Considering the comparatively low electron densities expected in a gradual release, it seems inadvisable to attempt such an experiment in the presence of such Es layers, particularly when the release is planned for an altitude exceeding 100 km. In the present case this Es was observed from Tyndall, Field-1 and Barin, in addition to A-4; it appears that it covered a large area to the south and west of A-4. We would suggest that this Es may be responsible for reports of signal enhancement during this experiment.

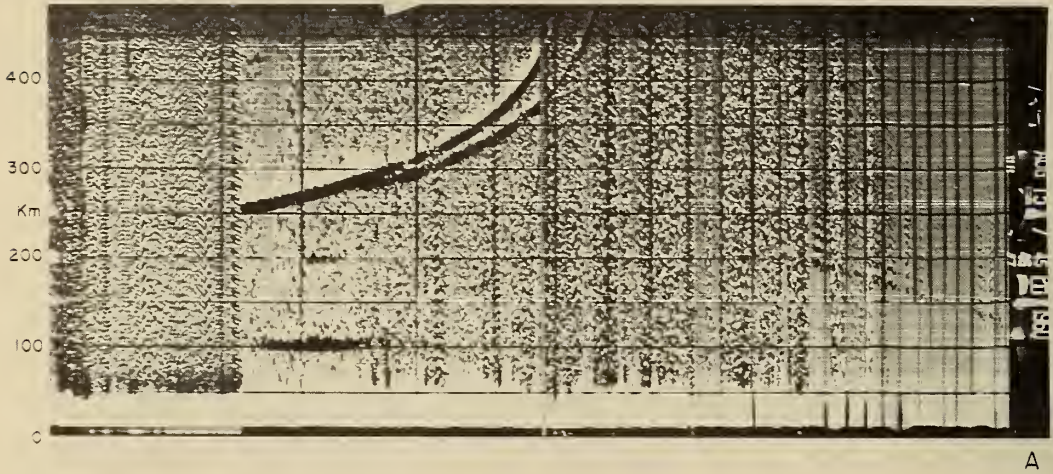
D. High Explosive Detonations

CARRY

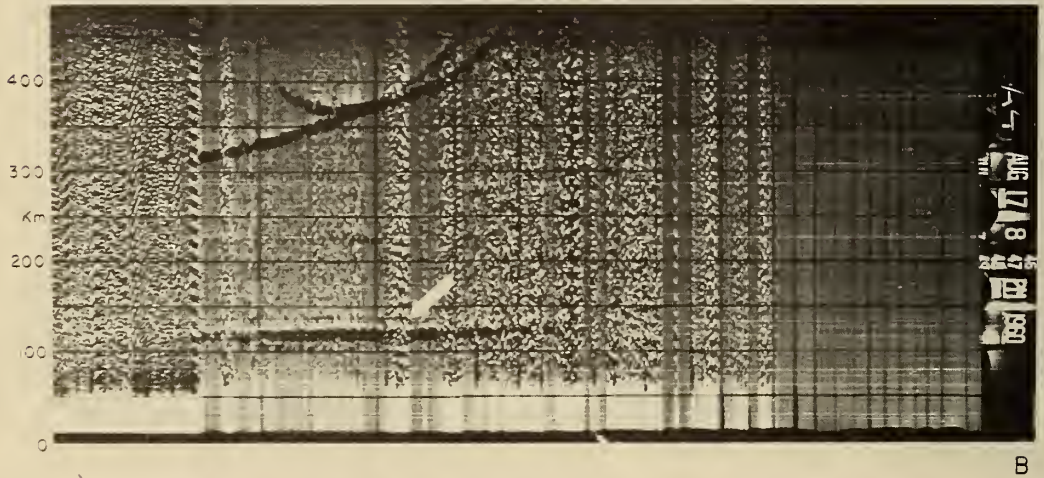
Carry (Burst 0403:27, July 18 at 129 km) was an early morning detonation of high explosive (19 kg). At and before burst, the A-4 ionograms showed intense sporadic-E at 100 km (foEs = 2.1 Mc), with many scattered reflections*.

No echo was observed that could be attributed to the detonation. Only the A-4 ionosonde was operating for this experiment.

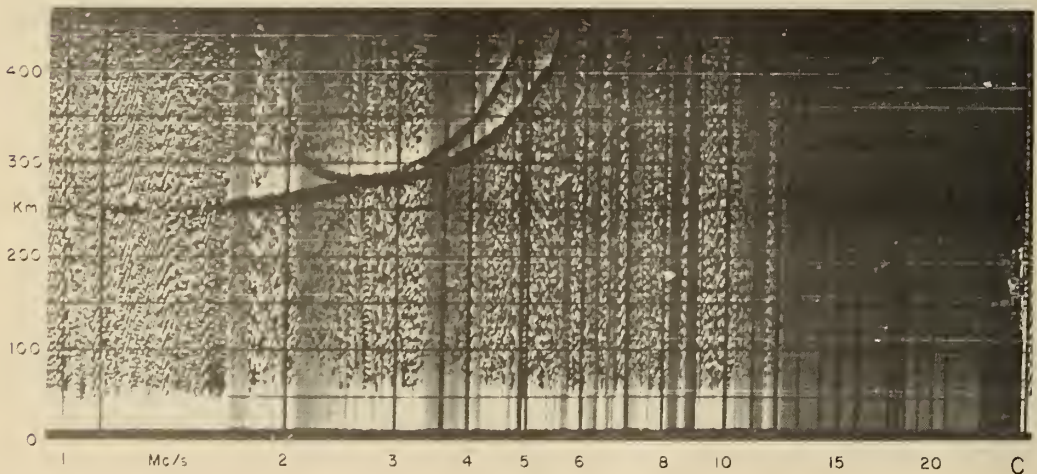
*It may be useful to recall here the suggestion of Clark (1957), that when ionogram sporadic E echoes showed such scattered reflections, it correlated well with extremely high drift speeds in the E region (100 - 300 m/sec.).



A



B



C

Figure 43A: FIREFLY ARLENE, HIGH EXPLOSIVE DETONATION AT 104 KM: A-4 IONOGRAM AT DETONATION (A, 1945:30).
 B. FIREFLY LENDA: A-4 IONOGRAM AT B + 120 (B, 2047).
 C. FIREFLY MAVIS: A-4 IONOGRAM AT B + 15 (C, 0415:45), ON JULY 29, 1960.

ARLENE

Arlene was an evening (1945:34, August 15) detonation of 18 kg. of high explosive at an altitude of 104 km. The ionogram from the A-4 site depicting the condition of the ionosphere at this time is shown in Figure 43 A. A layer of Es existed throughout this test at 95 km and about $3 \times 10^4 \text{ cm}^{-3}$ maximum electron density (1.55 Mc; only the magneto-ionic extraordinary component shows on the ionogram). No echo attributable to the detonation was observed at this or any of the ionosonde sites.

E. ONR Project TP Arc Experiments

During the Firefly 1960 series, two Electron Arc payloads were launched as part of ONR Project ~~TEEPÉE~~. Shots TP Annie and TP Norma were launched at 0119 and 0347, respectively, on August 13; the arc was ignited 144 sec later; the intended altitude was 120 km. Optical results, however, suggest that TP Annie may have failed to ignite, and that the maximum altitude reached by TP Norma (which was optically observed to ignite) was only 97 km.

Ionogram sequences from the NBS site A-4 for both TP experiments are found in Figure 44, showing conditions during and after (?) ignition of the arcs.

TP Annie: Comparing Figure 44 A (at 0121:00, before ignition), no echo at the predicted range can be found. However, Figures 44 C (at 0423, I+120), an echo is observed at 96 km, to 2.4 mc/s. It is only faintly visible at 0124 (I+180).

TP Norma: Shows a similar echo before the ignition time at 0349:00 (Figure 44 F). This echo is at 92 - 100 km slant range, and implies an

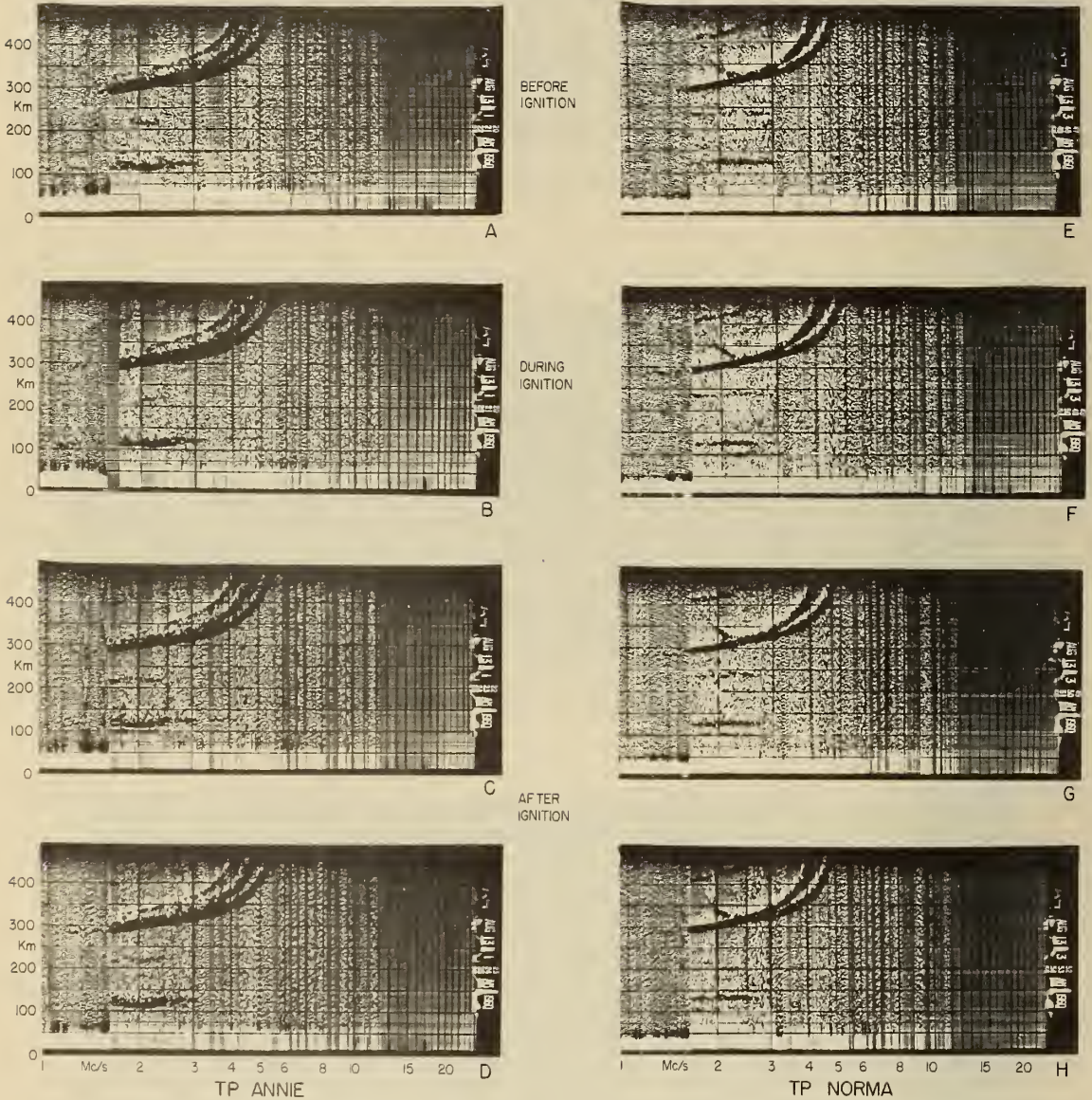


Figure 44: ELECTRON ARC EXPERIMENTS: A, B, C, D, IONOGRAMS FROM A-4. TP ANNIE, AUGUST 13 AT 0121:24. A-0121:00 AT I-24; B-0121:30 AT I+6; C-0123, AT I+120; D-0124 AT I+180. TP NORMA, AUGUST 13 AT 0349:24. E-0348:30 AT I-54; F-0349:00 AT IGNITION; G-0350 AT I+60; H-0353 AT I+240. NOTE IONOSONDE SWEEPS ARE OF 30 SECONDS DURATION.

electron density of $6 \times 10^4 \text{ cm}^{-3}$ (2.5 Mc). It was still visible at I + 60 and I + 240 (Figures 44 G at 0350; and 44 H at 0353, respectively). On the latter ionogram, the echo has moved out in range to 105 km; it was not seen later.

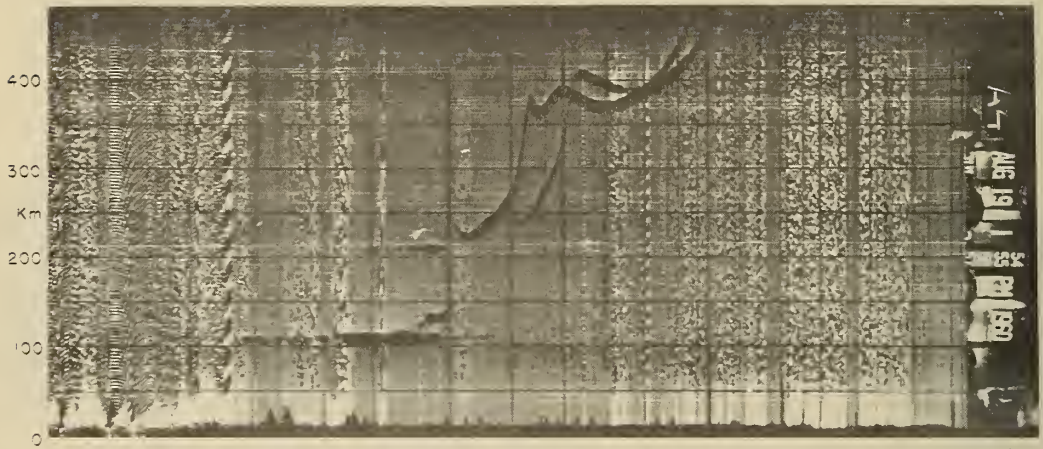
Our timing is accurate to probably ± 1 second, thereby making it rather doubtful that the echoes discussed above for TP Norma can be associated with the arc -- unless it should prove to have ignited prematurely. Furthermore, available evidence seems to be that TP Annie did not ignite at all -- yet we saw an echo at I + 120 very similar in appearance to the TP Norma observations. Since, in both cases, meteoric ionization could have been responsible for our observed echoes, we cannot conclude with certainty from ionosonde data that either of these electron production experiments was successful.

F. RENA: Electron Removal Experiment

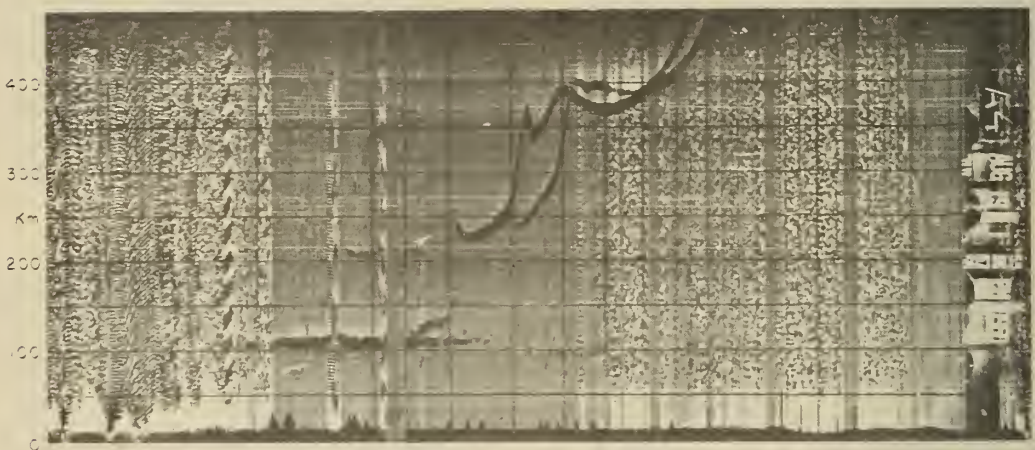
Rena (Electron Removal; burst 1356:40, August 19 at 105 km) was an experiment designed to test the efficiency of sulphur hexafluoride (14 Kg) as a "remover" of electrons in the E region, in competition with the daytime photoionization and photodetachment processes. It was hoped to produce a detectable decrease in E region electron densities, which could be observed by the ionosonde as either a decrease in foE, or a redistribution or change in shape of the E layer. It is clear that nothing dramatic happened, but it is not improbable that the release had a detectable effect.

Ionograms from A-4 before (-70 seconds) at, and after (+ 390 seconds) burst are shown in Figure 45 A, B, C. This was not a simple E region at this time; ultimately the following important levels should be noted:

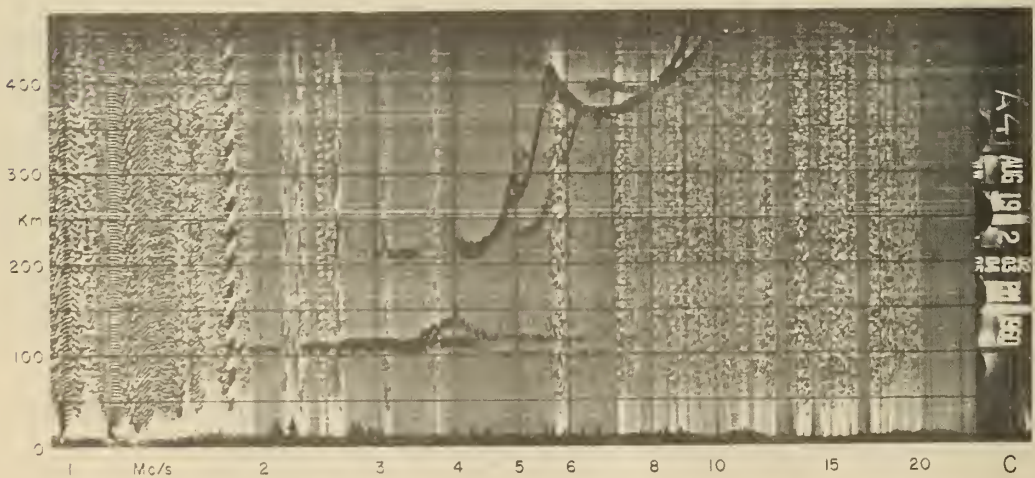
- a. The "normal" daytime E layer extending to altitudes presumably below 100 km in a fairly simple way.



A



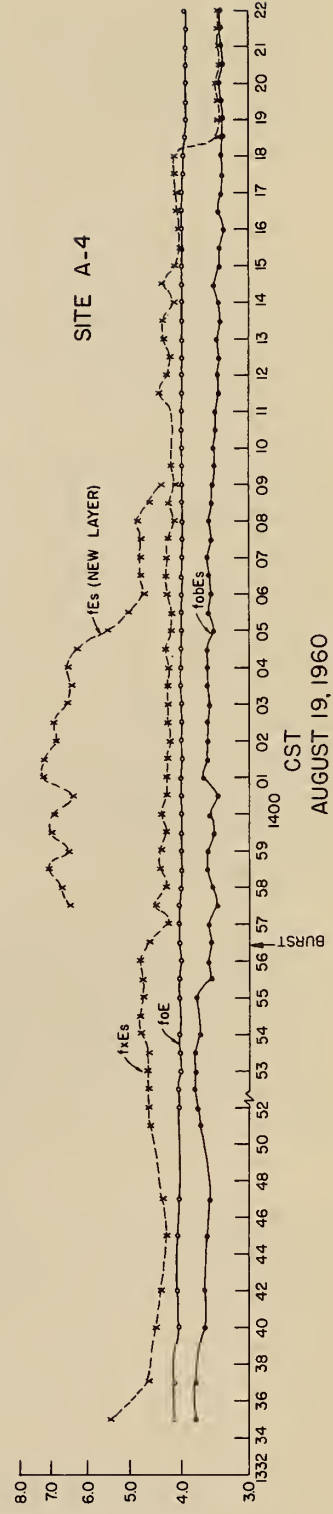
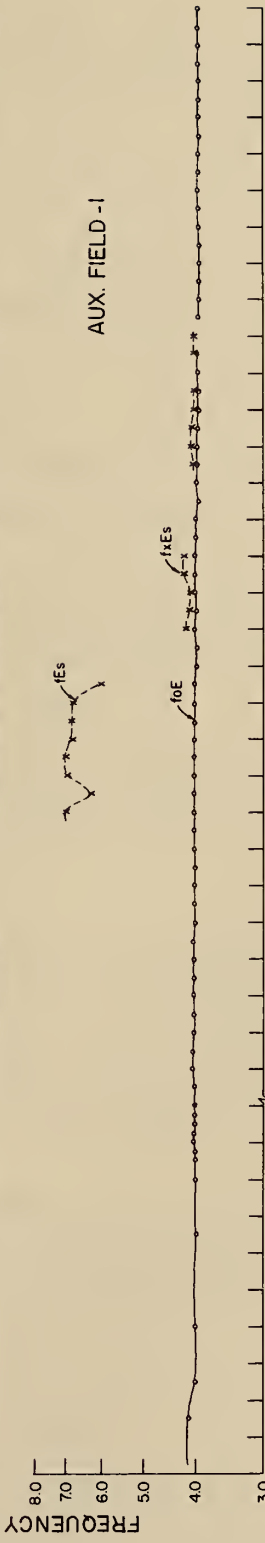
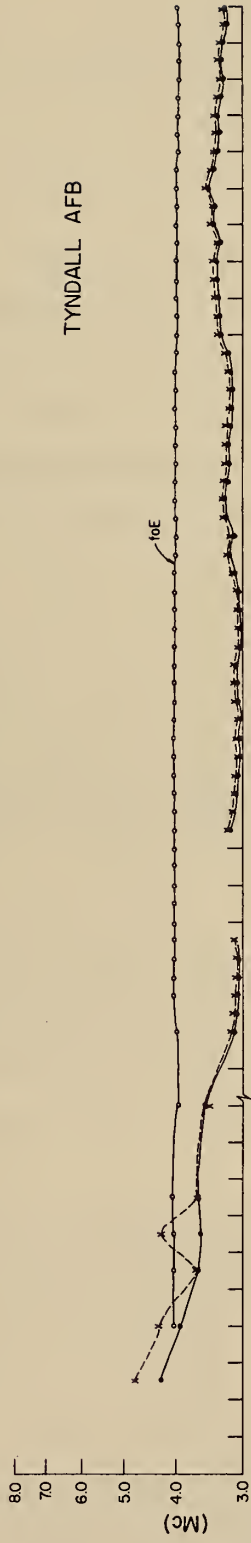
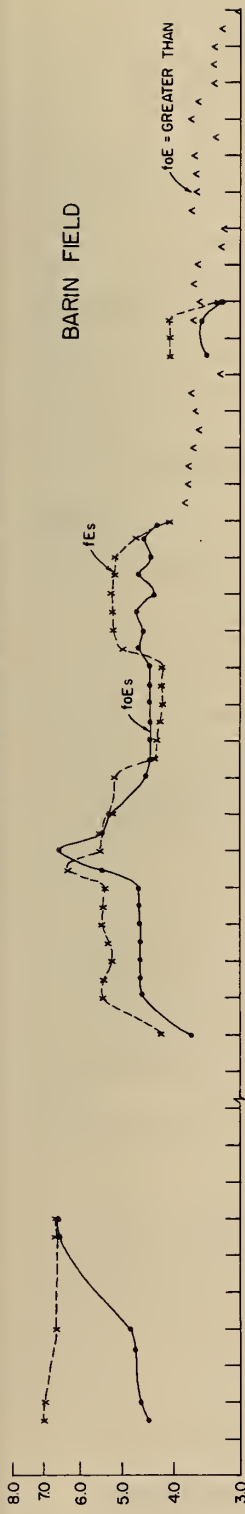
B



C

Figure 45: FIREFLY RENA, AUGUST 19 ELECTRON REMOVAL AT 105 KM: A-4 IONOGRAMS AT B-70 (A, 1355:15), AT BURST (B, 1356:45), AND AT B + 390 (C, 1403:00).

RENA, ELECTRON REMOVAL AT 105 Km



AUGUST 19, 1960

Figure 46: FIREFLY RENA: TIME VARIATION OF E REGION FREQUENCY PARAMETERS FROM FOUR IONOSONDES.

- b. A sporadic E stratum at 100 km, and at a level immediately below which the E layer electron density is about $8.1 \times 10^4 \text{ cm}^{-3}$. The Es stratum had an electron density of about $10.1 \times 10^4 \text{ cm}^{-3}$.
- c. A "ledge" or minor stratification in the E layer at approximately 108 (true height) km, where $N = 1.7 \times 10^4 \text{ cm}^{-3}$.
- d. The "peak" of the E region at 113 km with a maximum electron density of $2 \times 10^5 \text{ cm}^{-3}$.

The time variation of the frequency characteristics of these records from B - 1470 to B + 1530 is shown in Figure 46 for all of the stations. The solid line labeled fobEs shows the time variation of the peak density of the sporadic E described in (b) above. This quantity is measured by the lowest ordinary-wave frequency to penetrate the Es into the E region above it. The curve labeled fxEs measures the extraordinary wave critical frequency of this same Es layer; ideally, fobEs and fxEs should measure the same thing, viz, the electron density of the Es layer.

The curve labeled foE refers to the peak density of the E region (d), above. Similar graphs for Field-1, Tyndall, and Barin are also shown. Unfortunately, data at these stations are not sufficiently detailed to give the complete picture comparable to A-4.

For some minutes prior to burst (note the scale change at 1352), these parameters are fairly stable. At burst there is a definite detectable drop in fxEs, corresponding to a drop in electron density of the Es layer of 28%. The drop is rather permanent. Unfortunately, the expected drop in fobEs, which should also measure the electron density of this layer, does not occur. On the other hand, these frequencies are not related in the expected magnetoionic way in the first place. (At B - 30; fxEs = 4.80 Mc; this should give foEs 4.03, whereas a value

of 3.60 Mc is observed for fobEs; similar discrepancies exist throughout the sequence.) At the same time, a rise in the height of this Es layer is noted, as may be seen by careful comparison of Figures 45 A, and C (B - 70 and B + 390 respectively). This also is consistent with a decrease in electron density at or below this level.

Finally, a comment must be made concerning the new Es stratum appearing within 60 seconds of Burst, and represented in Figure 46 by the line labeled "fEs - new layer." It may also be seen in Figure 45 C (B + 390), at a range of 111 km. This appears to be a turbulent Es stratum embedded at or near the level of the E layer peak. It is not known what, if any, relation this may bear to the electron removal experiment.

G. Other Experiments

LINDA

Linda (Burst 2045, August 17 at 133 km) was an evening release of 2 μ cobalt powder. While no ionosonde echoes were expected from this release, it is of interest to note that an echo was observed at A-4 at the predicted range and time. Figure 43 B shows the ionogram obtained at B + 120 (2047). The Es at 112 km was present sporadically for some time before the launching. At burst a weak echo at 138 km appeared (predicted range to A-10 for Linda); it remained with about the same appearance through 2050, and by 2053 increased in range, then disappeared.

No similar behavior was detected at any of the other ionosonde sites; at Field 1, the next-nearest location, the ionograms were too poor to permit reliable judgment.

MAVIS

Mavis (Burst 0415:32, July 29 at 115 km) was a release of 3.2 kg. of 0.03 μ Al₂O₃ powder. The ionogram for site A-4 at B + 15 (0415:45),

is shown in Figure 43 C. There was no sporadic E at this time. By the technique discussed Section II C the quantity of ionization below the F region is found to be somewhat larger than average. There was no echo attributable to the release observed at any of the ionosonde sites.

FRANCES

Frances (Burst 0408:20, July 14 at 149 km) was a release of 7.7 kg. of aluminum oxide powder. At and prior to burst there was some sporadic E at 130 km ($f_oE_s = 1.95$ Mc), with evidence (Section II C) for ionization of lower density at lower heights. At A-4, no echo could be ascribed to this cloud; the other ionosonde stations were not operating.

LILY

Lily (Burst 0405:16, July 21 at 151 km) released 8.1 kg. of 2μ aluminum oxide. No observations were obtained at A-4 due to equipment malfunction; the other ionosonde stations were not operating.

HEDY

Hedy (Burst 0412:47, July 22 at 109 km) was a release of 18 kg. of cadmium sulphide. Prior to burst A-4 ionograms showed weak sporadic E near the predicted range (115 km), erratic in occurrence. At B + 15 this sporadic E became somewhat enhanced with $fE_s = 2.5$ Mc. At B + 28 a rather strong echo was observed at 132 km and 15 Mc; by B + 43 this had disappeared -- it was probably a meteor. The other ionosonde stations were not operating at this time.

IDA

Ida (Burst 1932:30, July 20 at 130 km), was a release of 10 kg. of kerosene. A-4 ionograms showed sporadic E of the "sharply bounded" partially reflecting type fEs = 3.4 Mc, at 100 km. No echoes were observed that could be related to the burst. The other ionosonde stations were not operating.

IV. SUMMARY

POSITION, DRIFT AND GROWTH OF ELECTRON CLOUDS

A. Practical Considerations

Initially, it was hoped that the use of four ionosondes would permit a precise radio location and tracking of the electron clouds, and perhaps also give unambiguous first-order estimates of the clouds' size. We still believe these hopes to be realizable, although our attempts recorded here have been far short of our goals. On the whole, the determinations of drift have compared well with optical data (for details, see discussions of individual experiments in Section III), and have given reasonable values of cloud speed. However, the attempts to determine cloud height or radius from range data (see Appendix 2, regarding methods) have been rather unsatisfactory except at burst, in a few notable cases. This is attributed to three main factors:

- a. errors in range calibrations at the three outlying sites (see Appendix 1, Part C),
- b. a weak station deployment, consisting of Barin, A-4 and Tyndall (and often the clouds) on nearly the same straight line, with Field-1 too nearby. This leads to singularities and near-singularities aggravated by the effect of small range errors,
- c. the considerable growth and assymetry of the clouds, rendering any "spherical" assumptions ineffective.

The inverse (and in a practical sense, useless) process of deriving the cloud slant-ranges to the ionosondes from optical position data, has given very encouraging results for properly calibrated ionosondes: the mean "range-error" so computed for A-4 (eleven experiments) was 0.54 km. Thus the problems lie more with the station-cloud geometry than with the instrumentation.

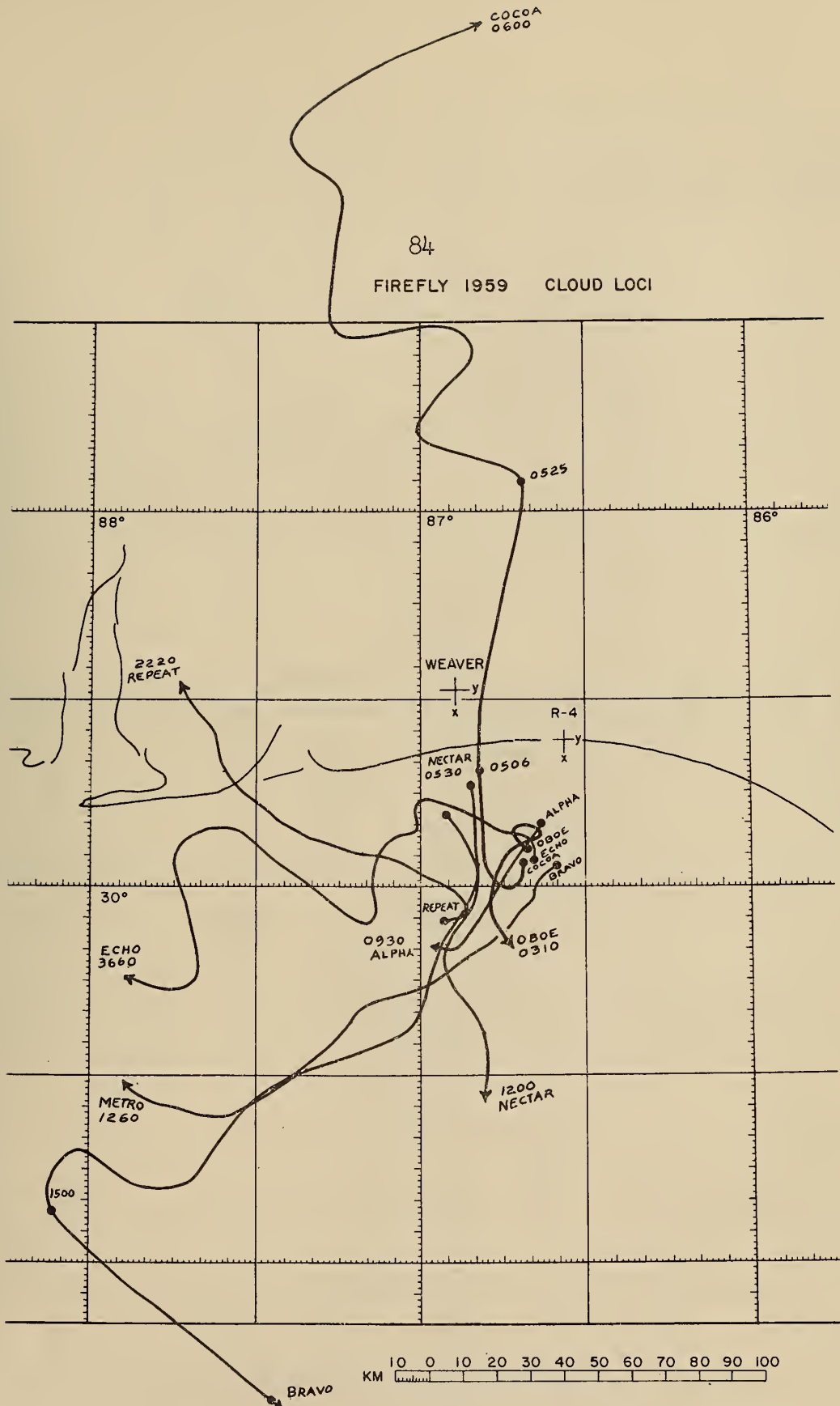


Figure 47: FIREFLY 1959 CLOUD LOCI SUMMARY, AS DEDUCED AT NBS FROM WEAVER AND A-4 IONOSONDES ASSUMING BURST HEIGHT THROUGHOUT.

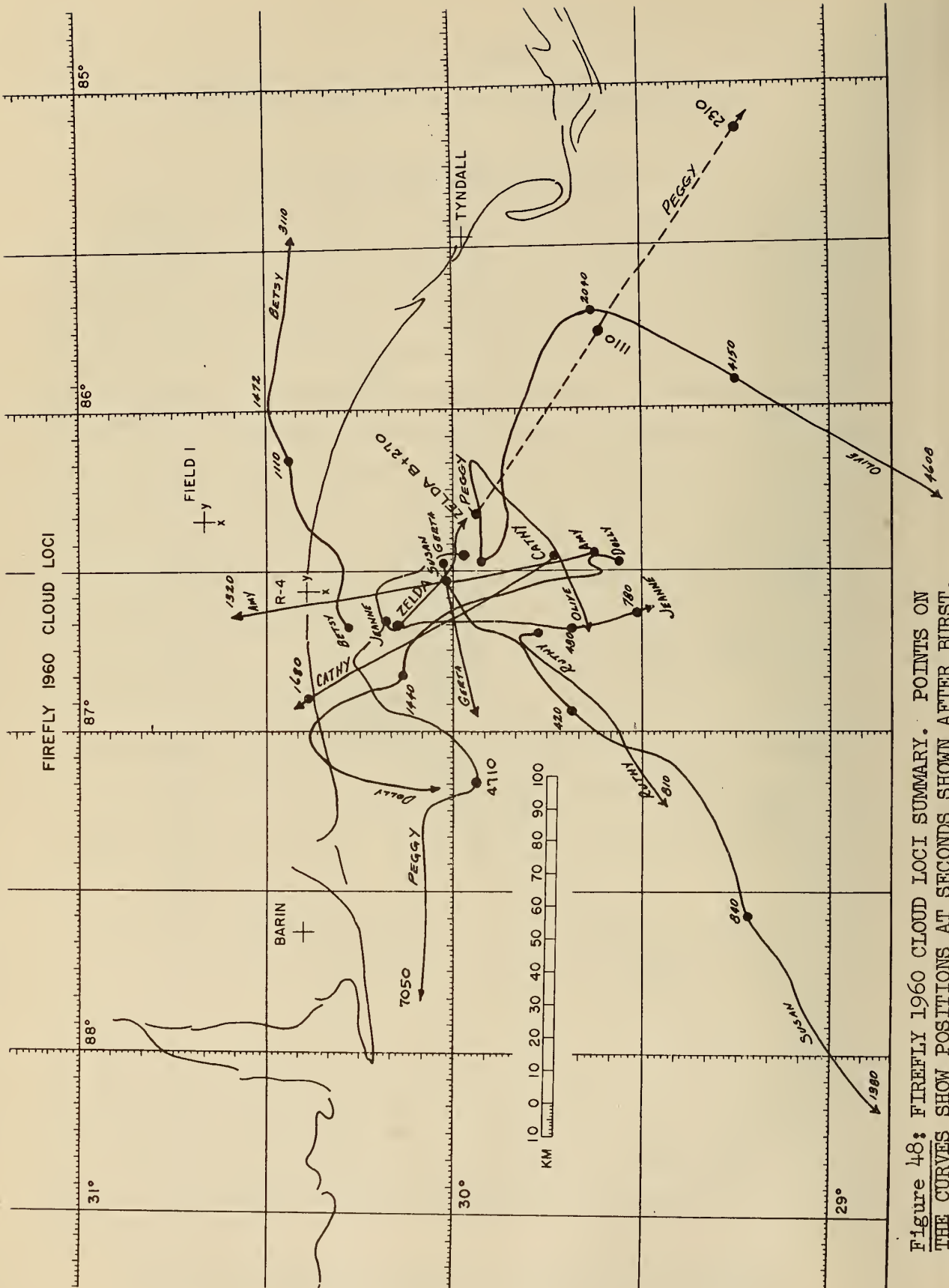


Figure 48: FIREFLY 1960 CLOUD LOCI SUMMARY. POINTS ON THE CURVES SHOW POSITIONS AT SECONDS SHOWN AFTER BURST.

N-S AND E-W COMPONENTS OF DRIFT SPEED, VS HEIGHT
 FIREFLY 1959 (-----) AND 1960 (——) CLOUD DATA

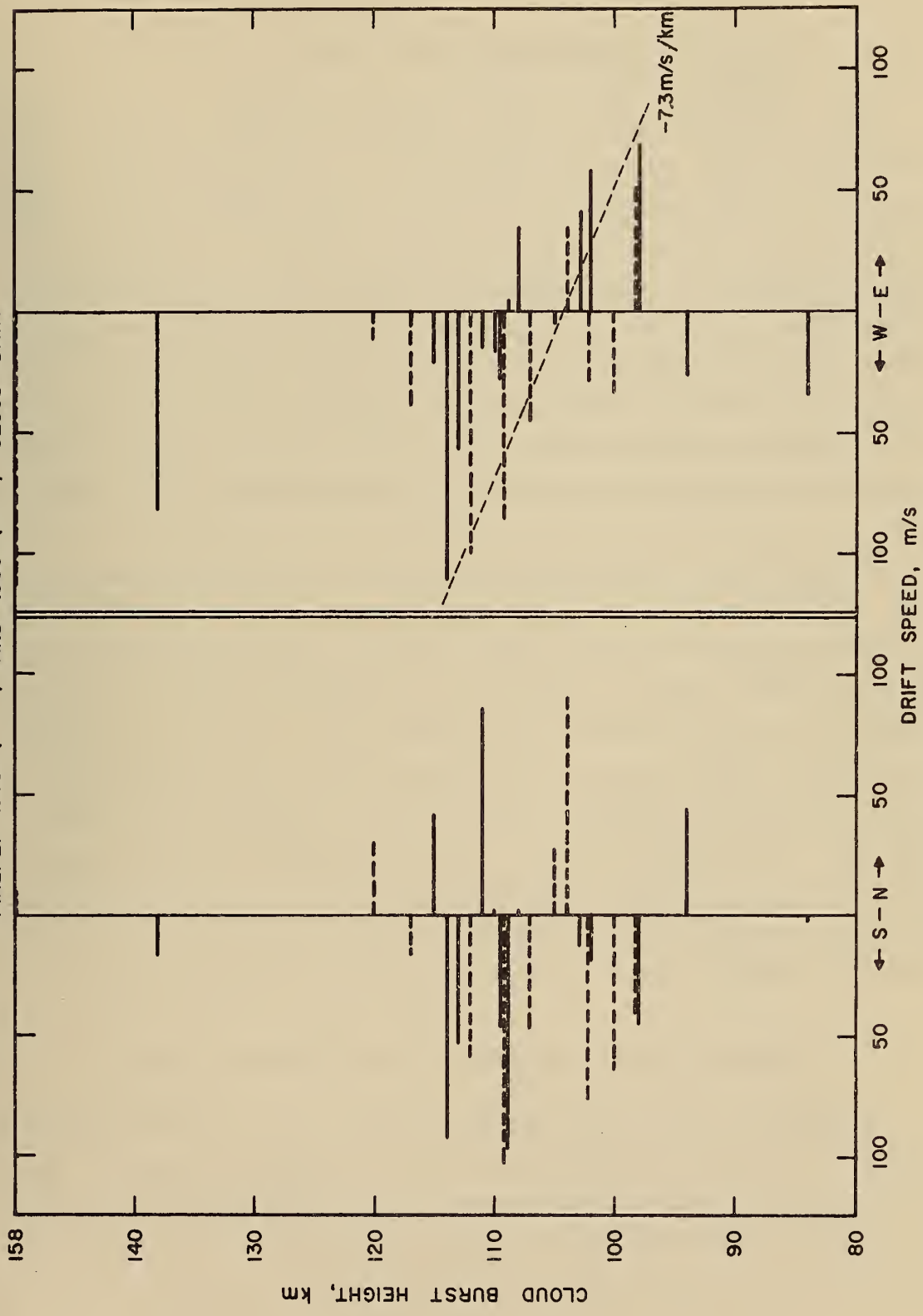


Figure 49: NORTH-SOUTH AND EAST-WEST COMPONENTS OF CLOUD DRIFT SPEED, VS. CLOUD BURST HEIGHT, FIREFLY 1959 (-----) AND 1960 (——) DATA.

B. Summary of Drift Results

Maps summarizing the drift of eight Point Electron clouds in 1959, and eleven in 1960, are shown in Figures 48 and 49, respectively. In both cases, a definite preference for the south-west quadrant is apparent, but this is brought out more clearly in Figure 50, showing the north-south and east-west components of the drift vs. cloud height at burst. Where the cloud was observed to divide into two differently-moving parts, at apparently differing altitudes, both are shown. It must be noted that past experience has suggested that the clouds rise by a few kilometers in their first few minutes; thus it is possible that this diagram should be interpreted at somewhat greater heights than shown.

In any event, it is interesting to note the definite change in east-west drift taking place at (apparently) 104 km. A value of -7.3 m/s/km is deduced for the east-west height gradient of drift, from this diagram. The north-south component appears to be in quadrature with the east-west component, as would be expected of a drift vector rotating with height. Maximum drift speeds occur at an average height of about 110 km and appear definitely to decrease above and below this level; the latter judgment is based entirely on the 1959 data ignoring the two results at relatively high altitudes. There does not seem to be any significant difference between 1959 and 1960 data, in this diagram; in fact, both series are constructive in defining the patterns discussed above.

C. Comment on Growth and Persistence of Electron Clouds

Although we did not find the cloud size to be a directly-computable quantity in the work reported here, there is abundant evidence to show that many of the sunlit clouds reached a very considerable size indeed, and that they have lifetimes exceeding by more than a factor of two the most persistent clouds reported in Firefly 1959.

Consider the following Point Electron clouds:

	<u>Altitude</u>	<u>Observed Duration</u>
Zelda	102	> 4500 seconds
Peggy	103	8760
Susan	114	6000
Dolly	115	6000

Each of these clouds were observed long after the development of the daytime E region; they then appeared as a "sporadic E" stratum embedded in the E layer. In most cases, these strata appeared to drift out of the field of view of the stations, rather than to disappear through a simple decay process. With stations located still farther from the clouds they undoubtedly could have been traced much longer. Unfortunately, however, the predominant motions were often to the south and east, emphasizing the need for stations located on shipboard in the Gulf of Mexico.

V. RECOMMENDATIONS FOR FUTURE PROGRAMS

A. Firefly Launchings

1. The expected potentialities of the trail releases do not seem to have been realized, yet the method is perhaps the only way of rapidly producing clouds of large size in the desired location. With somewhat better feeling for the prevailing wind speeds and directions it might be possible to produce a "sheet" cloud.

2. Point Electron cloud experiments should be more "controlled" in their relation to existing sporadic E. While in a sense, Es interferes with the observations, it seems that Es can give special properties of movement and persistence to artificially produced clouds.

3. Daytime launchings to heights above the maximum of the daytime E layer can give information about a valley minimum below the F region. This is of considerable interest since the region cannot be directly observed by conventional radio techniques.

4. Point Electron clouds in the F region should expand rapidly in a vertical direction due to diffusion, but the earth's magnetic field will tend to contain them laterally. Valuable information on the F-region itself, on long distance communications potentialities, and on similar ICBM F region effects would be anticipated.

5. The potentialities of the electron removal experiments must be explored. Although results of the recent Rena experiment are not impressive, it is likely that something was accomplished. Now more aware of the magnitude of effect to expect it is probable that more definitive results could be obtained, even with payloads no larger than Rena's. Again different effects in the presence or absence of sporadic E might be expected.

6. The possibilities of F-region electron removal have been discussed in detail by Van Zandt; his unpublished suggestions are contained here as Appendix III to this report.

B. Instrumentation

1. One of the powerful techniques of radio geophysics is the spaced-receiver method of measuring upper atmosphere drifts. It is our opinion that such instrumentation should be a part of future Firefly programs. Equipment designed to operate on several frequencies simultaneously would offer the following opportunities:

- a. direct observation of cloud drift
- b. comparison with drifts in the ambient ionization
- c. determination of drift height gradient in the ambient (i.e., at closely spaced frequencies).
- d. prediction of cloud motions, from drift observations in advance of the launching.

2. Improved ionosonde range determination equipment under development in this laboratory should permit range measurements to within 0.5 km or better. We suggest that this may greatly improve the possibility of determining cloud growth with time.

3. An improved station deployment is strongly suggested. The great need is for observations at a point 100 - 200 km off-shore from the Burst point. This should be supplemented with another instrument farther inland. The possibility of synchronization of the ionosondes should be explored as a means of giving additional independent range measurements at various aspect angles to the clouds.

4. It is considered that some improvement in the ability of ionosondes to track electron clouds at the longer ranges might be realized by the use of a somewhat more complex antenna system. For example, an azimuthal distribution of horizontal rhombic antennas clustered about the conventional vertical delta should permit the selection of an antenna appropriate to a cloud in any visible location.

REFERENCES

- Manning, L. A. and Eshlemann, V. R. , Proc. IRE 47, p. 186, 1959.
- Hawkins, G. S. , Interim Report No. 12, Harvard College Observatory, May 1956.
- Brown, L. C.; Bullough, K.; Evans, S. and Kaiser, T. R. , Proc. Phys. Soc. B, 69, pp. 83-97, 1956.
- Clark, C. , Tech. Report No. 24, Radio Prop. Lab. , Stanford Univ. , Sept. 1957.
- Titheridge, J. E. , J. Atmosph. Terr. Phys. 17, p. 110, Dec. 1959.
- Watts, J. M. , Brown, J. N; J. Geophys. Res. 59, p. 71, 1954.

APPENDIX I

NOTES ON INSTRUMENTATION

By

J. W. Wright
E. J. Violette
G. H. Stonehocker
J. J. Pitts

In the course of the 1960 Firefly launchings, it rapidly became clear that a great difference existed between electron clouds of the 1959 and 1960 series. The maximum radio reflection frequencies attained in 1959 were generally larger for a longer time than in 1960, and the cloud motions were somewhat more uniformly to the south and west. Possible reasons for these discrepancies have been discussed in this report but the true reasons are not yet known. It has been suggested that the differences between ionosonde installations in the two years might contain part of the answer. We will now examine this question, and simultaneously note a few of the characteristics of the ionosondes.

A. Characteristics of the C-4 Ionosondes

The following gives the important characteristics of the C-4 ionosondes and antennas and in the table following an indication wherever the 1959 and 1960 installations were thought to differ:

Typical C-4 CharacteristicsTransmitter

1. Frequency range: 1-25 Mc (logarithmic variation)
2. Sweep time: 15 or 30 seconds
3. Pulse recurrence frequency: 60 cps
4. Pulse length: 50 μ s

VARIANTS IN C-4 CHARACTERISTICS
DURING FIREFLY 1959/1960

SITE	1959			1960		
	WEAVER	A-4	A-4	FIELD 1	BARIN FIELD	TYNDALL
Ownership	Sig.C	Sig.C	NBS	AFCRL	Sig.C	AFCRL
Operation	Sig.C	Sig.C	NBS	Sig.C	Sig.C	Sig.C
Latitude			30° 23' 34" N	30° 40' 39"	30° 24' 13"	29° 58' 02"
Longitude			86° 34' 42"W	86° 21' 12"	87° 38' 11"	85° 28' 28"
Transmitter power	some- what	some- what				
2 Mc	less	less	28 kw	18 kw	18 kw	18 kw
10 Mc	than	than	17 kw	13 kw	13 kw	13 kw
20 Mc	1960	1960	11.5 kw	9 kw	9 kw	9 kw
Receiver bandwidth	>25 kc	>25 kc	20 kc	20 kc	20 kc	20 kc
Transmitting antenna base height feet	130 x 70	approx 190' changed 130'	200 by 84	130 x 70	130 x 70	130 x 70
Receiving antenna	130 x 70	see Sig Cs Rpt	150 by 84	130 x 70	130 x 70	130 x 70
Transmitting ant. orientation	45° off mag. north	45° east of mag north	30°W of mag north	prob. west of mag. north	45° east of mag north	45° of mag. north

B. Antennas

As can be seen from the table above, there is a real difference between the A-4 antenna system in 1959 and 1960. The A-4 antenna in 1960 was larger, and was oriented slightly differently than in 1959. This was done in order to improve its performance at low frequencies and (for the low frequencies) at lower radiation angles, so that weakly ionized clouds could be followed for longer periods. This undoubtedly changed the high-frequency radiation patterns, probably causing them to split, at some frequencies, into many small lobes at all angles. However, while this is undesirable for vertical sounding, it can only be of benefit to the cloud detection problem as it increases, rather than decreases, the radiation at low angles.

Perhaps a more weighty argument against the "instrumental" interpretation of the 1959/1960 discrepancies is that in 1960 the other three sites used exactly the same antenna size and orientation as A-4 and Weaver in 1959. Field-1 especially, was located and operated in a manner similar to Weaver. It is thus concluded that the 1959/1960 differences cannot be ascribed to the ionosonde antennas.

C. Range Accuracies*

Accurate range measurements with an ionosonde depend upon the following considerations:

* We are, unfortunately, not in a position to discuss fully the calibration of equipment at the three Signal Corps stations. NBS engineers visited each of these stations at various times to instruct Signal Corps personnel in calibration procedures, but -- as will be seen below -- it seems clear that the prescribed calibrations were not always followed. The discussion following pertains therefore to the NBS A-4 site, where equipment calibrations were done in advance of each experiment.

- a. accuracy of the range marker interval
- b. accuracy of the zero-point
- c. allowance for pulse delay in receiver and transmitter
- d. rise time of the echo signal
- e. faithfulness of the film recording
- f. linearity of the range scale

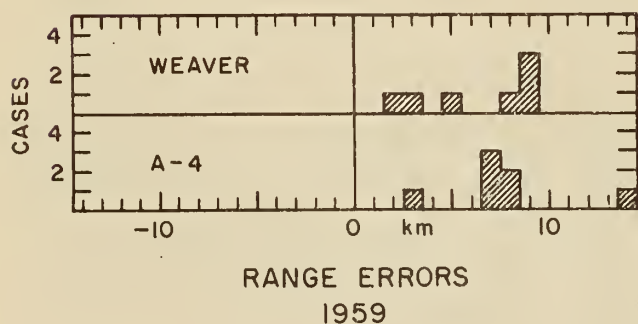
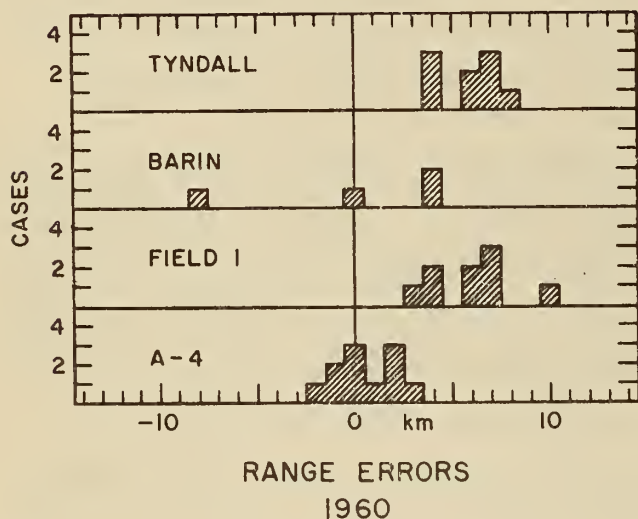
The range marker interval (usually 50 km) was crystal-controlled and compared with WWV; discrepancies of at most one cycle (out of 3 kc) were found. Non linearity (e) may be overcome by careful scaling, but in fact the C-4 range scale is quite linear and seldom gives any trouble. Item (c) (and to some extent d) may be compensated for by proper positioning of the ground zero-point. A method was developed expressly for the Firefly program* which greatly reduces the magnitude of this factor.

The transmitted pulse (greatly reduced in amplitude to simulate an echo signal and obtained at the receiver video output) is displayed on one trace of a dual beam oscilloscope. The range markers are displayed on the other trace expanded to show 0.75 km per centimeter. A careful adjustment of the transmitted pulse delay permits the alignment of the outgoing pulse, compensated for receiver and transmitter delays, to within 0.15 km. This assures that the zero of the range scale coincides with the zero range marker to within this accuracy for echoes of ordinary amplitudes.

The remaining factors are the faithfulness of the film recording and the rise time of the echo signal: to what extent does the film image represent the output of the receiver, after all the other difficulties have been eliminated, and how effective are weak echoes compared to strong echoes in this regard? The "A-scan" recordings described in

* By E. J. Violette of the NBS Equipment Development Group.

Section D provide an answer to this question. Here, the conventional ionogram recording is supplemented with a sequence of range vs amplitude recordings on 35 mm film. Using these recordings, the true position of the leading edge of the returning echo may be compared with that recorded on the ionogram. No significant error of the latter method of recording has been detected. Furthermore, echoes capable of "breaking" the A-scan range scale, appear on the ionogram without significant sacrifice of height accuracy. These findings were confirmed on a number of occasions at A-4 when many multiple echoes of sporadic E were observed. In most cases, accurate agreement was obtained, even where the echoes became fairly weak.



It is therefore concluded that within the range accuracies attempted (± 0.5 km), and with the generally good S/N ratios obtaining at A-4, there did not exist significant range errors at that station due to instrumental effects. However, there is evidence that these accuracies cannot be claimed for the other stations during 1959 and 1960. The histogram of the adjacent figure shows the distribution of "range-errors," defined as the observed burst slant range to the cloud minus the range computed from optical data, for each of the

ionosonde stations. Obviously, there was a great difference between the stations, with systematic errors at Tyndall and Field-1 and possibly Barin Field -- but not at A-4. It is also clear that the errors are not distance-dependent. It has unfortunately not been possible to take these errors into account for the position and drift results reported here. They would have only minor effect on the drift data, but might have permitted more conclusive results on cloud altitude and growth.

The average of the errors shown in the figure, for each station are: A-4: 0.54 km (11 observations); Barin Field: 0.12 km (4 observations); Field-1: 6.1 km (9 observations); and Tyndall: 5.8 km (9 observations).

D. Amplitude/Range vs. Time Recordings

Despite the very broad frequency range of this equipment (25:1), and the resulting considerable variations in its radiated power throughout this spectrum, it was felt that continuous recordings of echo amplitude vs time, when interpreted separately at selected frequencies, might be a useful extension of the ionosonde technique. Such recordings would reduce effects of definite rise-time of the pulse a possible source of error in range determinations. (See Section C.) They would also permit a study of the echo pulse shape, should that prove useful.

Accordingly, a device was developed* by which the range vs amplitude information could be recorded on a separate oscilloscope.

*By Mr. J. J. Pitts, NBS Equipment Development Group.

The pulse generator of the C4 recorder operating at a PRF of 60 pps was used to trigger a pulse divider, the output of which was adjustable from 1 pps to 6 pps. (3 pps was selected as the optimum rate). The pulse divider then triggered the external oscilloscope while a 35 mm camera exposed film at the rate of 55 ft/min. The external oscilloscope was connected to the last IF stage of the C4 receiver, ahead of any differentiation. The measured dynamic range of the receiver was approximately 70 db. Indications are that the receiver response is linear over most of the dynamic range (about 56 db). Precise linearity measurements have not performed.

Megacycle frequency markers were provided by an argon lamp which was flashed by a one-shot multivibrator, an integral part of the pulse divider unit. The C4 frequency marker unit supplied the negative pulse needed to trip this multivibrator. A standard IBM printtime unit was used to identify each frame once during each sweep. Height markers from the C4 recorder were injected into the amplitude measurements by means of an algebraic oscilloscope preamplifier.

Vertical incidence stations located on Tyndall Air Force Base, Barin Field, and Eglin Field-1 were operated by U. S. Signal Corps personnel. These three stations were supplied with complete NBS amplitude measuring equipment and technical assistance for putting this equipment into operation. Similar recordings were of course made also at A-4.

These recordings were employed when necessary to confirm range measurements used in this report. They were also analyzed for amplitude vs time vs frequency data by the U. S. Army Signal Corps, and form the basis for a parallel report from the Signal Corps Radio Propagation Agency on radar cross sections.

APPENDIX II

METHODS FOR DETERMINATION OF CLOUD POSITION, DRIFT,
AND GROWTH FROM IONOSONDE RANGE DATA.

by

D. E. McKinnis

Given ranges from four ionosondes, it is in principle possible to derive four numbers descriptive of the cloud: its three spatial coordinates (latitude, longitude, and height) and one number related to the size, necessarily the radius.

To derive the relations for four stations, we select one of the stations as the origin of a set of rectangular coordinates. The equations relating cloud radius r ; ranges R_i ; station locations x_i , y_i ; and the cloud coordinates x , y , h are:

$$(R_i + r)^2 = (x - x_i)^2 + (y - y_i)^2 + h^2 \quad i = 0, 1, 2, 3 \quad (1)$$

or, subtracting the relation for station 0,

$$(R_i - R_0)r + x_i x + y_i y = a_i \quad i = 1, 2, 3 \quad (2)$$

where $a_i =$

$$a_i = \frac{1}{2}(R_0^2 - R_i^2 + x_i^2 + y_i^2) \quad (3)$$

This system of equations has a solution if the determinant of the coefficients of the left-hand side does not vanish. The altitude is given by

$$h^2 = R_0^2 - x^2 - y_i^2 \quad (4)$$

Given only three ranges, no cloud size determination is possible, and the relations will be like (1) with $r = 0$, whence

$$x_i x + y_i y = a_i \quad (5)$$

as before. This system has a solution unless the three stations lie in a straight line. Given two ranges, the position is not determined unless further data is given. We may specify an estimated cloud height to determine the position, but as can be seen physically, this solution is two-valued; the two solutions will be equidistant from the line joining the locations from which the ranges are measured. The relations are found from

$$x_1 x + y_1 y = a_1, \text{ as before.}$$

Substituting this into (4), we get

$$x^2(x_1^2 + y_1^2) - P x_1 x - y^2(R_0^2 - h^2) = 0 \quad (6)$$

$$\text{where } P = R_0^2 - R_1^2 + x_1^2 + y_1^2$$

The solutions to this quadratic are

$$2(x_1^2 + y_1^2)x = x_1 P \pm y \left[4(x_1^2 + y_1^2)(R_1^2 - h^2) - P^2 \right]^{1/2} \quad (7a)$$

$$\text{and } 2(x_1^2 + y_1^2)y = y_1 P \pm x_1 \left[4(x_1^2 + y_1^2)(R_1^2 - h^2) - P^2 \right]^{1/2} \quad (7b)$$

This solution will not exist if the estimated height is so great that the two ranges in contact cannot reach it.

If data is available from only one station, it can be used with other (e.g., optical) data on geographic position to determine the cloud height.

A multipurpose program was prepared for the NBS CDC-1604 computer. The program was designed to accept data from one, two, three or four (or more) stations and provide the following information:

- a. Four or more stations:
 1. cloud size given: program computes position and height for all possible sets of three ranges and the average position and height for these sets.
 2. cloud size not given: program computes position, height and cloud radius for all possible sets of four ranges, and the average position, height, and radius for these sets.
- b. Three stations: program computes height and position for any assumed value of cloud radius.
- c. Two stations: height and radius of cloud given: program computes the two possible positions of the cloud.
- d. One station: position and range given: program computes cloud height.
- e. Cloud height and position given: program computes ranges to all specified stations.

When the configuration of three or four stations is near a configuration for which no solutions exist, the computed cloud parameters will be sensitive to small errors in the range determinations. During Firefly 1960 stations at Barin and Tyndall and site A-4 were in fact within 25° of a straight line; the computed positions will be highly uncertain in a direction normal to this line.

In practice, we found that reasonable values of cloud size seldom could be deduced from the four-ionosonde data of 1960 Firefly. The cloud radius when it was computed was erratic and often negative. This is the effect of the markedly non-spherical shape rapidly assumed by the clouds, and because the radius depends so delicately on the range information. Given a sphere resting on four stilts based on a plane, it is easy to picture a sphere of much different size "almost" resting on the same four stilts, making the computed size

very sensitive to small errors in range determination. On the other hand the considerable sizes attained by the clouds made it impossible to determine their heights accurately (in the three-station problem) if the cloud radii were assumed negligible.

There has not been adequate time to make full use of the present computer program in the examination of cloud size or height by trial and error. In future work we hope to deal with a more ideal deployment of stations, and to make a more elaborate study of the geometric problem.

APPENDIX III

A SUGGESTION FOR THE STUDY OF ELECTRON RECOMBINATION
IN THE F2 REGION BY THE RELEASE OF GASES FROM ROCKETS

by

Thomas E. Van Zandt

National Bureau of Standards
Boulder Laboratories
Boulder, Colorado

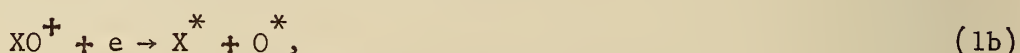
January 20, 1960

A SUGGESTION FOR THE STUDY OF ELECTRON RECOMBINATION
IN THE F2 REGION BY THE RELEASE OF GASES FROM ROCKETS

In the F region of the ionosphere, recombination of electrons is thought to be limited by the reactions¹ atom-ion exchange,



followed by dissociative recombination



Where XY is a molecule, probably either O₂ or N₂. X* and O* are excited states: The O* emits the 6300Å airglow observed from the F region.² Although ionospheric research shows that these reactions are qualitatively correct, some important problems remain: the identity of XY is open to conjecture, the densities of O₂ and N₂ are unknown, and determinations of the rate coefficients differ within a range of ten. The experiment proposed here is intended to resolve at least partially these uncertainties.

Solution of the rate equations for reactions (1a) and (1b) with the assumptions that the densities of XY and XO⁺ are independent of time leads to a rate of loss of electrons L(h,t) given by¹

$$L(h,t) = \frac{\alpha_{ex}N(h) \alpha_{dr}n(h,t)}{\alpha_{ex}N(h) + \alpha_{dr}n(h,t)} \cdot n(h,t), \quad (2)$$

where α_{ex} is the rate coefficient for dissociative recombination,
 α_{dr} is the rate coefficient for atom-ion exchange,
 N(h) is the number density of XY,
 n(h,t) is the number density of electrons.

In the F1 layer $\alpha_{ex}N(h) \gg \alpha_{dr}n(h,t)$ and,

$$L(h,t) \doteq \alpha_{dr}n(h,t)^2. \quad (3)$$

In the F2 layer, $\alpha_{ex}N(h) \ll \alpha_{dr}n(h,t)$ and,

$$L(h,t) \doteq \alpha_{ex}N(h)n(h,t). \quad (4)$$

Thus in the F2 layer the rate of recombination is proportional to the density $N(h)$ of XY, which is probably either O_2 or N_2 . The transition between (3) and (4) is uncertain and variable, but probably lies near 250 km.

It is evident that in the F2 region $L(h,t)$ can be increased by releasing XY from a rocket. The amount necessary for an appreciable effect can be estimated by comparison with the existing densities. At 300 km, the total atmospheric density is³ on the order of 0.1 kg/km^3 . Of this, only a few percent is O_2 and the fraction of N_2 may be as large as 90 percent or as small as one percent. In any case, it is evident that 10 kg of XY would be sufficient to double the density of XY in a volume of from 100 to $10,000 \text{ km}^3$, depending on the original density of XY.

In view of the uncertainty of the identity of XY, two or more experiments might be necessary.

The first release should be of O_2 at ≥ 250 km at night. If O_2 is XY the effects would be as follows. A visible red flash of the 6300\AA line of O would rapidly decay as the densities of O_2 and of the electrons decreased. The time and space variation of the 6300\AA and also the 5577\AA emission would be observed by monochromatic photometers long after they become invisible to the eye. Another photometer should observe the uncontaminated airglow not too far away. Most of the quantitative results of the experiment would be derived from a comparison of the observed 6300\AA emission with the theoretical emission based on reaction (1) and the rates of diffusion of O_2 and electrons.

The rapid recombination of electrons in the contaminated region will result in a hole in the bottom of the ionosphere (which is near 250 km at night). The hole will grow outward as the O_2 diffuses. Also it will grow upward as the electrons diffuse downward along the magnetic lines of force and recombine in the contaminated volume. These effects should be observed with one or more ionosondes, one of which should be as nearly as possible directly beneath the release (e.g., an airborne ionosonde). The hole will appear as an additional trace. Observation of its geometry and growth will be important to theories of the ionosphere.

If the hole grows upward long enough, the F layer along these lines of force will be emptied of electrons, forming a hole through the ionosphere. By measuring the increased cosmic noise intensity through the hole we could both gain information on the cosmic noise intensity at frequencies which are ordinarily reflected by the ionosphere and at the same time deduce the upward progress of the hole.

A hole made at night could not begin to fill until the O_2 had been dispersed. Then it would fill by horizontal diffusion of electrons at the lowest heights (about 250 km). In fact, the hole might last until sunrise. A hole made in the daytime would fill more rapidly by photoionization.

If O_2 caused no effect this would in itself be an important result, and would impel us to a release of N_2 . The observations and the nature of the deductions would be the same.

References

1. J. A. Ratcliffe, "The formation of the ionospheric layers F-1 and F-2", JATP 8, 260-9 (1956).
2. J. W. Chamberlain, "Oxygen red lines in the airglow. I. Twilight and night excitation processes", AP. J. 127, 54-66 pp 62-65 (1958).
3. E.g., G. F. Schilling and T. E. Sterne, "Densities and temperatures of the upper atmosphere inferred from satellite observations", JGR 64, 1-4 (1959).



THE NATIONAL BUREAU OF STANDARDS

The scope of activities of the National Bureau of Standards at its major laboratories in Washington, D.C., and Boulder, Colorado, is suggested in the following listing of the divisions and sections engaged in technical work. In general, each section carries out specialized research, development, and engineering in the field indicated by its title. A brief description of the activities, and of the resultant publications, appears on the inside of the front cover.

WASHINGTON, D.C.

Electricity. Resistance and Reactance. Electrochemistry. Electrical Instruments. Magnetic Measurements. Dielectrics. High Voltage.

Metrology. Photometry and Colorimetry. Refractometry. Photographic Research. Length. Engineering Metrology. Mass and Scale. Volumetry and Densimetry.

Heat. Temperature Physics. Heat Measurements. Cryogenic Physics. Equation of State. Statistical Physics.

Radiation Physics. X-ray. Radioactivity. Radiation Theory. High Energy Radiation. Radiological Equipment. Nucleonic Instrumentation. Neutron Physics.

Analytical and Inorganic Chemistry. Pure Substances. Spectrochemistry. Solution Chemistry. Standard Reference Materials. Applied Analytical Research.

Mechanics. Sound. Pressure and Vacuum. Fluid Mechanics. Engineering Mechanics. Rheology. Combustion Controls.

Organic and Fibrous Materials. Rubber. Textiles. Paper. Leather. Testing and Specifications. Polymer Structure. Plastics. Dental Research.

Metallurgy. Thermal Metallurgy. Chemical Metallurgy. Mechanical Metallurgy. Corrosion. Metal Physics. Electrolysis and Metal Deposition.

Mineral Products. Engineering Ceramics. Glass. Refractories. Enameled Metals. Crystal Growth. Physical Properties. Constitution and Microstructure.

Building Research. Structural Engineering. Fire Research. Mechanical Systems. Organic Building Materials. Codes and Safety Standards. Heat Transfer. Inorganic Building Materials.

Applied Mathematics. Numerical Analysis. Computation. Statistical Engineering. Mathematical Physics. Operations Research.

Data Processing Systems. Components and Techniques. Computer Technology. Measurements Automation. Engineering Applications. Systems Analysis.

Atomic Physics. Spectroscopy. Infrared Spectroscopy. Solid State Physics. Electron Physics. Atomic Physics.

Instrumentation. Engineering Electronics. Electron Devices. Electronic Instrumentation. Mechanical Instruments. Basic Instrumentation.

Physical Chemistry. Thermochemistry. Surface Chemistry. Organic Chemistry. Molecular Spectroscopy. Molecular Kinetics. Mass Spectrometry.

Office of Weights and Measures.

BOULDER, COLO.

Cryogenic Engineering. Cryogenic Equipment. Cryogenic Processes. Properties of Materials. Cryogenic Technical Services.

Ionosphere Research and Propagation. Low Frequency and Very Low Frequency Research. Ionosphere Research. Prediction Services. Sun-Earth Relationships. Field Engineering. Radio Warning Services. Vertical Soundings Research.

Radio Propagation Engineering. Data Reduction Instrumentation. Radio Noise. Tropospheric Measurements. Tropospheric Analysis. Propagation-Terrain Effects. Radio-Meteorology. Lower Atmosphere Physics.

Radio Standards. High Frequency Electrical Standards. Radio Broadcast Service. Radio and Microwave Materials. Atomic Frequency and Time Interval Standards. Electronic Calibration Center. Millimeter-Wave Research. Microwave Circuit Standards.

Radio Systems. Applied Electromagnetic Theory. High Frequency and Very High Frequency Research. Modulation Research. Antenna Research. Navigation Systems.

Upper Atmosphere and Space Physics. Upper Atmosphere and Plasma Physics. Ionosphere and Exosphere Scatter. Airlow and Aurora. Ionospheric Radio Astronomy.

